UDC 004
21.3
681.5
In print: ISSN 2545 – 4250
On line: ISSN 2545 – 4269

JOURNAL OF ELECTRICAL ENGINEERING AND INFORMATION TECHNOLOGIES

СПИСАНИЕ ЗА ЕЛЕКТРОТЕХНИКА И ИНФОРМАЦИСКИ ТЕХНОЛОГИИ

J. Electr. Eng. Inf.. Technol.	Vol. **8**	No. 2	pp. 43–132	Skopje 2023
Спис. Електротехн. Инф. Технол.	Год.	Број	стр.	Скопје

J. Electr. Eng. Inf.. Technol.	Vol.	No.	pp.	Skopje
	8	2	43–132	2023
Спис. Електротехн. Инф. Технол.	Год.	Број	стр.	Скопје

JOURNAL OF ELECTRICAL ENGINEERING AND INFORMATION TECHNOLOGIES
СПИСАНИЕ ЗА ЕЛЕКТРОТЕХНИКА И ИНФОРМАЦИСКИ ТЕХНОЛОГИИ

Published by:
Faculty of Electrical Engineering and Information Technologies, "Ss. Cyril and Methodius" University in Skopje,
P.O.Box 574, MK-1001 Skopje, North Macedonia

Издава:
Факултет за електротехника и информациски технологии, Универзитет „Св. Кирил и Методиј" во Скопје,
пошт. фах 574, МК-1001 Скопје, Северна Македонија

Published twice yearly – Излегува два пати годишно

UDC: "St. Kliment Ohridski" Library – Skopje	УДК: НУБ „Св.. Климент Охридски" – Скопје
Copies: 300	Тираж: 300
Price: 760 denars	Цена: 760 денари
Address	Адреса

http://jeeit.feit.ukim.edu.mk
jeeit@feit.ukim.edu.mk

JEEIT is indexed/abstracted in INIS (International Nuclear Information System)

JOURNAL OF ELECTRICAL ENGINEERING AND INFORMATION TECHNOLOGIES
СПИСАНИЕ ЗА ЕЛЕКТРОТЕХНИКА И ИНФОРМАЦИСКИ ТЕХНОЛОГИИ

J. Electr. Eng. Inf.. Technol.	Vol.	No.	pp.	Skopje
	8	2	43–132	2023
Спис. Електротехн. Инф. Технол.	Год.	Број	стр.	Скопје

TABLE OF CONTENTS
(С О Д Р Ж И Н А)

Renewable energies – Обновливи извори на енергија

Power distribution systems – Енергетски дистибутивни системи

Telecommunications – Телекомуникации

Metrology – Метрологија

Automation – Автоматика

Electronics – Електроника

Journal of Electrical Engineering and Information Technologies, Vol. **8,** No. 2, pp. 47–56 (2023)
Article 206 In print: ISSN 2545–4250
Received: November 12, 2023 On line: ISSN 2545–4269
Accepted: November 30, 2023 UDC: 621.548.4-192
https://doi.org/10.51466/JEEIT2382206047ck

Original scientific paper

VIABILITY AND PERFORMANCE INVESTIGATION OF SMALL WIND TURBINES

Maja Celeska Krstevska, Vlatko Stoilkov, Vladimir Dimčev

Faculty of Electrical Engineering and Information Technologies, "Ss. Cyril and Methodius" University in Skopje, Rugjer Bošković bb, P.O.Box 574, 1001 Skopje, Republic of North Macedonia
celeska@feit.ukim.edu.mk

A b s t r a c t: In the past decades, extensive and exhaustive research has been done on the analysis of the operation of large wind turbines, but detailed analyses on small wind turbines are still rare. In addition, two current situations are considered: i) the exhaustion of the possibilities for designing new large wind fields, and ii) the energy crisis, which is particularly current in Europe, so it comes naturally to analyze the possibilities for exploitation of small wind turbines defined according IEC 61400-2 standard. The paper analyzes five potential locations in North Macedonia. Based on two-year measurement period at those locations, the probability distribution of wind speeds was obtained and integrated with the power curve for a specific turbine, the electricity production of four different, commercially available, small wind turbines was investigated. Three wind turbines are horizontal axes wind turbines, with installed power in the range of 3–50 kWp, and one is vertical axis wind turbine with installed power of 4 kWp. In accordance with the Rulebook for amending and supplementing the rulebook for renewable energy sources from June 2022, calculations have been made for the profitability of energy production from grid-connected small wind turbines. Finally, a graphical comparative analysis of different models of small wind turbines for all locations is presented, and conclusions and further directions and recommendations for optimal utilization of wind energy are given.

Key words: small wind turbine; wind energy potential; profitability analysis

АНАЛИЗА НА ОДРЖЛИВОСТА И ПЕРФОРМАНСИТЕ НА МАЛИ ВЕТЕРНИ ТУРБИНИ

А п с т р а к т: Во изминатите децении се направени обемни и исцрпни истражувања за анализа на експлоатацијата на големите ветерни турбини, но детални анализи за мали ветерни турбини сѐ уште се реткост. Дополнително, ако се земат предвид и две клучни тековни состојби: i) исцрпеноста на можностите за проектирање нови големи ветерни полиња и ii) енергетската криза која е посебно актуелна во Европа, природна е потребата да се анализираат можностите за примена и на мали ветерни турбини дефинирани според стандардот IEC 61400-2. Во трудот се анализирани пет потенцијални локации во Северна Македонија. Врз основа на двегодишни мерења на тие локации, добиена е дистрибуцијата на веројатност на брзините на ветерот и во комбинација со кривата на моќноста на конкретна турбина е анализирано производството на електрична енергија од четири различни, комерцијално достапни, мали ветерни турбини. Три ветерни турбини се со хоризонтална оска, со инсталирани моќности во опсегот 3–50 kWp, а една е со вертикална оска и со инсталирана моќност од 4 kWp. Согласно Правилникот за изменување и дополнување на Правилникот за обновливи извори на енергија од јуни 2022 година, направени се пресметки на исплатливоста на производството од мали ветерни турбини. На крајот е претставена графичка компаративна анализа на различните модели на мали ветерни турбини за сите локации и се изведени заклучоци и понатамошни насоки и препораки за оптимално искористување на енергијата на ветерот.

Клучни зборови: мали ветерни турбини; потенцијал на енергијата на ветерот; анализа на профитабилност

1. INTRODUCTION

With Tremendous advances have occurred in the renewable energy sector in recent decades, among which one of the most important is wind energy. As shown in Figure 1, the rate of growth of global total installed wind power capacity increased annually from 2001 to 2022 [1]. The amount of electricity generated by wind increased by almost 273 TWh in 2021 (17%), 55% higher growth than that achieved in 2020, and the largest of all power generation technologies. Wind remains the leading non-hydro renewable technology, generating 1.870 TWh in 2021, almost as much as all the others combined [2].

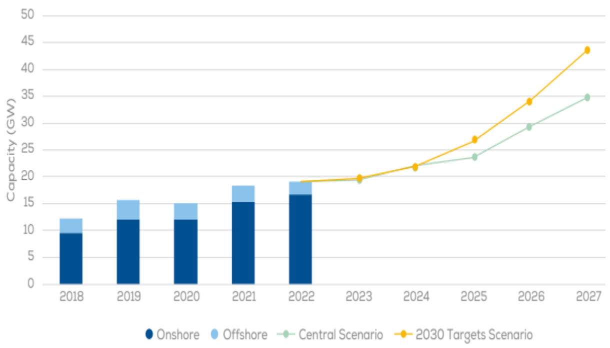

Fig. 1. 2023–-2027 new onshore and offshore wind installations in Europe – WindEurope's scenarios [7]

In our country, we cannot boast of following the trend of installing new wind energy capacities, as we've expected when this technology was new and promising. In 2010, the Macedonian Academy of Sciences and Arts published a strategy for the use of renewable energy sources [3]. The study predicts that the total installed capacity by 2030 will be around 360 MW, with an expected annual production of around 720 GWh [4]. Until the moment of writing this paper, only the first wind farm – Bogdanci, with an installed capacity of 36.8 MW, is operating in the country, which represents only the first phase of a projected wind farm [5]. By the end of 2023 it is expected the second wind plant to be finished. Furthermore, this is the first private wind energy project in the country, named „Bogoslovec". "Bogoslovec" will have total capacity of 36 MW and hopefully is a step forward in order to divert country's national electricity production, which is still dominated by coal (lignite), to renewable energy sources. So it is clear that intensification of the process is needed.

Within the wind energy sector, small wind turbines (SWTs) are a separate group of wind turbines that cater to localized or decentralized power generation. Unlike large-scale wind turbines commonly seen in wind farms, SWTs are designed for residential, commercial, or community-scale applications. In recent years, technological advancements and increased interest in renewable energy have led to the growth of the SWTs market. As technology continues to evolve, SWTs are becoming more efficient, quieter, and aesthetically acceptable, further expanding their potential application in the renewable energy landscape.

According to the IEC 61400-2 standard, SWTs are characterized by a rotor swept area of less than 200 m^2 and rated power below 50 kW, generating electricity at a voltage below 1 000 V (AC) or 1 500 V (DC) for both on-grid and off-grid applications [6].

Their compact size makes them suitable for installation on rooftops, towers, or other structures, and they are often used inrural or remote areas where grid connection may be challenging. They can provide power for individual homes, farms, small businesses, telecommunication units, isolated mountain objects, or even communities, reducing reliance on traditional energy sources and lowering carbon emissions. One of the primary advantages of SWTs is their ability to generate electricity in areas with lower wind speeds, as well as possibility of 24/7 electricity production. This is confirmed by data from a report from the Statista portal [8] showing the capacity of small wind turbines in the world from 2010 to 2018.

SWTs come in various designs, including horizontal-axis and vertical-axis configurations. Horizontal-axis wind turbines (HAWTs) are similar in design to larger wind turbines and consist of a rotor with two, three or more blades that rotate around a horizontal axis. Vertical-axis wind turbines (VAWTs), on the other hand, have blades that rotate around a vertical axis, allowing them to capture wind from any direction without the need for wind direction alignment.

The installation and maintenance of SWTs are generally more straightforward compared to large-scale turbines. However, it's essential to consider factors such as local regulations, zoning restrictions, and proper site assessment before installing an SWT.

While SWTs offer numerous benefits, they also have limitations. The disadvantages of SWTs are high initial cost, effective placement, wind fluctuation, lower electricity production due to wind share, change in wind direction and also aero-acoustic noise [6]. SWT profitability is determined by the combination of wind turbine efficiency, cost and reliability. At the preliminary stage of the SWT design process, there is a need for an inexpensive, effective and reliable methodology for estimating these factors when considering design solutions and variants [7].

The paper attempts to address this gap by examining the real parameters of SWTs, especially data on actual electricity generation and the profitability of power plant installations. The results will be valuable for economic assessments of wind turbine investments and for determining the real energy potential of SWTs in the country.

2. MEASUREMENT DATA

The wind data used in the study covers a period of two years (2012–2014) [9]. The input data is gained from three wind measurement masts, at five different locations (Berovo, Mogila, Sopište, St. Nagoričane and Sv. Nikole). The main parameters that are used in the analysis, wind speed and direction, are recorded at 10-minute intervals, expressed in meters per second (m/s) and degrees (^{o}) toward north. The data used in this research is measured with anemometers and wind vanes positioned at heights of 40 m and 38 m, respectively. Average wind speeds for each month across all years studied were calculated separately for each location. Figure 2 presents the results to facilitate the analysis of trends, differences and relationships. A constant trend of windiness between 3 and 4 m/s, can be observed across 3 locations – Berovo, Mogila and Sopište. For Mogila it can be concluded that windiness is usually higher in the autumn-winter period than in the spring-summer period. Opposite of this, the graphs show that for Sopište location the windiness trend is higher in the summer months, with an exception for January. Data from measuring mast located in Berovo also show higher windiness trend during spring and summer months. At Sv. Nikole the windiness is between 3.7 and 5 m/s and higher winds are measured during warm months. Completely different windiness conditions are observed at Staro Nagoričane, with wind speeds among 5.5–8.5 m/s, which qualifies this location as most suitable for exploitation of wind energy, even for commercial big wind turbines.

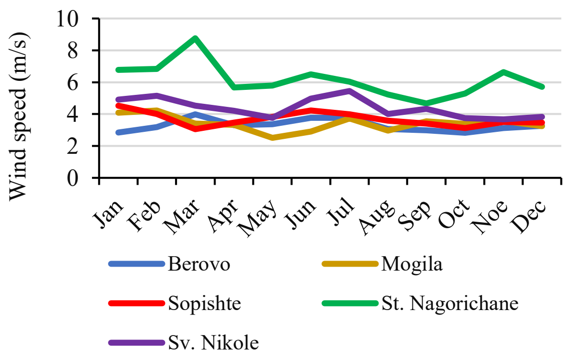

Fig. 2. Distribution of mean monthly wind speeds across the three year period 2012–2015 for five locations

When analyzing data for estimation of electricity production form SWT, the absence of big variations in wind speed is a positive side. In that case, electricity generation will be quite constant and all necessary maintenance operations as well as routine checks can be carried out anytime, even it is certainly recommended to be done during the calm (least windy) periods.

For better depiction of the real achievable wind speeds at these five locations, histograms were prepared to illustrate how frequently specific wind speeds occur at each location. Also, two-parameters Weibull function is applied at the same graphs, plotted with the values for shape and scaling parameters given in Table 1. From the calculated data in Table 1 it is expected that there won't be any significant differences among wind regimes at the first three locations – Berovo, Mogila and Sopište. All three locations are characterized with low value of mean wind speed – slightly above 3 m/s. At Berovo the lowest wind speed is measured 3 – 0.29 m/s, slightly higher at Mogila – 3.41 m/s, and 3.69 m/s at Sopište. Minor differences are calculated among shape parameters (k). Scale parameters (c) differ for Sopište – 4.34 m/s, compared to those of Berovo, 3.66 m/s, and Mogila, 3.72 m/s.

Table 1

Weibull parameters for the three measuring locations

Parameter	Berovo	Mogila	Sopište	St. Nagoričane	Sv. Nikole
v_{mean} (m/s)	3.29	3.41	3.69	6.16	4.38
Std (m/s)	2.21	2.57	2.72	3.84	3.29
k	1.54	1.36	1.45	1.78	1.36
c (m/s)	3.66	3.72	4.34	7.34	4.75

The dominance of all parameter's values at Staro Nagoričane are evident, with the maximum measured average wind speed of 6.16 m/s, except for the k parameter of 1.78 and it should be notified that a higher value was expected. At last, Sv. Nikole location is characterized with values in the middle among the above mentioned, with average wind speed of 4.38 m/s and a wider standard deviation, compared to the first three locations. Wind speed analysis is the basis for calculating the annual electricity production in each location by a specific wind turbine in this study (Figure 3).

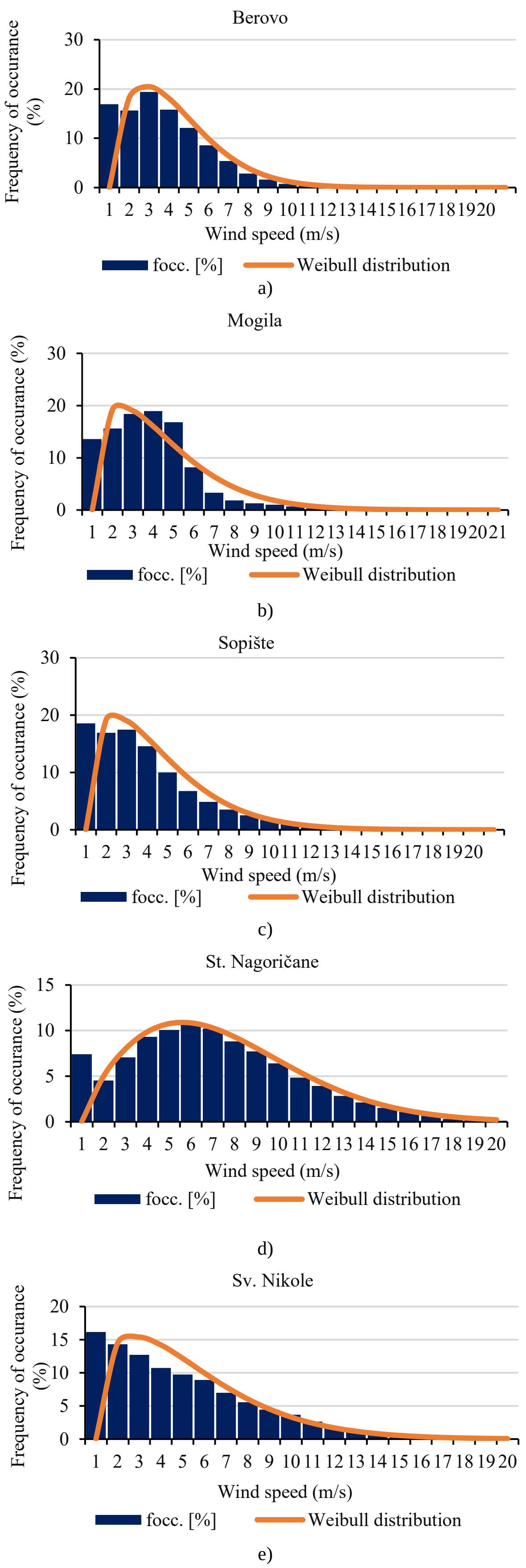

Fig. 3. Wind speed distribution and bivariant distribution for a) Berovo, b) Mogila, c) Sopište, d) Staro Nagoričane, e) Sv. Nikole

3. SMALL WIND TURBINES

The paper investigates the technical and economic feasibility of four small wind turbines at five measuring locations. The small wind turbines have rated power of 3, 4, 30, and 50 kW. Technical data and power curve data for each wind turbine are given in Table 2 [10]. The selection of these SWT is based on the following factors: i) commercial availability, ii) online available information for installation and operating costs, iii) examining different types of turbines (VAWT and HAWT) and iv) covering the widest possible range of installed power per SWT.

Table 2

SWT technical data and power curve [10]

SWT type/ Technical data	Type 1: Uge-4k (Urban Green Energy – UK) VAWT	Type 2: Skyline sl-30 (En-Eco Italy) HAWT	Type 3: Hz 30 k (Ge shandong – China) HAWT	Type 4: Redriven 50 kW (Redriven – Canada) HAWT
Nominal power (kW)	4	3	30	50
Rotor diameter (m)	2.75	3	12	14.3
Height (m)	7.5	8	18	36
Investment cost (EUR/kW)	3,561.00	3,218.00	2,764.00	3,259.00
Investment cost (EUR)	14,244.00	9,654.00	82,920.00	162,950.00

The prices of the turbines are given in the same table, expressed in euros per kW ([EUR/kW) and in euros. The net price of the turbines includes purchase cost and installation cost. Under installation cost the following cost are considered: building/foundation material cost; installation cost-crane rental, purchase of the equipment's used by the installation team; engineering cost-feasibility study; land purchase cost-circular area of the same radius is assumed necessary; grid connection cost, i.e. cables, power unit and control system and license fees [11].

From this data, we can see that the third type of SWT model is the cheapest (2.764 EUR/kW) and the first type which is VAWT is the most expensive, with 3.561 EUR/kW (Figure 4).

Figure 5 presents the energy characteristics of the analyzed SWTs as a power output curve, which shows the relationship between the wind speed captured by the rotor and its electrical output. The power curve allows the amount of electricity generated by the turbine to be estimated and is an essential component of wind turbine performance assessment [12]. When the detailed characteristics of wind conditions in a given location are known, the annual electricity production of a turbine can be forecast very accurately on the basis of the power curve, and the economic viability of the investment can be assessed [13].

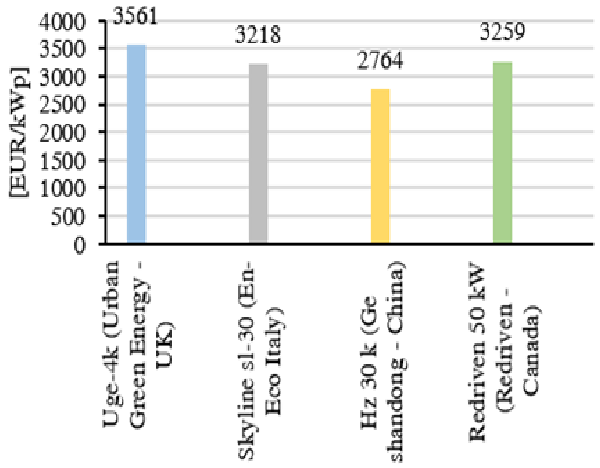

Fig. 4. Investment costs (EUR/kW) referred to each turbine model

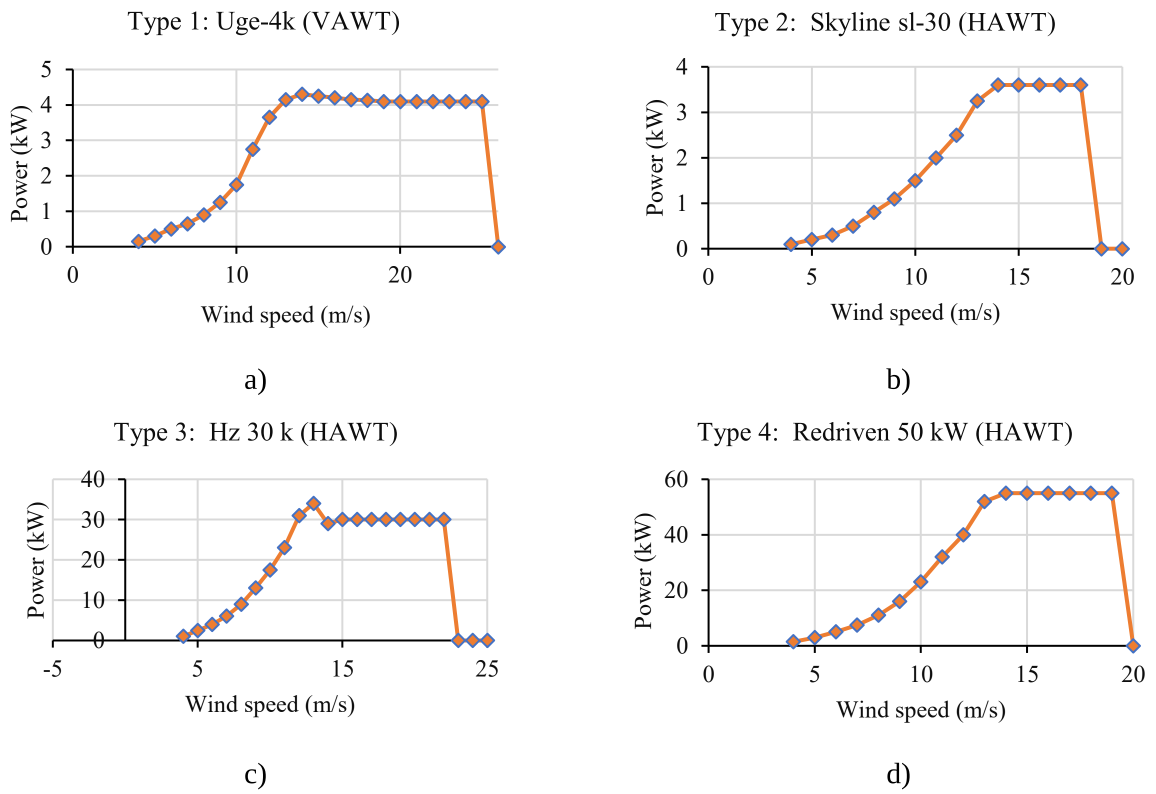

Fig. 5. Power curves for four examined SWT [10]

4. ECONOMIC ANALYSIS

The annual energy production (*AEP*) was calculated for each surveyed year for each location based on the wind characteristics, namely individual wind speeds and their frequency in a given period, and parameters from the turbine power curves for specific wind speeds. The *AEP* is calculated by successively multiplying the power for each wind speed from the turbine power curve by the measured wind frequency distribution and the number of hours per year [14]. For calculating the *AEP*, a fixed operating period was assumed, i.e., periods out of operation (e.g., due to repair and maintenance of equipment) were not considered. The results are summarized in Table 3 and in Figure 6 Capacity Factors (*CFs*) for each SWT are illustrated for easier comparison.

T a b l e 3

Calculated annual energy production and cost of energy from each SWT

Type : 1Uge-4k (Urban Green Energy – UK)	AEP (kWh)	CF (%)	COE (EUR/kWh)
Berovo	1,989.67	5.68	0.74
Mogila	1,965.61	5.61	0.75
Sopište	2,797.07	7.98	0.52
Staro Nagoričane	9,703.87	27.69	0.15
Sv. Nikole	4,731.50	13.50	0.29
Type 2: Skyline sl-30 (En-Eco Italy)	AEP (kWh)	CF (%)	COE (EUR/kWh)
Berovo	1,460.59	5.56	0.68
Mogila	1,412.45	5.37	0.70
Sopište	2,128.34	8.10	0.47
St. Nagoričane	7,507.10	28.57	0.13
Sv. Nikole	3,631.12	13.82	0.25
Type 3: Hz 30 k (Ge shandong – China)	AEP (kWh)	CF (%)	COE (EUR/kWh)
Berovo	17,296.00	6.58	0.49
Mogila	16,817.86	6.40	0.51
Sopište	24,305.30	9.25	0.35
St. Nagoričane	82,452.12	31.37	0.10
Sv. Nikole	41,499.90	15.79	0.21
Type 4: Redriven 50 kW (Redriven – Canada)	AEP (kWh)	CF (%)	COE (EUR/kWh)
Berovo	35,928.32	8.20	0.47
Mogila	35,431.93	8.09	0.47
Sopište	47,639.93	10.88	0.35
St. Nagoričane	146,578.77	33.47	0.11
Sv. Nikole	76,504.66	17.47	0.20

The main object of the analysis is the distribution of wind speeds over the year. On its basis, the time of occurrence of winds with specific speeds during the year and, consequently, the energy production of a wind power plant is estimated. It is clear, that at St. Nagoričane the highest *CF* values were calculated for all four types of STWs, above 27%. Data calculated for this location was not intended to be compared to other, less windy locations. Next is Sv. Nikole with calculated *CF*s above 13.5%. At Sopište location generally the *CF* is 2% higher, compared to Berovo and Mogila.

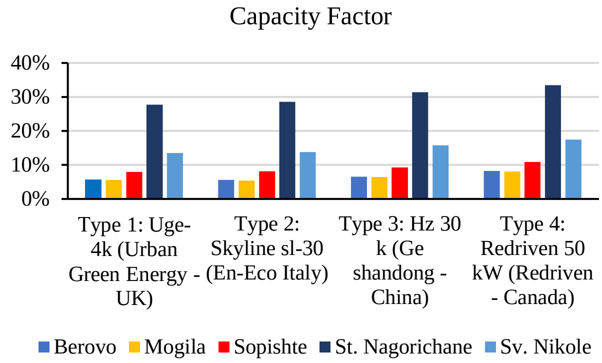

Fig. 6. Calculated *CF* [%] for each SWT at the tested locations

If we analyze the SWT models, it is clear that the first type, which is VAWT has the lowest *CF*s, and the fourth type of SWT – Redriven 50 kW, has the highest *CF*s at each location. This can be result of the lowest cut in speed, since this SWT starts producing electricity at 3 m/s, compared to the other three SWTs that start producing electricity above 4 m/s, as is shown in Table 2.

In the next step, a number of calculations were performed for which the cost of electricity in Macedonia was required. For evaluating the energy savings which can result from using different technologies for on-grid systems, the reference figure is household energy purchasing price [15]. The data was taken from the State Statistical Office: the average retail electricity price in 2022 for households was 6.486 MKD/kWh, which is 0.105 EUR/kWh [16], price quoted includes all taxes and fees. The general layout of grid-connected small wind turbine is in Figure 7.

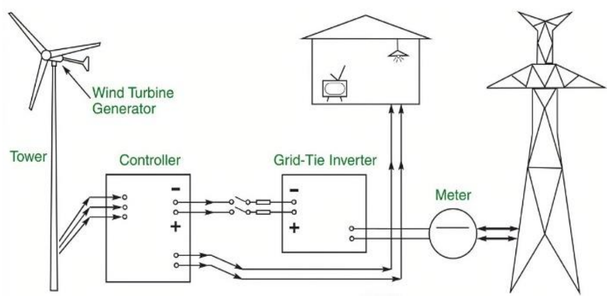

Fig. 7. Layout of on-grid wind turbine system [17]

This type of system is implemented for diminishing the energy bill of a residence. The small wind turbine is connected to the power grid via a dedicated inverter which maximizes the power transfer, via MPPT algorithm or predefined power curve.

In Macedonia, prosumers generating electricity for their own use sell excess produced energy to the grid, necessitating the use of two different electricity prices in the calculations. The price of the produced electricity that the supplier takes from the prosumer is determined in a manner that is established according to the Rulebook for renewable energy sources in the country:

$$c = PCE \cdot \frac{E_i}{E_p}, \quad (1)$$

if quantity of produced electricity E_p is higher of the consumed electricity E_i. In case when consumed electricity E_i is equal to or greater than the electricity produced E_p, then:

$$c = PCE \cdot 0.9. \quad (2)$$

PCE is the average price of electricity that the prosumer pays to the supplier for the purchased electricity, without compensation for using the network, other fees and taxes within a calculation period [18].

According to the State Statistical Office, the average monthly household electricity consumption was 410 kWh in Macedonia in 2022. This value was used with the average retail electricity price to calculate the price of 1.0 kWh for households. The investment costs for each SWT type are shown in Table 2. The cost of energy (*COE*) was also calculated for each considered case. *COE* is a metric used to assess the costs of electricity generation [19]. For one year of turbine operation, the formula for *COE* is as follows:

$$COE = \frac{CRF \cdot I}{AEP} + \frac{TO\&M}{AEP} \text{ (EUR/kWh)} \quad (3)$$

where:

I is investment wind turbine costs (EUR),

AEP is annual energy production (kWh),

TO&M is total yearly operation and maintenance costs (EUR) (estimated 0.015 EUR/kWh over the entire lifetime of the SWT [20, 21]), and

CRF is the capital recovery factor. CRF is the yearly interest [%/year], which depends on interest rate i = 6% and economic lifetime n = 15 years. The results of the calculations are shown in Table 3.

Furthermore, the return of investment in the form of payback time (SPBT) was calculated for each scenario, as follows:

$$Paybacktime = \frac{Investment\ cost}{Average\ animal\ cash\ flow} \text{ (years)}. \quad (4)$$

The result is the time (in years) after which the amount of money saved from the use of a small wind turbine will exceed the amount of funds invested in the project. To assess economic efficiency, appropriate calculations were used to determine whether the investment is profitable and after what period of use the wind power plant will start to generate profit.

If the *COE* values form Figure 8 are analyzed, it can be concluded that payback time for Berovo, Mogila and Sopište location are very pessimistic, which will be discussed more thoroughly in the next section.

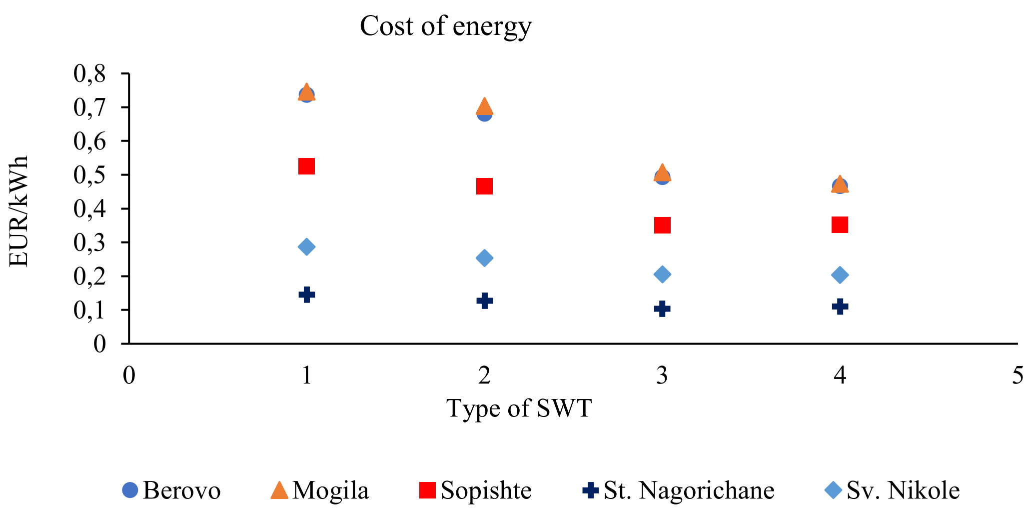

Fig. 8. Unit cost of energy production for each SWT at the tested locations

5. RESULTS AND DISCUSSION

When choosing to invest in an alternative source of energy for a household, the most important consideration is the economic aspect. The most desirable outcome is return of investment followed by the time after which the investment will start to yield a profit. By one Amendment in the Rulebook of RES, by the Macedonian Ministry of Economy, it is assumed an average rate of return on prosumer PV installations of 5 – 6 years. The initial idea for writing this paper was not to compare the profitability of different alternative sources, but to examine the sustainability and cost-effectiveness of SWTs for currently available commercial models.

Knowing the wind conditions at all sites, the motivation was to investigate the feasibility of SWTs at the first three sites (Berovo, Mogila and Sopište). While performing the analyses for annual energy production, then *COE* and at the end the payback time it was suggestively asserted that the same calculations should be performed for locations with better windiness, as Sv. Nikole and St. Nagoričane. Although it is known in advance that St. Nagoričane location is also eligible for the exploitation of wind energy from large scale wind farms.

The results of the simulations of energy production at the five selected locations for the period 2012–2014 are shown in Table 3, accompanied by *CF*s values. Based on the calculated total energy produced, location St. Nagoričane is the most effective location, with more than three times greater energy production compared with either of the other locations. *CF* provides information about the performance of the turbine and the utilization of its potential under the given conditions. The value obtained for Sv. Nikole is good, but *CF*s for St. Nagoričane are optimal and indicate relatively good adaptation of all four types of SWTs to the wind conditions. However, for the first three locations, the indicator reached a very low level and it can be concluded that none of the selected turbines are suitable for use under these conditions.

Figure 8 shows the trends in the costs of electricity generation at the five analyzed locations. Costs vary greatly depending on the location of the SWT, and location 4 is clearly the most cost-effective. Comparing the four types of SWT, slightly lower cost are calculated for type 4 – Redriven 50 kW (0.11–0.47 EUR/kWh), compared to type 3 – Hz 30 k (0.1–0.51 EUR/kWh). The cost is the lowest at St. Nagoričane for the analyzed period, with an average cost of 0.1225 EUR/kWh, in contrast to average costs of 0.24 EUR/kWh at Sv. Nikole. Average value of *COE* for Berovo, Mogila and Sopište are 0.6; 0.607 and 0.42 EUR/kWh, respectively. The analysis shows that Mogila is the most expensive – this can already be deduced from the value of the *AEP* index, which is the lowest at all four types of SWT. The cost calculations show the same for all locations, so if the least amount of electricity was produced during the year, the highest cost of electricity generation per kWh is gained.

A wide range of investment payback periods is obtained, highlighting the importance of a proper, in-depth analysis of location in the preliminary design of SWT installations and before the start of the investment. In the Rulebook for renewable energy sources for North Macedonia, it is clearly noted that a facility for the production of electricity from a renewable energy source can be build, since it uses the electricity produced for its own consumption, and the surplus of the electricity produced is handed over to the electricity distribution network only if:

i) the installed power of the facility should not exceed 6 kW, for household use,

ii) the installed power of the facility should not be greater than 40 kW, for a small budget company.

Due to these limitations, for the SWT type 3 and type 4 (with installed power of 30 kW and 50 kW, respectively) in the calculations, very small, almost none money returns are obtained from the delivered electricity (Eq. 1), so the calculated payback time is over 95 years. The best result was obtained for SWT type 2 (Skyline sl-30.3 kW) which is 15.99 years for the payback period, certainly at St. Nagoričane location.

If the profit was the main objective, the installation of a SWT is not the best option for households. Maybe it is reasonable to analyze the operation of the SWT under isolated conditions from the power grid, when it is unprofitable and unreasonable to connect a particular facility to the grid.

Another option can be a turbine with a shrouded rotor (diffuser). Despite extensive study, shrouded turbines are not yet widely used due to their complexity and high design and manufacturing costs. The diffuser acts as a wind gathering and accelerating device, allowing the turbine to achieve higher aerodynamic efficiency than allowed by the Betz limit [22].

6. CONCLUSION

The basic knowledge necessary for deciding to invest in a wind turbine in a given area is local wind energy resources. The results of the present paper emphasize the potential for large differences in average annual speed among measurement points and hence the importance of measurement of wind characteristics for decision-making. Wind potential clearly differs among the selected five locations and therefore consequently the per unit cost of electricity follows these differences.

Based on the results of this analysis, the following conclusions can be withdrawn:

i) The wind characteristics in the analyzed locations Berovo, Mogila and Sopište have a similar windiness trend, so we analyze them in one separate group. Sv. Nikole has slightly better wind regimes, but undoubtedly St. Nagoričane has the most desired wind regimes.

ii) The per unit cost of electricity generation is clearly different in each „group". This proves the necessity of thorough verification of the surroundings before investing in a SWT.

iii) The most favorable location for SWT installation from analyzed five locations is St. Nagoričane location.

iv) The conducted analysis gives an overview of the costs of wind resources in different parts of the country, but it is not truly complete as the authors did not have all the required data for calculations, and therefore they partly used assumptions from the literature.

v) Current SWTs are promising solutions for use in sparsely populated areas where there is no access to electricity from the distribution grid.

vi) The addition to SWTs of equipment such as diffusers to tunnel the rotor could increase SWT efficiency and promote further growth of the wind energy industry. Rotor tunnelling can also ensure efficient wind turbine operation, even in areas with less than ideal wind conditions.

REFERENCES

[1] Statista (2023): Cumulative installed wind power capacity worldwide from 2001 to 2022. Available*: Global installed wind energy capacity 2022 | Statista*. Online-release date: March 2023 [Accessed 05.07.2023]

[2] International Energy Agency (2022): Wind Electricity – Technology deep dive. Available: *Wind Electricity – Analysis – IEA*. Online release date: September 2022. [Accessed 05.07.2023]

[3] Македонска академија на науки и уметностите (2010): *Стратегија за искористувањето на обновливите извори на енергија во Република Македонија до 2020 година*, Скопје, Јуни 2010.

[4] Министерство за економија на Р. Македонија (2010): *Стратегија за развој на енергетиката во Република Македонија до 2030 година*, Скопје, 2010.

[5] Celeska, M., Najdenkoski, K., Dimchev, V., Stoilkov, V. (October, 2018): Modeling the arrangement of turbines for onshore wind power plants under varying wind conditions, In: *17th Wind Integration Workshop*, Stockholm, Sweden.

[6] International Electrotechnical Commission (2013): *Wind Turbines.* Part 2*: Small Wind Turbines*, Geneva, Switzerland.

[7] Wind Europe, Report: *Wind energy in Eurpoe – Statistics and outlooks for 2023–2027,* Online-release date: 28. 02. 2023

[81] Statista (2019): Available: *Capacity of small wind turbines worldwide 2018* | Online-release date: 6 Sepmetber 2019. [Accessed 15.06.2023]

[9] Факултет за електротехника и информациски технологии (2016): *Збирен извештај за втората мерна кампања за ветер во Република Македонија*, Скопје, април 2016.

[10] Bortolini, M., Gamberi, M., Graziani, A., Manzini, R., Pilati, F. (2013): Performance and viability analysis of small wind turbines in the EU, *Renewable Energy*, Vol. **62**, pp. 629–639.

[11] Karczewski, M., Sobczak, K., Lipian, M., Jozwik, K. (2018): Numerical and experimental tools for small wind turbine load analysis, *Structural Control and Fault Detection of Wind Turbine Systems*, pp. 45–79.

[12] Celeska, M., Najdenkoski, K., Dimchev, V., Stoilkov, V. (2017): Equivalent wind farm power curve estimation, *Journal of Electrical Engineering and Information Technologies*, Vol. **2**, No. 2, pp. 105–111, ISSN 2545–4269.

[13] Tummala, A., Kishore Velamati, R., Kumar Sinha, D., Indraja, V., Krishnam H. (2015): A review on small scale wind turbines, *Renewable and Sustainable Energy Reviews*, Vol. **56**, pp. 1351–1371.

[14] Saint-Drenan, Y., Besseau, R., Jansen, M., Staffell, I., Troccoli, A., Dubus, L., Schmidt, J., Gruber, K., Simões, S., Heier, S. (2020): A parametric model for wind turbine power curves incorporating environmental conditions, *Renewable Energy*, Vol. **157**, pp. 754–768.

[15] Predescu, M. (2016): Economic evaluation of small wind turbines and hybrid systems for residential use: The case of Romania, *Revista Brasileria de Planejamento e Desevovlvimento*, Vol. **5**, No. 2, pp. 185–197, ISSN 2317-2363.

[16] State Statistical Office of North Macedonia (2023): *Electrical energy and natural gas prices*, report. Available: Државен завод за статистика: Цени на електрична енергија и природен гас, второ полугодие од 2022 година *(stat.gov.mk)*. Online-released date: 30 March 2023. [Accessed 29.06.2023]

[17] WindEnergy7 (2008): *Understand Net Metering for Home Wind Turbines and Solar*. Available: http://windenergy7.com/turbines/wind-energy/understanding-net-metering-for-sma ll-wind-turbines/. Online release date: September 2008. [Accessed 30.10.2023]

[18] Ministry of Economy of North Macedonia (2019): *Rulebook for renewable energy sources*, Online-release date 30 May 2019.

[19] Zalewska, J., Damaziak, K., Malachowski, J. (2021): An energy efficiency estimation procedure for small wind turbines at chosen locations in Poland, *Energies MDPI*, 21.06.2021.

[20] Bussel, G. (2013*): Electricity Generation with Small Wind Turbines*. New York, USA, Springer, pp. 696–727.

[21] Rao, K. R. (2019): *Wind Energy Economics in Wind Energy for Power Generation*. Cham, Switzerland, Springer, pp. 427–701.

[22] Lipian, M., Dobrev, I., Karczewski, M., Massouh, F., Jozwik, K. (2019): Small wind turbine augmentation: experimental investigations of shrouded- and twin-rotor wind turbine systems, *Energy*, Vol. **186**, No. 115855.

Journal of Electrical Engineering and Information Technologies, Vol. **8,** No. 2, pp.57–67 (2023)
Article 207
In print: ISSN 2545–4250
Received: April 4, 2023
On line: ISSN 2545–4269
Accepted: May 6, 2023
UDC: 621.311:342(497.7:4-672EU)
https://doi.org/10.51466/JEEIT2382207057km

Original scientific paper

GAP ANALYSES BETWEEN THE LEGISLATIVE FRAMEWORK OF THE ELECTRICITY SECTOR IN THE REPUBLIC OF NORTH MACEDONIA AND THE EUROPEAN LEGISLATION

Aleksandra Krkoleva Mateska[1], Vesna Borozan[1], Petar Krstevski[1], Rubin Taleski[1], Stefan Borozan[1,2]

[1]*Faculty of Electrical Engineering and Information Technologies, "Ss. Cyril and Methodius" University in Skopje, Rugjer Bošković bb, P.O.Box 574, 1001 Skopje, Republic of North Macedonia*
[2]*Imperial College London, Department of Electrical and Electronic Engineering*
krkoleva@feit.ukim.edu.mk

A b s t r a c t: This paper conducts a comprehensive evaluation of the ongoing development of legislation within North Macedonia's electricity sector when compared against the corresponding legal framework of the European Union (EU). Specifically, the initial overview promptly identifies North Macedonia's strategic alignment within the EU's political sphere and emphasizes the imperative need for consistent harmonization of national laws. Moreover, it becomes evident that achieving full EU harmonization in the electricity sector necessitates cooperation and the fulfilment of obligations stipulated in the Energy Community (EnC) Treaty. This treaty holds particular significance for North Macedonia as it stands as the country's legally binding agreement with the EU. Hence, monitoring the consistent fulfilment of the treaty requirements, along with assessing the stance adopted by competent institutions and the perceptions of professionals and the broader public in North Macedonia, portrays an overall image of the nation's readiness and commitment to the reform process in preparation for EU accession. Furthermore, given the dynamic nature of EU energy law evolution, especially amid the current tumultuous state of energy crises, EnC Contracting Parties consistently lag in the transposition and implementation of these laws. This paper delineates the imminent pending obligations that North Macedonia must address within this ongoing process.

Key words; electricity legal framework; national law harmonization; gap analysis

АНАЛИЗА НА ПРАВНАТА РАМКА НА ЕЛЕКТРОЕНЕРГЕТСКИОТ СЕКТОР ВО РЕПУБЛИКА СЕВЕРНА МАКЕДОНИЈА ВО СПОРЕДБА СО ПРАВОТО НА ЕВРОПСКАТА УНИЈА

А п с т р а к т: Овој труд прикажува критичка анализа на сегашниот развој на правната рамка во електроенергетскиот сектор на Република Северна Македонија во споредба со соодветната рамка во Европската Унија (ЕУ). Во рамките на трудот е претставена потребата од соодветно усогласување на националното право со правото на ЕУ, што всушност треба да се постигне преку соработка и исполнување на обврските преземени со Договорот за Енергетска заедница (ЕнЗ). Овој договор е значаен и поради фактот што тој е прв законски обврзувачки договор кој Северна Македонија го има склучено со ЕУ. Затоа навременото исполнување на обврските, како и целокупниот однос на надлежните институции, стручната и пошироката јавност кон овој договор, ја проектира сликата на подготвеноста и сериозноста на реформите во процесот на пристапување на нашата држава кон ЕУ. Имајќи ја предвид динамиката на развој на законодавството на ЕУ, особено во тековното турбулентно време на енергетска криза, договорните страни на ЕнЗ секогаш доцнат при транспозицијата и имплементацијата на правото на ЕнЗ. Овој труд ги идентификува постигнувањата, но и неминовните заостанати обврски на Северна Македонија во тој процес.

Клучни зборови: правна рамка на електроенергетскиот сектор; хармонизација на националното право; споредбена анализа

1. INTRODUCTION

The implementation of energy sector reforms under the EnC legislation serves as more than just a prerequisite for aligning with EU Law. These reforms constitute a comprehensive undertaking aimed at fostering the establishment of a cost-effective and sustainable energy system. This process stands as a crucial component of North Macedonia's preparations for EU accession and, more broadly, for the nation's economic advancement. Namely, as a contracting party of the EnC, North Macedonia has the obligation to harmonize its legislation with the EnC acquis, which requires adoption, harmonization and implementation of legislation in the fields of energy, competition, renewable energy sources (RES), energy efficiency, oil and gas, statistics, infrastructure, environment and climate. The process, which started in 2005, aimed to prepare the contracting parties for the EU accession requirements and to support the transformation of the vital sectors. At present, the aims of the process have broadened and comprise support of the energy transition process and decarbonisation of the economy.

This paper is divided into two parts. The first part offers a concise examination of EU and EnC Law concerning electricity markets. It is utilized to conduct a comparative analysis between national legislation and the EnC's target regulations. The results of the comparative analyses are presented in the latter part of this paper. This analysis stems from extensive research into North Macedonia's electricity sector legislation, as previously published in the authors' works [1] and [2].

The primary objective of this paper is to present a brief update on the current status of the electricity related legislation in North Macedonia, augmenting the information outlined in [1] and [1], while also providing a comparison of achievements against both EnC and EU objectives. This comprehensive overview of the current situation and objectives establishes the foundation for ongoing monitoring of legislative changes in relevant domains. Additionally, it offers an assessment of the country's progress toward meeting the objectives stipulated in the EnC Treaty.

2. ELECTRICITY MARKET LEGISLATION AT EUROPEAN LEVEL

Until recently, the EU's electricity sector operated under the framework of the Third Legislative Package for Electricity and Gas Markets (Third Package). However, this package lacked defining and enabling the utilization of innovative flexible technologies and numerous emerging concepts related to power system operations and power market dynamics. Subsequently, legislative advancements have occurred, primarily through the introduction of the Clean Energy for all Europeans Package (CEP). This newer legislation has eliminated certain obstacles hindering advanced technologies and has recognized various innovative concepts associated with electricity markets, as well as the security, operation, and management of power systems.

Nonetheless, the process of reforming legislation remains ongoing, and there are several crucial regulations that need development and adoption to fully implement the concepts advocated within the CEP.

A. *Clean energy for all Europeans package*

CEP was adopted in 2019 and its primary goal is to aid the decarbonization of EU's energy system, considering the mandatory climate targets by 2030. These targets are introduced in the Governance Regulation of the Energy Union and Climate Action (Governance Regulation) [3], which is one of the acts comprising CEP.

In addition to the Governance Regulation, the following acts, which may conditionally be classified as follows, legal acts that comprise CEP can be conditionally classified in two groups based on their dominant contribution to the priority measures:

- Climate targets of the Energy Union (energy efficiency and renewable energy):
  - Directive (EU) 2018/844 on the energy performance of buildings,
  - Directive (EU) 2018/2001 on the promotion of the use of energy from renewable sources (recast) (RED II), and
  - Directive (EU) 2018/2002 on energy efficiency.
- Electricity market and security of supply:
  - Directive (EU) 2019/944 on common rules for the internal market for electricity (recast) (IEM-Directive),
  - Regulation (EU) 2019/943 on the internal electricity market (recast) (IEM-Regulation).
  - Regulation (EU) 2019/941 on risk-preparedness in the electricity sector (Risk Regulation), and

- Regulation (EU) 2019/942 on the establishment of the Agency for Cooperation of Energy Regulators (ACER) (recast).

In the following subsections a short description of the novelties introduced by the legal acts that create the electricity market legislation is given.

1) *Renewables directive*

The RED II [4] introduces the following three key concepts for the first time:

- Enabling self-consumption, i.e. enabling end users or customers to generate electricity from RES for their own consumption and allowing them to store and sell surplus electricity.
- Establishment of renewable energy cooperatives.

Implementation of new or redefined criteria concerning sustainability and reductions in greenhouse gas emissions from individual biofuels, bioliquids, or biomass fuels.

In addition to these concepts, RED II sets a new obligatory target for the EU to achieve 32% RES in energy consumption by 2030. It includes a review clause scheduled for 2023, aimed at potentially increasing the EU-level target. The directive aims to enhance the structure and stability of RES Support Schemes, simplify administrative processes, and create a clear and steady regulatory framework for self-consumption of RES.

Furthermore, RED II raises the bar for the integration of RES in transportation and heating/cooling sectors, fostering collaboration among EU Member States (MSs) and non-EU countries. It encourages joint efforts to achieve the RES target through mechanisms such as statistical renewable energy transfers, collaborative RES projects, and unified Support Schemes for RES.

The adoption of the Fit for 55 package required significant alterations to the existing EU energy legislation, aiming to incorporate a higher RES share within the energy composition of both the European Union and its Member States (MSs). This initiative also called for a revision of RED II. Consequently, in July 2021, concurrent with the adoption of Fit for 55, the European Commission (EC) puts forth a proposed amendment to RED II [4]. The EC's proposal for the revised RED II aims to achieve a twofold increase in the share of RES in the energy mix by 2030, accomplished by elevating the mandatory EU minimum RES share in final energy consumption to 40%. To accomplish this goal, a comprehensive framework for the deployment of RES across all sectors of the economy is set to be initiated and reinforced by sector-specific targets at both the EU and national levels.

Among the provisions of the revised RED II is the obligation to create a credit mechanism incentivizing renewable energy consumption in transport, facilitating collective Power Purchase Agreements for RES generators, introducing a new EU-wide labelling methodology for industrial products manufactured using renewable energy, and establishing a pilot project to foster cross-border cooperation on renewables. The sustainability of biofuels has also been addressed, for instance through the creation of Support Schemes that align with the biomass cascading principle.

Amidst the Parliamentary process for the adoption of an updated RED II in July 2022, the Parliamentary Committee on Industry, Research, and Energy highlighted the necessity for additional adjustments to the legislative proposal. This was to ensure alignment with the objectives and targets outlined in the REPowerEU plan. The report presents several promising insights. Specifically, Member States (MSs) are urged to target a 5% increase in newly installed capacities for both storage technologies and innovative RES technologies. Additionally, they are mandated to develop a minimum of two cross-border RES projects by 2026. In October 2023, the Council adopted the updated Directive, with the new objectives to raise the share of renewable energy in the EU's overall energy consumption to 42.5% by 2030 with an additional 2.5% indicative top up to allow the target of 45% to be achieved.

2) *Electricity directive and electricity regulation*

The IEM-Directive [5] and IEM-Regulation [6] aim to introduce a new energy market design. This section of the CEP focuses on adapting the EU's internal electricity market model to address the demands posed by the energy transition. Its aims to enhance the connectivity and resilience of the market, while safeguarding it against power system failures. Furthermore, this segment of the CEP is designed to facilitate the incorporation of renewable electricity into the grid and to better cater to the diverse requirements of all consumers.

The acts introduce a definition of energy storage systems, acknowledging their significance as vital resources within power systems. They are crucial in enhancing flexibility to accommodate the increasing integration of renewable energy into the grid. Additionally, these acts acknowledge the emergence of citizen energy communities as a distinct category of collaboration among citizens or local stakeholders in the energy sector. The new market model is designed to incentivize consumers to actively participate and contribute to maintaining stability within the electricity system by leveraging their consumption flexibility. This flexibility encompasses practices like intelligent charging of electric vehicles and utilizing self-generated electricity. Moreover, these legislations significantly tackle issues related to customer protection, facilitating energy supply transitions, and addressing concerns regarding energy poverty.

The IEM-Regulation also introduces cyber security care as part of the tasks of ACER, the European Network of Transmission System Operators (ENTSO-E) and of the Association for the European Distribution System Operators (EU DSO Entity) and it imposes an establishment of a new Network Code on Cyber Security.

3) *Risk regulation*

Secure operation of power systems and functioning electricity markets are prerequisites for secure and continuous supply of electricity. But even when these conditions are expected to be met, there are factors that may influence or disrupt supply of electricity. These factors may be both natural and man-made. Their effects can be easily spread to neighbouring systems as power systems are interconnected infrastructures. The consequences of disruptions in supply may have regional impacts in economy, environment and social interactions.

The secure power system operation and efficient electricity markets are fundamental requirements for ensuring a continuous and secure electricity supply. However, despite meeting these conditions, various factors – both natural and human-induced – can influence or potentially disrupt the supply of electricity. Given the interconnected nature of power systems, the effects of these factors can swiftly propagate to neighbouring systems. Consequently, these disruptions can lead to regional impacts affecting the economy, environment, and social interactions.

The Risk Regulation [7] is a legal act from the CEP which focuses on the issue of secure supply of electricity. It sets a framework for cooperation among EU MSs in preventing, preparing for and managing large scale electricity crisis, as well as for monitoring the security of electricity supply in the EU. This regulation also considers the possible cooperation between EU MSs and EnC Contracting Parties in the area of secure electricity supply, which may include identification of electricity crisis scenarios, defining electricity crisis and establishment of risk-preparedness plans.

The Article 5 of the Risk Regulation [7] stipulates adoption of a Methodology for Identifying Regional Electricity Crisis Scenarios. The Methodology sets the framework for the transmission system operators (TSOs) to establish electricity crisis scenarios on regional level, based on common scenarios rating scales. Table 1 and Table 2 show the current scenario classification scales, which are elaborated in more detail in [8].

T a b l e 1

Six-step likelihood classification scale [8]

Classification	Events per year	1 × years	Description/example of initiating event
Very likely	≥ 0.5	2 or less	Event expected practically every year, e.g. winds/storms causing multiple failures of overhead lines may be expected nearly every year in some areas
Likely	0.2–0.5	2–5	Event expected once in a couple of years, e.g. heat wave causing limits on output of open-loop water-cooled power plants, low water levels at hydro plants, higher load, etc.
Possible	0.1–0.2	5–10	Event expected or taken into consideration as a potential threat, e.g. cyber or malicious attack
Unlikely	0.01–0.1	10–100	Rare event, e.g. simultaneous floods causing unavailability ofgeneration, distribution and transmission infrastructure
Very unlikely	0.001–0.01	100 – 1000	Vvery rare event, e.g. earthquake causing a huge destruction of transmission, distribution and generation infrastructure
Extremely unlikely	≤ 0.001	1000 or more	Not applicable, impossible, or extremely rare event, expected beyond 1 in 1000 years

Table 2

Five-step impact classification scale [8]

Classification	Expected energy not served% (of average annual consumption)	Loss of load expectations (hours)
Disastrous	≥0.25%	≥168
Critical	≥0.05% and <0.25%	≥48 and <168
Major	≥0.01% and <0.05%	≥12 and <48
Minor	≥0.002% and <0.01%	≥3 and <12
Insignificant	<0.002%	<3

At the beginning of December 2023, the second public consultation on this Methodology has finished. The consultation process aims to ensure that the Methodology, developed by ENTSO-E, is updated according to the latest information and developments. Such approach is required as the risk factors that influence the risk scenarios are continuously evolving.

B. *Network codes*

The electricity sectors in EU MSs are further governed by a set of regulations that are known as Network Codes (NCs). The existing Electricity NCs were adopted in the period 2015 – 2017 with the aim to unify power system operation and market rules across the EU for the purpose of creating a functional Internal Market for Electricity. This set of regulations formally belongs to the Third Package and comprises the following acts:

- Connection Codes

  High Voltage Direct Current Connections,

  Demand Connection Code (DCC), and

  Requirements for Generators (RfG).
- Market Codes

  Capacity Allocation & Congestion Management (CACM),

  Forward Capacity Allocation (FCA), and

  Electricity Balancing (EBGL).
- Operation Codes

  System Operations (SOGL), and

  Emergency and Restoration (ER).

The process of preparation of amendments to these NCs and their subsequent adoption to comply with the legislation introduced by CEP is ongoing within EU institutions.

1) *Forward capacity allocation*

The FCA [9] sets out regulations governing long-term markets, which enable market participants to mitigate future price risks within defined periods specified in forward contracts (such as weeks, months, quarters, or years). To facilitate cross-border electricity exchange, this regulation also establishes the rules for the forward allocation of both physical and financial transmission rights. However, the new stipulations outlined in CEP emphasize the imperative need for establishing a new EU Electricity Market Model. ACER's recent Policy Paper on the Further Development of the EU Electricity Forward Market [10] argues for revisions to the forward market in line with these developments.

2) *Capacity allocation and congestion management*

The CACM [11] forms the basis of the European single electricity market. It establishes methodologies for computing and allocating transmission capacities across the different market timeframes. Additionally, it defines regions for capacity calculations, bidding zones, and rules governing the operation of day-ahead and intraday electricity markets. CACM specifically emphasizes implicit coordinated capacity auctions and aims to standardize the operation of cross-border markets across Europe, fostering increased competitiveness and the integration of RES. The implementation of CACM has demonstrated significant progress in advancing both the EU's day-ahead and intraday electricity markets [12].

3) *Electricity balancing*

EBGL [13] promotes integration, coordination and harmonization of electricity balancing rules, thus facilitating the efficient use of available balancing resources and allowing new players such as demand response and renewables to participate in this market. This should help to increase security of supply, limit emissions and diminish costs to customers.

Namely, the objective of EBGL is to foster balancing market integration with the aim of reducing total costs and to increase social welfare while ensuring operational security. EBGL introduces a definition of the concept of “Balancing energy”, which should be provided by Balance Service Providers (BSPs). The TSOs can use this energy to balance the deviations between supply and demand in real-time. Balancing can be provided by a wide range of technologies, including small-scale, renewable, and conventional generation, energy storage and demand response. Therefore, one of the major impacts of the implementation of EBGL is that it provides opportunities for all potential sources of balancing, fostering competition and maximizing social welfare. The EBGL are guided by the notion that actions which are not explicitly forbidden, like participation or initiative for cooperation, are allowed.

The requirements of EBGL include establishment of balancing platforms for frequency containment, frequency replacement and reserve replacement, which are already operational and increase the number of participating TSOs, as presented on Fig. **1** below. These platforms have been developing in the last few years and the results of their implementation confirm the benefits of regional cooperation.

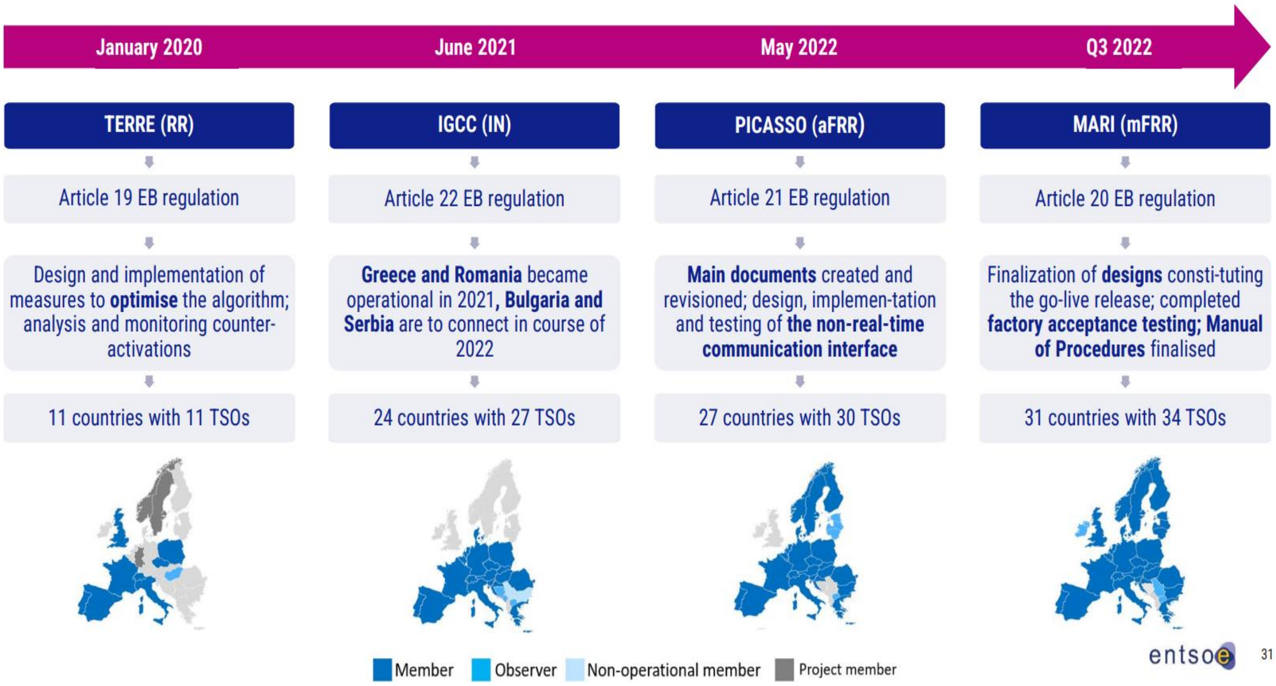

Fig. 1. Overview of balancing platforms development in Europe [14]

Balancing market design and arrangements cannot be fully decoupled from real time system operation. As a result, SOGL [15] is also relevant for the discussion of electricity balancing. The SOGL primarily addresses three aspects of balancing: the harmonisation of reserve categories, the activation strategy for balancing energy in real-time and the sizing of reserves.

4) *System operation*

SOGL [15] specifies TSO activities to manage secure operation of their electricity grid, considering the integration of RES and flexibility resources, as well as increased interconnections and cross-border competition. This regulation also introduces regional coordination a legal obligation for TSOs.

SOGL introduces provisions related to coordination and data exchange between TSOs, between TSOs and Distribution System Operators (DSOs), as well as between TSOs or DSOs and Significant Grid Users (SGUs), both during planning and close to real-time operations. This includes rules and responsibilities for the approval of Key Organization Requirements, Roles and Responsibilities (KORRR) relating to Data Exchange [16], the implementation of specific aspects of the data exchange, and the agreements on processes and format for data exchanges between key players.

5) *Emergency and restoration*

While SOGL refers to normal power system operation, ER [17] considers emergency operation of power systems. The ER [17] outlines the specific steps and protocols that TSOs must adhere to in the event of incidents within their grid. These procedures are designed to meet the highest standards and best practices for handling emergencies, blackouts, and the restoration of normal grid operations. ER establishes standardized requirements for TSOs to develop both the System Defence Plan and the Restoration Plan. The standardized approach ensures the effectiveness and coherence of these plans on a European scale. Moreover, ER aims to maintain the continuity of energy transactions during states of emergency, blackout, or restoration. It also defines the conditions [17] under which such transactions could be temporarily suspended.

6) *Connection codes*

RfG [18] prescribes the standards that generators have to meet in order to connect to the grid. The implementation of the RfG aims to boost the market participation of generation technology and increase competitiveness.

DCC [19] sets the requirements for grid connection of: i) transmission-connected demand facilities; ii) transmission-connected distribution facilities; iii) distribution systems, including closed distribution systems; iv) demand units, used by a demand facility or a closed distribution system to provide demand response services to relevant system operators and relevant TSOs. DCC introduces obligations for system operators to make appropriate use of the demand facilities' and distribution systems' capabilities in a transparent and non-discriminatory manner.

C. *Legal framework of the Energy Community*

In general, the implementation level of the EU energy and environmental law in the Energy Community Contracting Parties is limited to the documents of the EU Third Package for Electricity and Gas Markets. However, the activities to introduce new acts in EnC Law, which are related to the CEP package, have already started.

The first step towards alignment with the current EU law in the related areas was done at the 19th EnC Ministerial Council of 30 November 2021 [20], when the first set of CEP documents and commitments was adopted in the EnC Law. This set covers legislation in the areas of governance, energy efficiency, renewables, electricity market design, and security of supply rules. The alignment with the current EU law continued with the Decision of the 20th EnC Ministerial Council of 15 December 2022 [20] and the adopting additional set of CEP related documents. The most important development for the SEE Electricity Market happened on the same Ministerial Council [20] by adoption, based on the previous long-lasting negotiation and adaptation process with the EC, of the Market and System Operation NCs deriving from the Third Package for Electricity and Gas Markets. The adoption of the Market and System Operation NCs has become a reality after incorporating a new reciprocity mechanism within the EnC Treaty, which makes possible market couplings between EU MSs and EnC Contracting Parties. Finally, the renewables, energy efficiency and greenhouse gas reduction targets for 2030 were adopted at the Ministerial Council in December 2022, following the finalization of a study by the European Commission.

Table 3

EnC – Obligations for contracting parties [21]

Act from	Name of document	Deadline for transposition
CEP	Governance Regulation	31 December 2021
	RED II	31 December 2022
	Directive (EU) 2018/2002 on energy efficiency	31 December 2022
	IEM-Directive	31 December 2023
	IEM-Regulation	31 December 2024
	Risk Regulation	31 December 2024
	Regulation (EU) 2019/942 on the establishment of the ACER (recast)	31 December 2024
NCs	FCA	1 January2024
	CACM	1 January 2024
	EBGL	1 January 2024
	SOGL	1 January 2024
	ER	1 January 2024

It is noteworthy to observe that the EU is already in the process of updating some of the legislative acts comprising CEP with the aim of increasing the targets and objectives related to RES use, energy efficiency and greenhouse gas emissions.

3. IMPLEMENTATION OF ELECTRICITY MARKET LEGISLATION IN NORTH MACEDONIA

The content found in references [1] and [2] clearly shows that the Energy Law [22] serves as the foundation for executing a strong reform base to align EU Law within North Macedonia's electricity sector. By enacting this law and accompanying secondary regulations, the country can be considered among EnC Contracting Parties that have successfully integrated the Third Package into their national legislation.

This section presents an overview of the most relevant bylaws and other documents which set the legislative will in the area related to the electricity market. As an update to the situation presented in [1] and [2], this paper highlights the main achievements in the past three to four years. Hence, it considers the implemented actions aimed to further harmonise the provisions of the Energy Law [22] and to prepare for full implementation of the NCs. It is important to note that since the first half of 2023, a new Energy Law is under preparation. This Law should transpose the requested CEP documents from the EnC Law. As presented in the section 2, subsection C, the implementation deadlines for all these legal acts are in the near future.

Fig. **2** presents part of the legislative acts adopted or approved by relevant institutions, which enable the most significant reform achievements related to the implementation of European legislation.

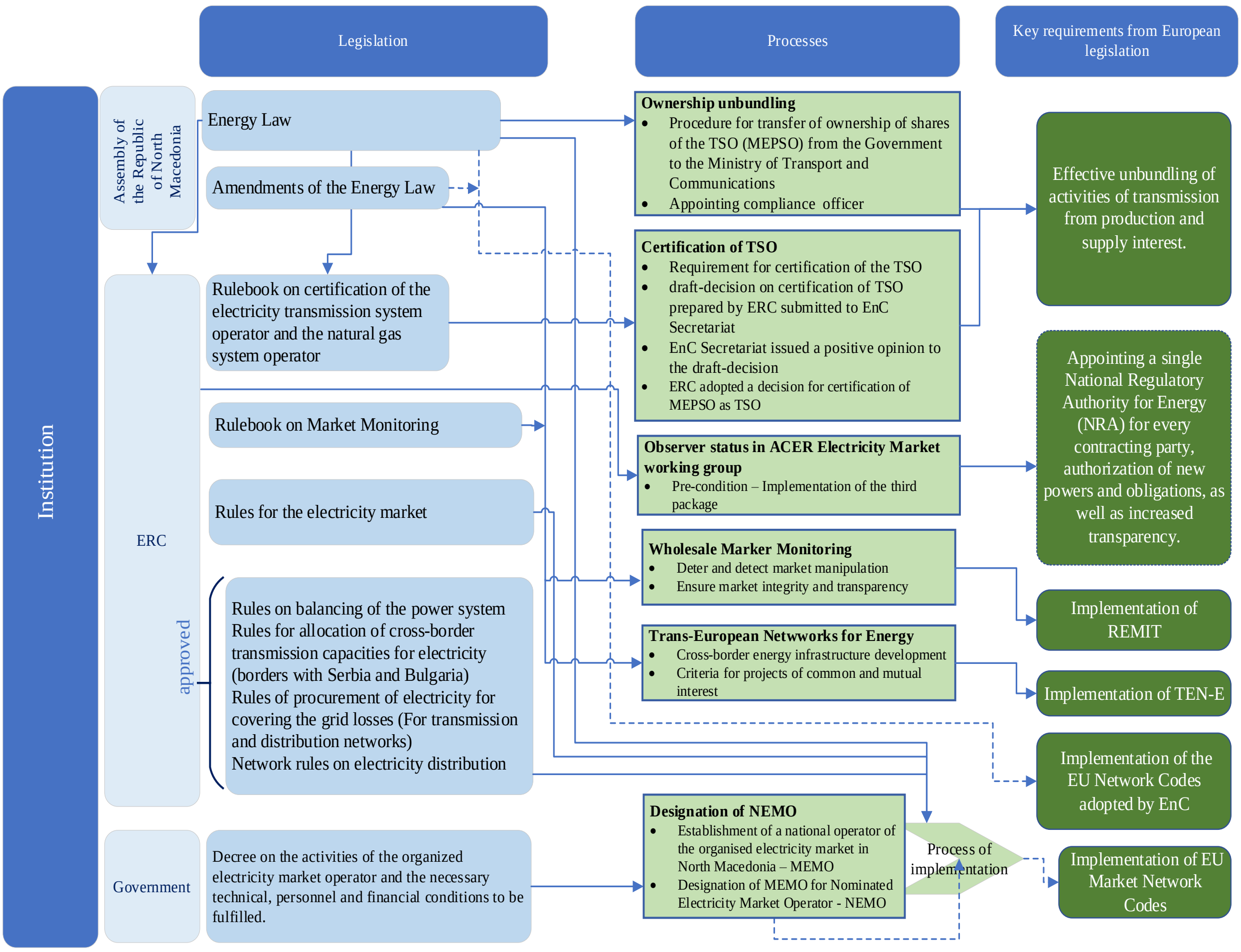

Fig. 2. Overview of the key achievements from the implementation of EnC legislation

One of the key requirements from the Third Package was met by implementation of the Energy Law and completing the process of ownership unbundling of the TSO – MEPSO. Shortly after, another obligation was completed, i.e., the certification process of MEPSO as a TSO was concluded successfully. The implementation of the Energy Law extended the competences of the Energy and

Water Services Regulatory Commission of the Republic of North Macedonia (ERC). As a result, ERC could apply for membership in the working bodies of ACER which is an essential aspect for further development of the work of the national regulatory body. At present, ERC has a status of observer in the ACER's Electricity Working Group. An important contribution to achieving this status was the complete implementation of the EU REMIT Regulation [23] after adequately amending Energy Law [22] and adopting the new Rulebook on Market Monitoring [24]. By the last amendments to the Energy Law [22], the EU TEN-E Regulation [25] was transposed to the national legislation, thus achieving one more milestone on the way to EU harmonization. All these achievements are acknowledged by the last EnC Secretariat Annual Implementation Report 2022, [26].

Fig. **2** presents another essential step for the process of implementation of Market NCs, i.e. the establishment of a National Operator of the organized electricity market in North Macedonia – MEMO. Furthermore, in September 2020, by a government decision, MEMO was designated as the Nominated Electricity Market Operator (NEMO), in line with the Market NCs of the EU. The completion of these actions, which are considered as outstanding achievements, made our country the first of the EnC Contracting Parties to have implemented such a decision. Within this period, MEMO undertook a number of activities for the establishment of the first organized electricity market (the Day-ahead and Intraday market) in North Macedonia, and for its coupling with neighbouring markets into a single electricity market of the EU. On a session held on 6th of April 2023, the ERC adopted a Decision to approve the Rules for Operation of the organized electricity market. This has led to the first live Day-ahead auctions, which were held on 10th of May 2023 [27]. The establishment of the organized Day-ahead market operated by MEMO is a key step towards achieving the European Electricity Market Target Model and further market coupling with neighbouring markets.

As per the evaluation conducted on the implementation of EnC legislation in North Macedonia [26], it is estimated that the collective efforts made to implement the Energy Law [22] and create and endorse secondary regulations, primarily driven by the expertise of the ERC, have resulted in the establishment of an "advanced electricity market model characterized by a high degree of openness."

In relation to the implementation of the NCs, the Energy Law prescribes their direct applicability, however, [26] states that no NC has been translated and published officially as a legislative act. The transmission grid code was amended in December 2021 to implement some requirements of the NCs. The distribution grid code was amended in 2022, but it still requires introduction of further changes to reflect the required parameters of the Connection Codes [26].

Upon adoption of the Energy Law and of series of bylaws described in detail in [27], the wholesale and retail electricity market were completely transformed.

Fig. **3** presents a general overview of the achievements related to the market development.

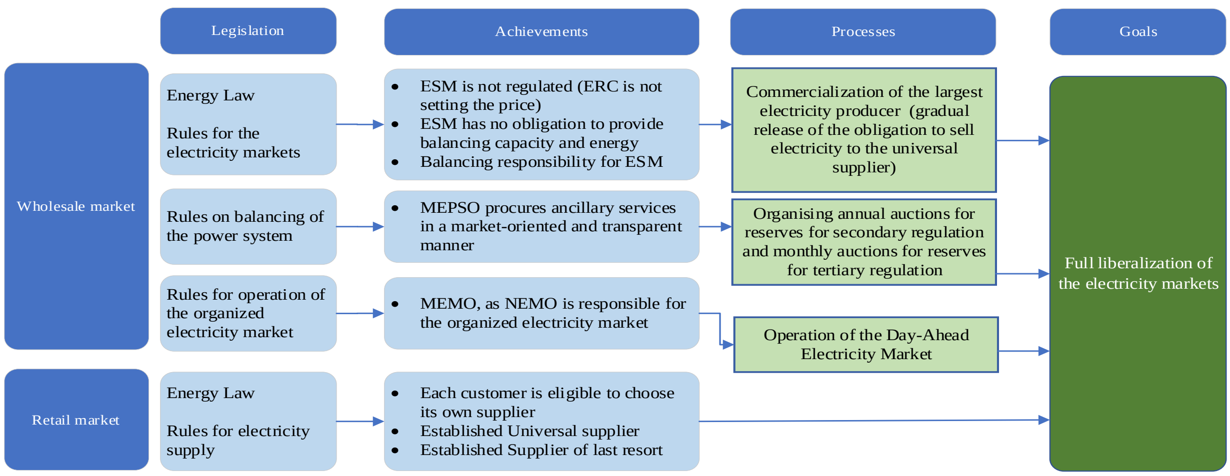

Fig. 3. Achievements and processes in relation to electricity market liberalization processes

4. CONCLUSION

This paper provides comprehensive analyses of the developments of the EU electricity market related legislation. This paper also considers EnC Law latest developments and the obligations for the stakeholders in the electricity sector of North Macedonia. The focus is both on the achieved results and the challenges ahead.

The analyses show that despite North Macedonia's notable accomplishments in implementing the Third Package, there are remaining actions to be taken, particularly regarding the complete implementation of the necessary NCs. As outlined in subsection C of section 2, there are new tasks and obligations that must be met to initiate the implementation process of the CEP. In essence, this paper clearly demonstrates that the alignment with EU law is a continuous process that shall continue in the future. This is due to the numerous challenges faced by EnC Contracting Parties, which are reiterated with each new development in both EU Law and EnC Law.

Acknowledgment: This research has been supported by the EU Horizon project TRANSIT (grant agreement 101075747) and UK Research and Innovation. The paper reflects only the authors' views and neither the Agency nor the Commission are responsible for any use that may be made of the information contained therein.

REFERENCES

[1] Borozan, V., Krkoleva Mateska, A., Krstevski, P. (2020): *Legislative Framework of the Electricity Sector in the Republic of North Macedonia and its International Standing*, Friedrich-Ebert-Stiftung (FES), Skopje, November 2020. ISBN 978-9989-109-96-6

[2] Borozan, V., Krkoleva Mateska, A., Krstevski, P. (2020): *Gap Analysis of the Electricity Sector Legal Framework of the Republic of North Macedonia and EU Law*, Friedrich-Ebert-Stiftung FES), Skopje, November 2020. ISBN 978-9989-109-96-6

[3] European Commission, "Regulation (EU) 2018/1999 of the European Parliament and of the Council of 11 December 2018 on the Governance of the Energy Union and Climate Action, amending Regulations (EC) No 663/2009 and (EC) No 715/2009 of the European Parliament and of the Council," Council Directives 2009/119/EC and (EU) 2015/652 and repealing Regulation (EU) No 525/2013 of the European Parliament and of the Council (Text with EEA relevance.), 11 December 2018, Directives 94/22/ EC, 98/70/EC, 2009/31/EC, 2009/73/EC, 2010/31/EU, 2012/27/EU and 2013/30/EU of the European Parliament and of the Council.

[4] European Commission, "Proposal for a DIRECTIVE OF THE EUROPEAN PARLIAMENT AND OF THE COUNCIL amending Directive (EU) 2018/2001 of the European Parliament and of the Council, Regulation (EU) 2018/1999 of the European Parliament and of the Council, and Directive 98/70/EC" of the European Parliament and of the Council as regards the promotion of energy from renewable sources, and repealing Council Directive (EU) 2015/652 COM/2021/557 final, Brussels, 14.7.2021.

[5] European Commission, "DIRECTIVE (EU) 2019/944 OF THE EUROPEAN PARLIAMENT AND OF THE COUNCIL of 5 June 2019 on common rules for the internal market for electricity and amending Directive 2012/27/EU (recast)", 5.06.2019.

[6] European Commission, "REGULATION (EU) 2019/943 OF THE EUROPEAN PARLIAMENT AND OF THE COUNCIL of 5 June 2019 on the internal market for electricity", 5.06.2019.

[7] European Parliament, Council of the European Union, Regulation (EU) 2019/941 of the European Parliament and of the Council of 5 June 2019 on risk-preparedness in the electricity sector and repealing Directive 2005/89/EC, Brussels: OJ L 158, 14.6.2019, pp. 1–21.

[8] METHODOLOGY FOR IDENTIFYING REGIONAL ELECTRICITY CRISIS SCENARIOS in accordance with Article 5 of Regulation (EU) 2019/941 of the European Parliament and of the Council on risk-preparedness in the electricity sector and repealing Directive 2005/ 89/EC (For Public Consultation), 3 November 2023.

[9] European Commission, "COMMISSION REGULATION (EU) 2016/1719 of 26 September 2016 establishing a guideline on forward capacity allocation", 26.9.2016.

[10] ACER, "Policy Paper on the Further Development of the EU Electricity Forward Market", February 2023.

[11] European Commission, "COMMISSION REGULATION (EU) 2015/1222 of 24 July 2015 establishing a guideline on capacity allocation and congestion management", 24.7.2015.

[12] ENTSO-E, "ENTSO-E Market Report 2022", 29.6.2022.

[13] European Commission, "COMMISSION REGULATION (EU) 2017/2195 of 23 November 2017 establishing a guideline on electricity balancing", 23.1. 2017.

[14] ENTSO-E, "ENTSO-E Market Report and Balancing Report 2022", June 2022.

[15] European Commission, "COMMISSION REGULATION (EU) 2017/1485 of 2 August 2017 establishing a guideline on electricity transmission system operation". 2.8.2017.

[16] All TSOs' proposal for the Key Organisational Requirements, Roles and Responsibilities (KORRR) relating to Data Exchange in accordance with Article 40(6) of "Commission Regulation (EU) 2017/1485 of 2 August 2017 establishing a Guideline on Electricity Transmission System Operation", 19 December 2018.

[17] European Commission, "COMMISSION REGULATION (EU) 2017/2196 of 24 November 2017 establishing a network code on electricity emergency and restoration", 24.11.2017.

[18] European Commission, "COMMISSION REGULATION (EU) 2016/631 of 14 April 2016 establishing a network

code on requirements for grid connection of generators", 14.04.2016.

[19] European Commission, "COMMISSION REGULATION (EU) 2016/1388 of 17 August 2016 establishing a Network Code on Demand Connection", 17.08.2016.

[20] Energy Community, *Energy Community Decisions repository*, https://www.energy-community.org/legal/decisions.html.

[21] Energy Community, *Energy Community Acquis*, https://www.energy-community.org/legal/acquis.html.

[22] Energy Law, *Official Gazette of the Republic of North Macedonia*, no. 96/18, 96/19 and 236/22, http://www.erc.org.mk/pages.aspx?id=8.

[23] European Commission, "COMMISSION REGULATION (EU) 1227/2011 of 25 October 2011 on wholesale energy market integrity and transparency", 25.10.2011.

[24] Energy and Water Services Regulatory Commission of the Republic of North Macedonia, "RULEBOOK ON THE MANNER AND PROCEDURE FOR MONITORING THE FUNCTIONING OF ENERGY MARKETS", 27 April 2023.

[25] European Commission, "Regulation (EU) No 347/2013 of the European Parliament and of the Council of 17 April 2013 on guidelines for trans-European energy infrastructure and repealing Decision No 1364/2006/EC and amending Regulations (EC) No 713/2009, (EC) No 714/2009 and (EC) No 715/2009, Text with EEA relevance", 17 April 2013.

[26] Energy Community Secretariat, "Annual Implementation Report 2022", 1 November 2022, [Online]. Available: https://www.energy-community.org/implementation/report.html.

[27] MEMO, https://dam.memo.mk/?page_id=30312.

Journal of Electrical Engineering and Information Technologies, Vol. **8,** No. 2, pp 69–82 (2023)
Article 208
Received: October 22, 2023
Accepted: December 5, 2023
In print: ISSN 2545–4250
On line: ISSN 2545–4269
UDC: 621.311:519.86/.87(497.7)
https://doi.org/10.51466/JEEIT2382208069m

Original scientific paper

ASSESSMENT OF THE FUTURE FLEXIBILITY NEEDS OF THE MACEDONIAN POWER SYSTEM

Stojan Malčeski[1], Sime Kuzarevski[1], Jovica Vuletić[2], Jordančo Angelov[2], Mirko Todorovski[2]

[1]*Electricity Transmission System Operator of the Republic of North Macedonia,*
1000 Skopje, Republic of North Macedonia
[2]*Faculty of Electrical Engineering and Information Technologies, "Ss. Cyril and Methodius" University in Skopje,*
Rugjer Bošković bb, P.O.Box 574, 1001 Skopje, Republic of North Macedonia
stojan.malcheski@mepso.com.mk

A b s t r a c t: To achieve the strategic goals in the energy sector during the ascension path towards the European Union, North Macedonia has set ambitious goals in the Macedonian strategic framework for the power sector. Namely, the investment plans in conventional generation technologies are ambiguous, while the planned investments in variable renewable energy sources (VRES) are quick paced. Furthermore, with interest in VRES investment with total installed capacities above the hourly load during hours of maximal VRES generation, it is crucial to assess the future flexibility needs of the Macedonian power system. This paper uses multiple metrics to obtain a high-level estimate of the system inertia and flexibility needs of the Macedonian power system on a mid-term planning horizon. The system inertia and flexibility need estimates are calculated using a multi-scenario approach where the model dispatch is calculated using a Monte Carlo optimization on a market model enclosing Southeast Europe. The obtained results give a high-level estimate of the evolution of flexibility needs and system inertia of the Macedonian power system on a mid-term planning horizon.

Key words: power system flexibility; power system inertia; res integration; market simulation

ПРОЦЕНА НА ИДНИТЕ ПОТРЕБИ ОД ФЛЕКСИБИЛНОСТ НА МАКЕДОНСКИОТ ЕЛЕКТРОПРЕНОСЕН СИСТЕМ

А п с т р а к т: За да се постигнат стратешките цели во енергетскиот сектор на патот кон Европската Унија, Северна Македонија во својата стратешка рамка има поставено амбициозни цели за електроенергетскиот сектор. Во Македонската стратешка рамка инвестицискиот план за конвенционалните електрични централи е проследен со голем број неизвесности, додека инвестициите во обновливите извори на електрична енергија (ОИЕ) се реализираат со брзо темпо. Имајќи предвид дека вкупниот интерес за инвестиции во обновливи извори по капацитет го надминува системското оптоварување во часови кога производството од ОИЕ е најголемо, неопходно е да се направи процена на идните потреби од флексибилност на македонскиот електроенергетски систем. Во овој труд се пресметани неколку метрики со цел да се направи процена на системските потреби од флексибилност и инерција на македонскиот електроенергетски систем на среднорочен планирачки хоризонт. Потребите од системска инерција и флексибилност се пресметуваат со помош на методот Монте Карло на повеќе сценарија на пазарниот модел за Југоисточна Европа со часовна резолуција. Резултатите од истражувањето даваат јасна слика на системската потреба од флексибилност и инерција на среднорочен планирачки хоризонт.

Клучни зборови: флексибилност на ЕЕС; инерција на ЕЕС; интеграција на обновливи извори; пазарни симулации

INTRODUCTION

With the evolution of the Macedonian power sector towards a green energy sector, the Macedonian generation portfolio is supposed to undergo drastic structural changes in the years to come where the plan is to substitute the heavy emission power plants with VRES. According to the Macedonian strategic framework [1–3], the decommissioning of the lignite and fuel oil power plants will take place from 2019 to 2027. While the strategic goals for investments in VRES are ambitious, the investment plans in conventional generation technologies remain ambiguous. The possible changes to the conventional generation portfolio, combined with ambitious investment plans in VRES, will result in increased flexibility needs [4] and may reduce the system inertia on a national level. The difficulties of VRES integration and exploitation in the Macedonian power system will vary depending on the VRES production and installed capacity, the system load profile for the analyzed time horizon, and the flexibility of the power system [5]. Hence, the uncertain nature of the Macedonian energy strategy is analyzed using a multi-scenario approach to cover a broad spectrum of possible future scenarios.

As defined by [6], power system flexibility is the capability of a power system to cope with the variability and uncertainty that VRES generation introduces into the system in different time scales, from the very short to the long term, avoiding curtailment of VRES and reliably supplying all the demanded energy to customers. For a transmission system operator tasked to integrate large-scale VRES projects in their power system, a reasonable estimate of the future system flexibility needs, and inertia is essential. There are multiple approaches to assessing the flexibility and inertia of a power system differing in their complexity and computation resource requirements. So far, in academia and the power sector, there is no consensus on the best approach to tackle this problem since power system flexibility and inertia are system-specific [4].

There are numerous papers and technical reports covering the assessment of flexibility needs on a planning horizon written to this date. While the research focus is on algorithms that treat time series to assess the flexibility needs of a power system, such as in [7] and [8], there are not many papers that treat the problem using a stochastic market modeling approach.

Recent papers that treat the problem using a stochastic market modeling approach are [9], where the authors use flexibility metrics to analyze the flexibility needs from a ramp requirements point of view, while in [10] the authors focus on the impact of time-step granularity of the stochastic market modeling approach. The authors in [9] and [10] opt for a stochastic modeling approach using a European market model. In [11], the authors explore various scenarios and flexibility mechanisms to analyze a high share of RES scenarios. Furthermore, the authors in [11] developed a linear programming model POWER to solve a US-based market model.

Additionally, there are papers and studies on system flexibility that treat the problem on a national level while considering the regional implications on the national results. Such is the case in [12], where the authors examine the impact on system inertia during high penetrations of wind power to the power system of Ireland using the non-synchronous penetration ratio (SNSP) metric, and in [13], where the authors assess the flexibility needs of the Greek power system using two metrics, the flexibility index (FIX) and present VRE penetration potential (PVP). From the power system sector in Europe, two reports are of outstanding quality, namely [14] and [15].

When analyzing system inertia and flexibility, it is crucial to get a rough estimate of future needs before developing a complicated methodology that would cover the system specifics. In this paper, the inertia and flexibility assessment of the Macedonian power system is based on the net load, which represents the difference between system load and non-dispatchable power generation [16]. More specifically, the research focus is on the following flexibility metrics: a renewable penetration index (RPI) and renewable energy penetration index (REPI) [17], system probability for VRES curtailment (LORE) [18], and system inertia metric SNSP [19]. Furthermore, the ramp-up and ramp-down capability of the Macedonian power system was analyzed for two VRES development scenarios to obtain an estimate of the most frequent and volatile ramps in the future. The analysis was done, and the parameters were calculated using a regional market model of Southeast Europe, where each country is modeled with one/or multiple areas on the copper plate principle where the total production and load on a power system level are aggregated to the area/s representing a given country and interconnected with other neighboring countries on NTC-based interfaces [20].

Our research aims to provide energy system planners with assessment of the power system flexibility and inertia needs which is supposed to help them take this aspect of the power system into account when drafting the national strategy framework. The proposed metrics are calculated based on the outputs of a Monte Carlo based market simulation, and by doing so the variability of Load, RES, water inflows, and outages is properly considered. The proposed methodology should serve as a link between the process of energy and power system planning.

The remainder of this paper is organized as follows: Section 2 gives an overview of the market model from a national and regional point of view and scenario definitions for analysis, Section 3 gives a detailed overview of the methodology for calculation of the selected metrics, Section 4 presents the results of the analysis, while Section 5 presents a summary of the findings.

2. MEASUREMENT SYSTEM DESCRIPTION

The developed market model is for a mid-term time horizon (2030), based on the Energy Market Initiative Data Base (EMIDB) by USEA, [23], and Pan-European Climate Database (PECD) by ENTSO [20]. The EMIDB contains data on a unit-by-unit basis for the thermal and hydropower plants in the region, data for the installed capacity of VRES, data for demand, and data for the net transmission capacities on an interface level between the countries of SEE. The PECD dataset contains weather data for Europe from 1982 to 2016. This data is processed to obtain the production profiles for wind and solar on a country basis.

The simulation scope is the area of Southeast Europe in light gray in Figure 1. In this research, the following countries from the SEE region were modeled in detail: Albania, Bosnia and Herzegovina, Bulgaria, Croatia, Greece, Hungary, Kosovo, Montenegro, North Macedonia, Romania, Serbia, and Slovenia.

Fig. 1 Modeling scope of the Regional Market Model

The exchanges with the exogenous power systems, given in dark gray in Figure 1, represent the rest of the European power system modeled as hourly market-driven power flows.

The Macedonian strategy framework for the power sector is ambiguous when it comes to the investment plan in conventional power plants. Namely, there is uncertainty in the mid and long term whether the investments will be in gas power plants or a pump storage power plant (PSP). According to the Macedonian strategy framework, the investments in gas power plants by 2030 might amount to 450 MW. On the other hand, the PSP potential is around 333 MW in turbine mode and 363 MW in pump mode, based on the authors' best estimate.

Since both investments in gas power plants and PSP contribute to power system flexibility, both scenarios are analyzed, comparing the results of both scenarios to a base case scenario that takes no investment decision in conventional power plants. Moreover, the analysis considers two VRES profiles (wind and solar) named slow-paced and rapid development. The two VRES development profiles paired with the business-as-usual and the investment in gas and PSP scenarios yield a total of six scenarios:

Low RES BC: a base case with slow-paced VRES development.

Low RES wTPP: investment in gas power plants with slow-paced VRES development.

Low RES wPSP: investment in PSP with slow-paced VRES development.

High RES BC: a base case with rapid VRES development.

High RES wTPP: investment in gas power plants with rapid VRES development.

High RES wPSP: investment in PSP with rapid VRES development.

Figure 2 shows the installed capacities of different production technologies for the six scenarios of the Macedonian power system analyzed in this paper.

Table 1 shows the installed capacities per fuel type technology in MW for each of the modeled countries in the region for the 2030 planning horizon excluding the data for North Macedonia. From the table data, we can see that in 2030 the installed capacities from VRES and hydro are dominant in the region, while the capacity from the conventional power plants is on the lower end.

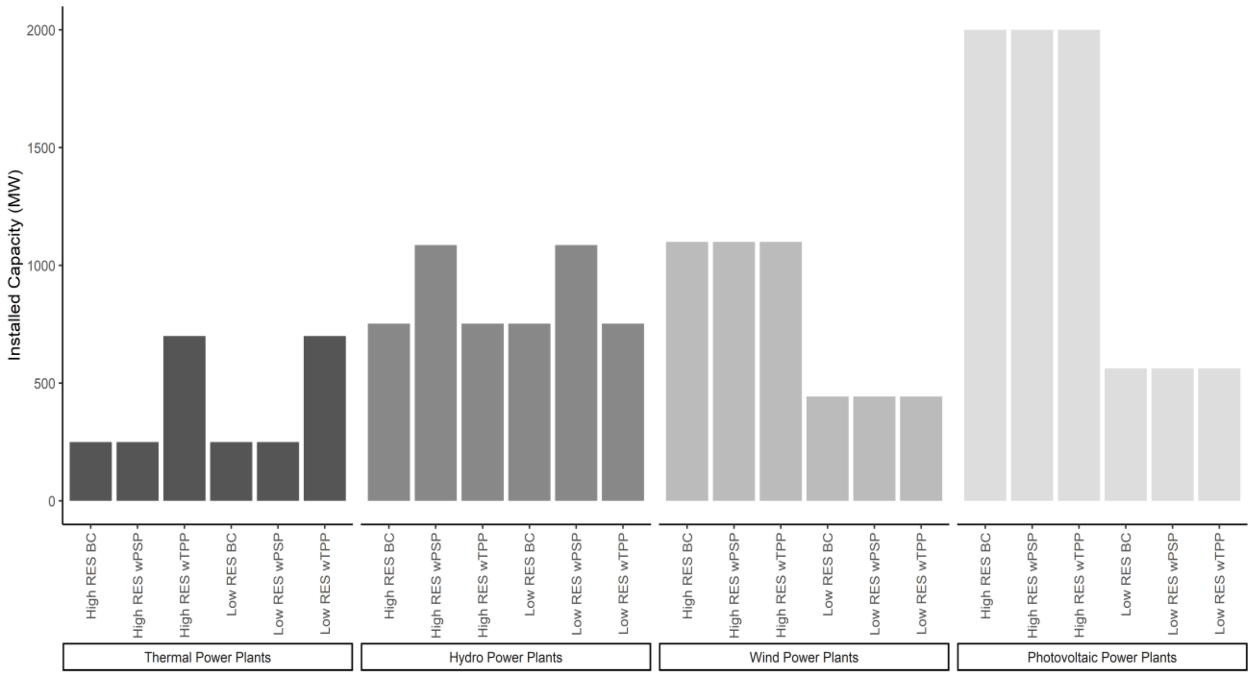

Fig. 2. Installed capacity per generation technology for the six scenarios in North Macedonia on a mid-term planning horizon

Table 1

Installed capacities per technology in the region in MW of Southeast Europe

Capacity (MW)	AL	BA	BG	GR	HR	HU	ME	RO	RS	SI	SUM
Nuclear	0	1632	0	0	297	165	225	2174	5406	584	10483
Coal	300	0	2728	7477	684	2981	0	5742	410	529	21101
Gas	0	0	0	290	0	0	0	0	0	0	290
Oil	0	0	2000	0	0	4248	0	1965	0	703	8916
Hydro	2949	2493	3207	4545	3117	0	1117	6783	3469	1715	30438
Wind	384	500	3216	7700	600	3589	250	5054	4889	150	26895
Solar	445	650	948	7000	1300	304	243	5255	657	1866	19111
Batteries	0	0	0	1000	0	0	0	0	0	0	1000

Table 2 shows the transfer capacities of the NTC-based interfaces connecting the areas that represent countries where their capacity is in MW. The NTC-based interfaces allow for bidirectional power flow between each country (node).

Table 3 shows the economic and technical parameters for each thermal power plant technology per fuel type as in [20]. These parameters were used to create the market model.

Using the data from Table 3 for each of the technologies given in [20], we can calculate the marginal price of each TPP unit χ_θ (€/MWh) by the following formula:

$$\chi_\theta = VO\&M + \frac{CO_2\ emmissions}{efficiency} \cdot CO_2\ price + \\ + \frac{Fuel\ Price \cdot 3.6\ (GJ/MWh)}{efficiency} \quad (1)$$

where the CO_2 price in our research is 66 €/t.

Table 4 shows the parameters for the forced and planned outage and maintenance rate for the thermal power plant technologies per fuel type as in [20]

Table 2

Transfer capacities of NTC-interfaces connecting areas

Link name	Capacity (MW)	Link name	Capacity (MW)
AL – GR	400	ME – RS	600
AL – ME	450	ME – XK	300
AL – MK	500	MK – AL	1000
AL – XK	650	MK – BG	800
BA – HR	1200	MK – GR	850
BA – ME	800	MK – RS	400
BA – RS	1100	MK – XK	330
BG – GR	1700	RO – BG	2600
BG – MK	800	RO – HU	1400
BG – RO	2600	RO – RS	2000
BG – RS	800	RS – BA	1200
GR – AL	400	RS – BG	800
GR – BG	1400	RS – HR	500
GR – MK	1100	RS – HU	1000
HR – BA	1200	RS – ME	600
HR – HU	1700	RS – MK	400
HR – RS	500	RS – RO	2000
HR – SI	2000	RS – XK	300
HU – HR	1700	SI – HR	2000
HU – RO	1300	SI – HU	1200
HU – RS	1000	XK – AL	500
HU – SI	1200	XK – ME	300
ME – AL	450	XK – MK	350
ME – BA	750	XK – RS	400
AL – GR	400	ME – RS	600

Table 3

Economic and technical parameters for thermal power plants per fuel type

Technology	Fuel Price (€/GJ)	Efficiency (%)	CO_2 emissions (kg/Net GJ)	VO&M cost (€/MWh)	Heat Rate (GJ/MWh)
Nuclear	0.47	33	0	9	10.9
Lignite	1.1	35 – 46	101	3.3 – 6.6	7.8 – 10.3
Hard Coal	4.3	35 – 46	94	3.3 – 6.6	7.8 – 10.3
Gas	6.91	36 – 58	57	1.1 – 1.6	7.1 – 10.3
Heavy Oil	14.6	35 – 40	78	3.3	9 – 10.3

Table 4

Forced and planned outage rate for thermal power plants per fuel type

Technology	Forced outage		Planned outage annual rate (days)
	Annual rate (%)	Repair time (days)	
Nuclear	5	7	54
Lignite	7.5 – 10	1	27
Hard coal	7.5 – 10	1	27
Gas	5 – 8	1	13 – 27
Heavy oil	10	1	27

The parameters from Table 4 were used to create random yearly outage patterns for each of the TPPs modeled in ANTARES while the data from PECD was used to create Climatic Years (CY) from the weather data. Each CY is a combination of hourly time series for load, wind, solar, hydro inflows, run-of-river, and other renewable energy sources for one of the PECD weather yearly data.

Table 5 shows the flexibility parameters data for the hydropower and thermal power plants which are eligible for flexibility provision.

Table 5

Flexibility parameters of the hydro and thermal power plants in North Macedonia

Power plant	No. Units	Ramp up/down (MW/min)	Cold start (min)
HPP 1	4	10	15
HPP 2	2	10	15
HPP 3	4	25	15
HPP 4	2	10	15
HPP 5	2	10	15
HPP 6	3	10	15
TPP 1	1	6	56

3. PROBLEM FORMULATION

Using the detailed economy and power system data, we can create market models in the tool ANTARES. In this tool, each power system modeled is represented as a vertex (area) that is connected to other areas (vertices) through links (edges, NTC-based interfaces) based on the actual interconnections between each power system that are modeled. The areas and links form an undirected graph (2) of the regional power system that's being modeled.

$$G(N,L), \forall\, n \in N, \forall\, l \in L \tag{2}$$

where $G(N,L)$ is the undirected graph of the power system, N is the ordered set of vertices of G, n is a vertex of N, L is the set of edges of G, and l is an edge of L.

Each of the modeled links allows for energy in both directions either from u_l to d_l or vice versa where: u_l is a vertex upstream from l, and d_l is a vertex downstream from l.

ANTARES uses the Monte Carlo optimization method with weekly resolution T where in each optimization period it dispatches an optimal mix of dispatchable generators for each hour t to serve the hourly net load. Hence, each optimization period consists of 168 hours, and we have 54 optimization periods in each MCY.

To achieve this the ANTARES simulator aims to minimize the system cost using the following objective function:

$$\min_{M_\theta \epsilon ArgMin(\Omega_{Unit\ com})} \left(\Omega_{dispatched}\right) \tag{3}$$

$$\Omega_{dispatched} = \Omega_{thermal} + \Omega_{hydro+} \\ +\Omega_{unsyplied} + \Omega_{spillage} \tag{4}$$

$$\Omega_{thermal} = \sum_{n\in N} \sum_{\theta\epsilon\Theta_n} (\chi_n P_\theta) \tag{5}$$

$$\Omega_{hydro} = \sum_{n\in N} \sum_{\lambda\epsilon\Lambda_n} (\varepsilon_\lambda + \varepsilon_\lambda^*)\,(H_\lambda - \rho_\lambda \Pi_\lambda + O_\lambda) \tag{6}$$

$$\Omega_{unsyplied} = \delta_n^+ G_n^+ \tag{7}$$

$$\Omega_{spillage} = \delta_n^- G_n^- \tag{8}$$

$\Omega_{Unit\ com}$, committed dispatchable units in each time step (9)

where Θ_n, a set of all thermal clusters connected to n: θ, a cluster which is an element of Θ_n; Λ_n, the set of all reservoirs connected to n; λ, a reservoir which is an element of Λ_n; $\chi_\theta \in \mathbb{R}^T$, cost proportional to the output of the running unit in θ; $P_\theta \in \mathbb{R}_+^T$, power output from cluster θ; $\varepsilon_\lambda \in \mathbb{R}$, reference water value associated with the reservoirs initial state; $\varepsilon_\lambda^* \in \mathbb{R}^T$, random component added to the water value; $H_\lambda \in \mathbb{R}_+^T$, power output from reservoir λ; $\rho_\lambda \in \mathbb{R}_+$, efficiency ratio of pumping units (or equivalent devices) available in reservoir λ; $\Pi_\lambda \in \mathbb{R}_+^T$, power output from reservoir λ; $O_\lambda \in \mathbb{R}_+^T$, power overflowing from reservoir λ; $\delta_n^- \in \mathbb{R}_+^T$, value of lost load; $\delta_n^+ \in \mathbb{R}_+^T$, value of wasted energy; $G_n^+ \in \mathbb{R}_+^T$, power not supplied, and $G_n^- \in \mathbb{R}_+^T$, supplied energy.

In the optimization process the following constraints were applied:

$$\forall\, n \in N: 0 \le G_n^+ \le \max(0, D_n) \quad (10)$$

$$\forall\, n \in N: 0 \le G_n^- \le -\min 0, Dn + + \textstyle\sum_{\lambda\epsilon\Lambda_n} H_\lambda + \sum_{\theta\epsilon\Theta_n} P_\theta \quad (11)$$

$$\forall\, l \in L: 0 \le F_l^+ \le C_l^+ \quad (12)$$

$$\forall\, l \in L: 0 \le F_l^- \le C_l^- \quad (13)$$

$$\forall\, l \in L: F_l = F_l^+ + F_l^- \quad (14)$$

$$\forall\, n \in N, \forall\, \lambda \in \Lambda_n: \underline{W_\lambda} \le \textstyle\sum_{t\in T} H_{\lambda_t} \le \overline{W_\lambda} \quad (15)$$

$$\forall\, n \in N, \forall\, \lambda \in \Lambda_n: \underline{W_\lambda} \le \le \textstyle\sum_{t\in T} H_{\lambda_t} - \sum_{t\in T} \rho_\lambda \Pi_{\lambda_t} \le \overline{W_\lambda} \quad (16)$$

$$\forall\, n \in N, \forall\, \lambda \in \Lambda_n: \underline{H_\lambda} \le H_\lambda \le \overline{H_\lambda} \quad (17)$$

$$\forall\, n \in N, \forall\, \lambda \in \Lambda_n: 0 \le \Pi_\lambda \le \overline{\Pi}_\lambda \quad (18)$$

$$\forall\, n \in N, \forall\, \lambda \in \Lambda_n: 0 \le \Pi_\lambda \le \overline{\Pi}_\lambda \quad (19)$$

$$\forall\, n \in N, \forall\, \lambda \in \Lambda_n, \forall\, t \in T: R_{\lambda_t} - R_{\lambda_{t-1}} = = \rho_\lambda \Pi_{\lambda_t} - H_{\lambda_t} - I_{\lambda_t} - O_{\lambda_t} \quad (20)$$

$R_{\lambda_{t-1}}$ is not a viable parameter for the first time slot and because of so the Initial Reservoir State is used in its stead.

$$\forall\, n \in N, \forall\, \lambda \in \Lambda_n: \underline{R_\lambda} \le R_\lambda \le \overline{R_\lambda} \quad (21)$$

$$\forall\, n \in N, \theta \in \Theta_n: \underline{P_\theta} \le P_\theta \le \overline{P_\theta} \quad (22)$$

$$\forall\, n \in N, \theta \in \Theta_n: \underline{M_\theta} \le M_\theta \le \overline{M_\theta} \quad (23)$$

$$\forall\, n \in N, \theta \in \Theta_n: l_\theta M_\theta \le M_\theta \le u_\theta M_\theta \quad (24)$$

$$\forall\, n \in N, \theta \in \Theta_n, \forall\, t \in T: M_{\theta_t} = = M_{\theta_{t-1}} + M_{\theta_t}^+ - M_{\theta_t}^- \quad (25)$$

$$\forall\, n \in N, \theta \in \Theta_n, \forall\, t \in T: M_{\theta\ t}^{-} \le \le \max\left(0, \overline{M}_{\theta_{t-1}} - \overline{M}_{\theta_t}\right) \quad (26)$$

$$\forall\, n \in N, \theta \in \Theta_n, \forall\, t \in T: M_{\theta_t}^- \le M_{\theta_t}^- \quad (27)$$

$$\forall\, n \in N, \theta \in \Theta_n, \forall\, t \in T: M_{\theta_t} \ge \ge \textstyle\sum_{k=t+1-\Delta_\theta^+}^{k=t} \left(M_{\theta_t}^+ - M_{\theta\ k}^{--}\right) \quad (28)$$

$$\forall\, n \in N, \theta \in \Theta_n, \forall\, t \in T: M_{\theta_t} \ge \ge \sum_{k=t+1-\Delta_\theta^-}^{k=t} \max\left(0, \overline{M}_{\theta_k} - \overline{M}_{\theta_{k-1}}\right) - - \textstyle\sum_{k=t+1-\Delta_\theta^-}^{k=t} \left(M_{\theta\ k}^-\right) \quad (29)$$

while one of the following conditions must be satisfied always:

$$\Delta_\theta^- \le \Delta_\theta^+ \quad (30)$$

$$\overline{M}_\theta \le 1_T \quad (31)$$

where $D_n \in \mathbb{R}^T$, net load expressed in node n; $F_l^+ \in \mathbb{R}_+^T$, power flow through l from u_l to d_l; $F_l^- \in \mathbb{R}_+^T$, power flow through l from d_l to u_l; $C_l^+ \in \mathbb{R}_+^T$, initial transmission capacity from u_l to d_l; $C_l^- \in \mathbb{R}_+^T$, initial transmission capacity from d_l to u_l; $F_l \in \mathbb{R}^T$, total power flow through l; $\overline{W_\lambda} \in \mathbb{R}_+$, maximum energy output from λ through the optimization period; $\underline{W_\lambda} \in \mathbb{R}_+$, minimum energy output from λ through the optimization period; $\overline{H_\lambda} \in \mathbb{R}_+^T$, maximum power output from reservoir λ; $\underline{H_\lambda} \in \mathbb{R}_+^T$, minimum power output from reservoir λ; $\overline{\Pi}_\lambda \in \mathbb{R}_+^T$, maximum power absorbed by pumps of reservoir λ; $\overline{R_\lambda} \in \mathbb{R}_+^T$, upper bound of the admissible level in reservoir λ; $\underline{R_\lambda} \in \mathbb{R}_+^T$, lower bound of the admissible level in reservoir λ; $R_\lambda \in \mathbb{R}_+^T$, stored energy level in reservoir λ; $\overline{P_\theta} \in \mathbb{R}_+^T$, maximal power output from cluster θ; $\underline{P_\theta} \in \mathbb{R}_+^T$, minimal power output from cluster θ; $P_\theta \in \mathbb{R}_+^T$, stored energy level in reservoir λ; $\overline{M_\theta} \in \mathbb{N}^T$, maximal number of running units in cluster θ; $\underline{M_\theta} \in \mathbb{N}^T$, minimal number of running units in cluster θ; $M_\theta^+ \in \mathbb{N}^T$, number of units changing from off state to on state in cluster θ; $M_\theta^- \in \mathbb{N}^T$, number of units changing from on state to off state in cluster θ; $M_\theta^{--} \in \mathbb{N}^T$, number of units changing from on state to outage state in cluster θ; $\Delta_\theta^+ \in \{1, \ldots, |T|\}$, minimum on time when running for an unit in θ; and $\Delta_\theta^- \in \{1, \ldots, |T|\}$, minimum off time when not running for a unit in θ.

The models consist of thirty-five climatic years which represent a combination of load, solar, wind, and hydro production profiles from the PECD database. The use of a high number of climatic years helps to account for the VRES and load variability. Each climatic year is paired with one of the twenty outage patterns for the thermal power plants, which outage patterns are generated using Three-state Markov Chain, yielding seven hundred Monte Carlo years (MCY) or seven hundred future states of the regional power system. The simulation results are with hourly resolution on an annual basis for each of the seven hundred simulated MCY.

4. FLEXIBILITY METRICS

The flexibility analysis is based on the following flexibility metrics: RPI, REPI, LORE, and SNSP. The RPI and REPI metrics are calculated based on the climatic years' data (correlated load, wind, PV, and run-of-river time series). The LORE and SNSP metrics are calculated by analyzing the annual dispatch results from the market simulation on an hourly level. Additionally, net load (NL) and net load ramp (NLR) were calculated before calculating the LORE metric.

Calculation of RPI and REPI

The *RPI* and REPI metrics are calculated in a deterministic manner using the data from all the *CY*. The RPI metric is calculated using the following three step algorithm:

Step 1: Calculate RPI for each hour for the selected CY based on:

$$RPI = \max\left(\frac{Wind(t)+PV(t)}{Load(t)}\right), \forall t \in [1{,}8760] \quad (32)$$

Step 2: Repeat Step 1 for each of the thirty-five CY.

Step 3: From all calculated values for each hour of the thirty-five CY RPI is equal to the maximal value.

The REPI metric is calculated using the following three step algorithm:

Step 1: Calculate REPI for the selected CY as:

$$REPI = \frac{\sum_{t=1}^{8760}(Wind(t)+PV(t))}{\sum_{t=1}^{8760}(Load(t))} \quad (33)$$

Step 2: Repeat Step 1 for each of the thirty-five CY.

Step 3: From all calculated annual values for each of the thirty-five CY REPI is equal to the mean value.

In (32) and (33), $Wind(t)$ is the hourly production of wind power plants in MW, $PV(t)$ is the hourly production of solar power plants in MW, and $Load(t)$ is the hourly load in MW.

Calculation of LORE

The system probability for VRES curtailment is calculated similarly to the Loss of Wind Estimation (LOWE) metric presented in [18]. Since, in this paper, the research is extended to cover Wind and PV curtailment probability, the metric name is modified to Loss of renewable energy estimation (LORE).

Before calculating LORE, the *NL* and *NLR* were calculated, where *NL* is calculated as:

$$NL(t) = Load(t) - Wind(t) - PV(t) - Must\_Run(t) \quad (34)$$

while NLR is calculated as:

$$NLR(t) = NL(t+1) - NL(t) \quad (35)$$

$$NLR_+(t) = NLR(t), \forall NLR(t) \geq 0 \quad (36)$$

$$NLR_-(t) = NLR(t), \forall NLR(t) < 0 \quad (37)$$

where $Must\_Run(t)$ consists of the production of all technologies that are hard constrained to produce energy during predetermined periods on annual level in MW.

Calculating the *NL* and *NLR* with different time steps, e.g., two, four, or another arbitrary system-specific time step will yield different results. *NL* and *NLR* were calculated with an hourly time step.

The periods during which VRES curtailment might occur are similar to the ones described in [18], which are: *NL* lower than zero, NLR_+ is higher than the ramp-up capability of online generators and offline generators that cannot be brought online, and NLR_- is higher than the ramp-down capability of online generators and online generators that can be shut down.

The Ramp-up or Ramp-down capability more commonly known as the Ramping capability of a generator is defined as the sustained rate of change of generator output, in MW/s. In this paper the Ramp-up and Ramp-down capability of the generators is expressed in MW/h due to the time step granularity of the market simulation.

The first recognized period during which VRES curtailment might occur is when *NL* is lower than zero, so the probability of this event is computed as:

$$P(Period_1) = P(NL(t) \leq 0) \quad (38)$$

The second period is the one where NLR_+ is higher than the Ramp-up capability of online generators and offline generators that cannot be brought online, for which the probability of occurrence is calculated as:

$$P(Period_2) = P\left(NLR_+(t) \geq \sum Ramp\_up(t)\right) \quad (39)$$

The last period is the one where $NLR\_$ is higher than the ramp-down capability of online generators and online generators that can be shut down, for which the probability of occurrence is calculated as:

$$P(Period_3) = P|NLR\_(t)| > \\ > \sum Ramp\_down(t) \quad (40)$$

The $\sum Ramp\_up(t)$ and $\sum Ramp\_down(t)$ capability of the Macedonian power system were calculated using the data in Table 5.

Finally, the $LORE$ metric is calculated as:

$$LORE = 1 - \left(1 - P(Period_1)\right) \cdot \\ \cdot (1 - P(Period_2)) \cdot (1 - P(Period_3)) \quad (41)$$

The LORE parameter is calculated by processing the results for all the seven hundred MCY. The results are given for each of the three periods (38 – 40) as well as the total probability represented by LORE (41).

Calculation of SNSP

The SNSP (Non-synchronous penetration ratio) is calculated as:

$$SNSP(t) = \frac{\sum P_{in_{inverter}}(t)}{\sum P_{out}(t)} = \frac{Wind(t)+PV(t)}{Load(t)+Export(t)} \quad (42)$$

where $Export(t)$ is the export to the neighboring countries in MW [19].

The SNSP parameter (42) is calculated by processing the results for all the seven hundred MCY.

5. RESULTS AND DISCUSSION

The flexibility analysis of the Macedonian power system was carried out using a regional market model covering Southeast Europe. Six different market models were created with the regional SEE model as a basis covering six scenarios for the development of the national generation portfolio. To account for the stochastic nature of VRES, in the analysis, the thirty-five unique climatic year scenarios for VRES and twenty outage patterns for the conventional power plants were used, which accounts for a total of seven hundred Monte Carlo years per scenario. Four main metrics were calculated: RPI, REPI, LORE, and SNSP, where RPI and REPI were calculated based on time-series analysis of the thirty-five different CY, while LORE and SNSP were calculated using the market model output for the seven hundred MCY. Furthermore, the ramp-up and ramp-down capability of the Macedonian power system was analyzed for two VRES development scenarios to obtain an estimate of the most frequent and volatile ramps that may occur in the future.

Table 6 shows the minimum, maximum, average, and standard deviation for RPI and REPI for the Macedonian power system. The data was calculated for the Low-RES and High-RES development scenarios.

Figures 3 and 4 display the histograms of RPI, while Figures 5 and 6 display the histograms of REPI for both RES development scenarios. From Figures 3 and 4 it can be concluded that for both RES development scenarios the distributions are similar, and, in both cases, centered around the mean. In both cases, the maximal recorded value is an outlier of the dataset. From Figures 5 and 6 it's clear that the data is skewed to the left where most of the data is closer to the maximal value centered around the mean. Since high RPI were noted for both Low-RES and High-RES, in the future, to avoid VRES production curtailment, the Macedonian strategic framework should be reworked to consider different energy storage technologies or a shift from a fossil fuel-powered industry to an electricity-powered industry to increase the overall load profile [22]. As an alternative approach, the Macedonian strategic framework may be reworked to develop a generation portfolio with suitable flexibility, which would allow the country to become export oriented.

Table 6

RPI and REPI for the Macedonian power system on a mid-term planning horizon

VRES development scenario	RPI				REPI			
	Min	Max	Mean	Standard deviation	Min	Max	Mean	Standard deviation
Low RES	0.938	1.811	1.114	0.148336	0.14	0.17	0.16	0.00004
High RES	2.804	5.403	3.320	0.447087	0.46	0.52	0.49	0.00030

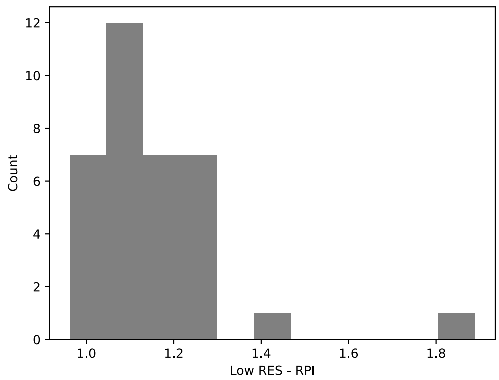

Fig. 3. RPI histogram for Low RES

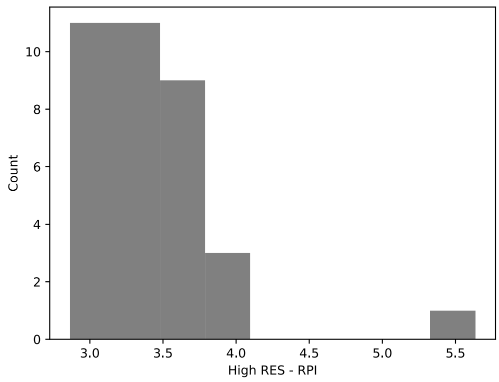

Fig. 4. RPI histogram for High RES

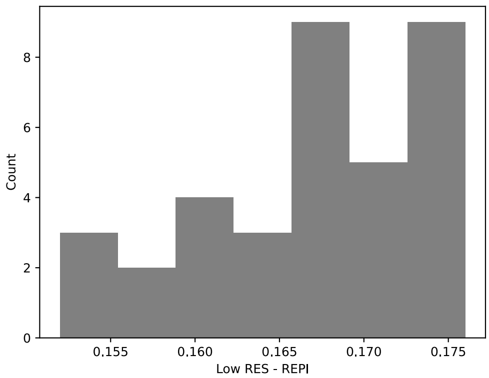

Fig. 5. REPI histogram for Low RES

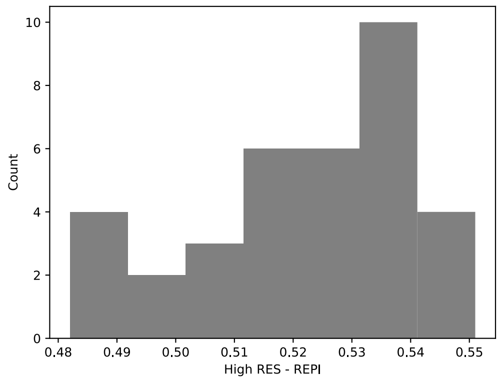

Fig. 6. REPI histogram for High RES

Figure 7 and Figure 8 present the RPI and REPI values on a regional basis for the Low-RES and High-RES development scenario in MK, respectively. Figure 3 and Figure 4 show that the VRES data in EMIDB and PECD for Southeast Europe is modest at best, while in most cases, it can be considered quite low, with VRES participation usually below 30%. Hence, the calculated flexibility metrics for North Macedonia might underestimate the flexibility needs since the needs are dependent on the development of the VRES generation portfolios in the region.

Fig. 7. Regional RPI distribution

Fig. 8. Regional REPI distribution

Table 7 shows the loss of renewable energy estimation (LORE) for the six analyzed scenarios as well as the results for the three different periods of interest. Period 3, or period during which the ramp-down capability of the system cannot match the $NLR_{-}(t)$, has an insignificant contribution to LORE in all six scenarios. Period 2, or period during which the ramp-up capability of the system cannot match the $NLR_{+}(t)$ contributes to LORE for all six scenarios. The commissioning of new TPPs (450 MW TPPs on gas) or the PSP project (333 MW) is crucial to reduce the curtailment probability, but we must check if this conclusion holds if we account for the latest interest of the private sector for RES connection. Period 1 contributes significantly to LORE in the High-RES scenarios due to the relatively low demand profile that the Macedonian power system experiences. In the future, to lower the probability of RES curtailment technologies such as power to hydrogen and hydrogen to power as well as power to gas and gas to power technologies (X2P and P2X) should be included in the energy and power mix on national level.

It is important to note that the results from the market model did not show curtailment of VRES as a result of the well-developed interconnections in the region of interest, but at the same time, the installed VRES capacities in the neighboring countries are quite modest, with exception to the installed capacities in Romania, Greece, Bulgaria, and the rapid development VRES scenarios for North Macedonia. From the results, it is expected that if each country follows a VRES development scenario, such as the rapid one we are using for North Macedonia, the region will experience curtailment of VRES.

T a b l e 7

LORE for the for the Macedonian power system on a mid-term planning horizon

Scenario	Periods of interest (%)			LORE
	Period 1	Period 2	Period 3	
Low RES BC	0.12	4.17	0.00	4.29
Low RES wTPP	0.12	1.36	0.00	1.48
Low RES wPSP	0.12	0.99	0.00	1.11
High RES BC	23.47	8.37	0.50	30.23
High RES wTPP	23.47	2.35	0.35	25.53
High RES wPSP	23.47	1.62	0.50	25.09

Figure 9 and Figure 10 show the rate of occurrence of ramps for the slow-paced and rapid VRES development scenarios, respectively. The rate of occurrence of ramps is calculated as an average of the measurement of the duration of up and down periods of $NLR(t)$ for the thirty-five climatic years for the slow-paced and rapid VRES development scenarios, respectively. Based on the obtained results, we can conclude for both VRES development scenarios that the one-hour ramps are the most frequent. Moreover, the two-hour, three-hour, four-hour, eight-hour, nine-hour, ten-hour, and eleven-hour ramps occur frequently enough so that their effects should be analyzed in more detail in future flexibility studies of the Macedonian power system.

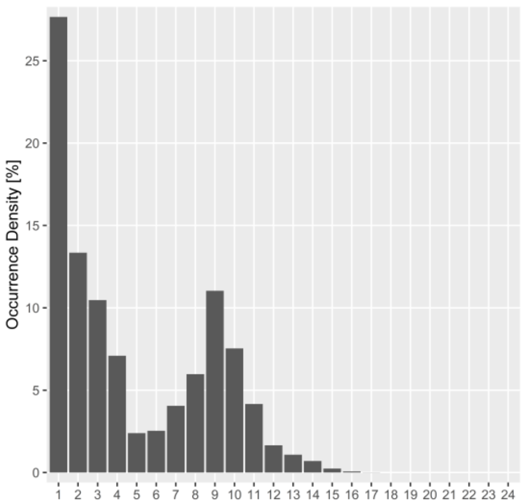

Fig. 9. Ramp span occurrence for the slow-paced VRES development scenario

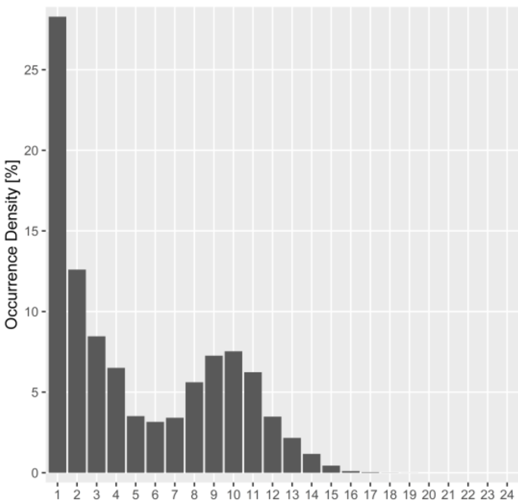

Fig. 10. Ramp span occurrence for the rapid VRES development scenario

Figure 11 shows the SNSP density for the analyzed scenarios of the Macedonian power system. In comparison to the slow-pace VRES development scenarios (Scenarios 1, 2, and 3), the rapid VRES development scenarios (Scenarios 4, 5, and 6) have a notable SNSP evolution which suggests that with the development of VRES and decommissioning of conventional brown power plants in MK and the region, the system inertia might be inadequate to maintain system stability. From the results for Scenarios 4, 5, and 6 in Figure 11, we can see that the tail of the graph goes to 1, and for Scenario 6, even above 1, which suggests that in the future in MK, we will have numerous regimes with extremely low inertia.

The results in Figure 11 clearly show that as the VRES profile in MK evolves, the Macedonian power system would rely on the neighboring power systems for system inertia provision. Additionally, as more and more conventional brown power plants get decommissioned, the region will have even fewer power plants that could provide the needed system inertia. Hence, with the VRES evolution on a regional level, the focus should be on a share of reserves and regional balancing market in Southeast Europe, which will lead to an optimal interconnection use and investments in synthetic inertia from large VRES plants.

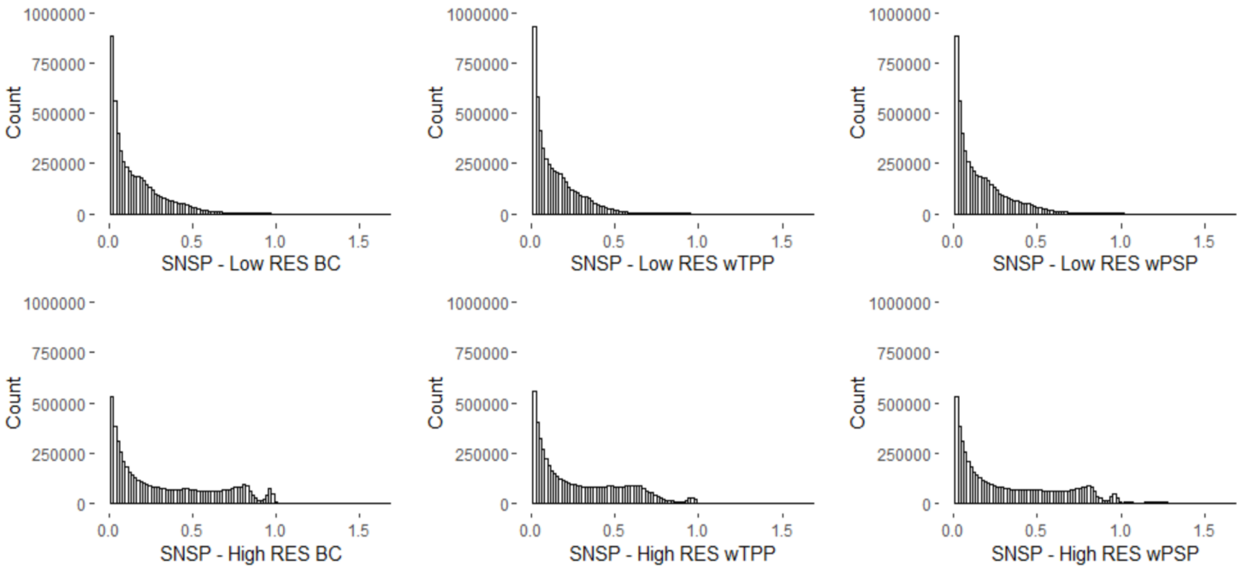

Fig. 11. Non-synchronous penetration ratio (SNSP) on a national level for the analyzed scenarios

6. CONCLUSION

The flexibility analysis for the Macedonian power system was done using a probabilistic market-based calculation on a PEMMDB-based market model for Southeast Europe. For North Macedonia, six national scenarios were analyzed as a combination of three development scenarios for the conventional power plants in MK and two VRES development scenarios, Section 3. The flexibility was assessed by computing the RPI, REPI, LORE, and SNSP metrics. Additionally, an analysis of the ramp span occurrence was done for the two VRES development scenarios.

The introduction of VRES to the system leads to a high ratio between RPI and REPI, which is mainly driven by the low load levels during the periods where the VRES production is the highest. Moreover, as shown in Table 2, the LORE parameter increases as more VRES are introduced to the system, which means that the risk for VRES curtailment in the future will be high. Since the flexibility needs are dependent on the regional evolution of the generation profiles in the neighboring countries, it is expected that as more VRES are introduced, the curtailment risk in MK and the region will be even higher. To avoid future VRES curtailment, it is important to run dedicated flexibility studies to assess the flexibility needs and optimize the conventional generation portfolio to a sufficiently flexible one while introducing smart technologies and techniques for flexibility provision. Furthermore, the Macedonian strategic framework for the energy sector should be reworked to consider different energy storage technologies, a shift from a fossil fuel-powered industry to an electricity-powered industry so to increase the overall load profile, or a redesign of the investment plan in the generation and storage portfolio to be suitably flexible to allow the country to become export oriented. Lastly, as the evolution of the generation profile is optimized, the national and regional legislation must be appropriately updated to support the needed changes.

Figures 5 and 6 show the ramp span occurrence for the slow-paced and rapid VRES development scenarios, respectively. As the results show, the one-hour ramp is the most frequent, followed by the two-hour, three-hour, four-hour, eight-hour, nine-hour, ten-hour, and eleven-hour ramps. In future flexibility studies, the one, two-hour, three-hour, four-hour, eight-hour, nine-hour, ten-hour, and eleven-hour ramps on system flexibility should be analyzed in more detail on a national level.

With the rapid development of the VRES profile in the region, a decarbonization phase is envisioned where conventional brown power plants are planned to be decommissioned. This will lead to a reduction of the available system inertia in the region, and in MK, it is expected that there will be periods with extremely low system inertia in the future if the evolution of the generation profile follows the rapid VRES development scenario. To avoid long periods of system instability, the focus should be on participation in regional markets for a share of reserves to optimally use the well-developed interconnections as well as developing the national markets to facilitate synthetic inertia provision from the large VRES parks.

The metrics in this paper are relatively easy to compute, and their computation isn’t computationally intensive compared to other more detailed methods. The obtained results represent a first-of-a-kind screening of the future flexibility needs in the Macedonian power sector, and they pave the way for future developments in this field on a national level. In the future, on a national level, the research focus should be on optimizing the flexibility portfolio from two aspects: reducing cost for adequate flexibility provision and introducing a flexibility analysis as an integrated part of the national adequacy studies. Furthermore, since the analysis of the system inertia showed that in the future, with the rapid development of VRES, the Macedonian power system would experience periods of extremely low system inertia, an analysis of the expected Rate of Change of Frequency (RoCoF) should be carried with a regional scope.

REFERENCES

[1] Price water house Coopers (PwC), MANU (2019): *The Strategy for Energy Development of the Republic of North Macedonia until 2040*.

[2] GIZ (2020): *National Energy and Climate Plan of the Republic of North Macedonia*.

[3] TAF-WB (2021): *Programme for the realisation of the Energy Development Strategy 2021 – 2025*.

[4] Cochran, J & Miller, Mackay & Zinaman, Owen & Milligan, Michael & Arent, Doug & Palmintier, Bryan & O'Malley, Mark & Mueller, S & Lannoye, Eamonn & Tuohy, Aidan & Kujala, B & Sommer, M & Holttinen, Hannele & Kiviluoma, Juha & Soonee, Sushil. (2014): *Flexibility in 21st Century Power Systems*.

[5] Lannoye, E., Flynn, D., O'Malley, M. (2012): Evaluation of Power System Flexibility, *IEEE Transactions on Power Systems*, Vol. **27**, no. 2, pp. 922–931. DOI: 10.1109/TPWRS.2011.2177280.

[6] IRENA (2018): *Power System Flexibility for the Energy Transition*, Part 2: *IRENA FlexTool Methodology*, International Renewable Energy Agency, Abu Dhabi.

[7] Tejada-Arango, D. A., Morales-España, G., Wogrin, S., Centeno, E. (2020): Power-Based Generation Expansion Planning for Flexibility Requirements, *IEEE Transactions on Power Systems*, Vol. **35**, no. 3, pp. 2012–2023, DOI:10.1109/TPWRS.2019.2940286

[8] Cañas-Carretón, M., Carrión, M. (2020): Generation capacity expansion considering reserve provision by wind power units, *IEEE Transactions on Power Systems*, Vol. **35**, no. 6, pp. 4564–4573. DOI: 10.1109/TPWRS.2020.2994173

[9] Huber, M., Dimkova, D., Hamacher, T. (2014): Integration of wind and solar power in Europe: Assessment of flexibility requirements, *Energy*, Vol. **69**, pp. 236–246, ISSN 0360–5442. https://doi.org/10.1016/j.energy.2014.02.109

[10] Ringkjøb, H-K., Haugan, P. M., Seljom, P., Lind, A., Wagner, F., Mesfun, S. (2020): Short-term solar and wind variability in long-term energy system models – A European case study, *Energy*, Vol. **209**, 118377, ISSN 0360-5442, https://doi.org/10.1016/j.energy.2020.118377.

[11] Frew, B. A., Becker, S., Dvorak, M.J., Andresen, G. B., Jacobson, M. Z. (2016): Flexibility mechanisms and pathways to a highly renewable US electricity future, *Energy*, Vol. **101**, pp. 65–78. https://doi.org/10.1016/j.energy.2016.01.079

[12] O'Sullivan, J., Rogers, A., Flynn, D., Smith, P., Mullane, A., O'Malley, M. (2014): Studying the maximum instantaneous non -synchronous generation in an island system – frequency stability challenges in Ireland, *IEEE Transactions on Power Systems*, Vol. **29**, no. 6, pp. 2943–2951. DOI: 10.1109/TPWRS.2014.2316974

[13] Stratigakos, A. C., Krommydas, K. F., Papageorgiou, P. C., Dikaiakos, C., Papaioannou, G. P. (2019): A suitable flexibility assessment approach for the pre-screening phase of power system planning applied on the Greek Power System, *IEEE EUROCON 2019 – 18th International Conference on Smart Technologies*, pp. 1–6. DOI: 10.1109/EUROCON.2019.8861888

[14] ELIA, Adequacy and Flexibility Study for Belgium 2022–2032. https://www.elia.be/en/electricity-market-and-system/adequacy/a dequacy-studies

[15] Bardet, R., Khallouf, P., Fournié, L. et al. (2019): *Mainstreaming RES : flexibility portfolios : design of flexibility portfolios at Member State level to facilitate a cost-efficient integration of high shares of renewables*, European Commission, Directorate-General for Energy, Publications Office. https://data.europa.eu/doi/10.2833/97595

[16] IEA (2011): *Harnessing Variable Renewables: A Guide to the Balancing Challenge*, OECD Publishing, Paris. https://doi.org/10.1787/9789264111394-en

[17] Bauknecht, D., Heinemann, C., Vogel, M. (2019): Study on the impact assessment for a new Directive mainstreaming deployment of renewable energy and ensuring that the EU meets its 2030 renewable energy target, Task 3.1: Historical assessment of progress made since 2005 in integration of renewable electricity in Europe and first-tier indicators for flexibility. https://energy.ec.europa.eu/design-flexibility-portfolios-member-state-level-facilitate-cost-efficient-integration-high-shares_en

[18] Ma, J., Silva, V., Belhomme, R., Kirschen, D. S., Ochoa, L. F. (2012): Exploring the use of flexibility indices in low carbon power systems, *3rd IEEE PES Innovative Smart Grid Technologies Europe (ISGT Europe)*, pp. 1–5. DOI: 10.1109/ISGTEurope.2012.6465757

[19] Blanco Poncela, M., Purvins, A., Chondrogiannis, S. (2018): Pan-European analysis on power system flexibility, *Energies*, **11** (7), JRC110658. ISSN 1996-1073,

[20] ENTSOE, European Resource Adequacy Assessment 2021 Edition – Executive Report, Brussels, 2021. https://www.entsoe.eu/outlooks/eraa/eraa-downloads

[21] RTE, Antares Simulator 7.1.0 – Optimization problems formulation. https://antares-simulator.org

[22] Ćosić, B., Krajačić, G., Duić, N. (2012): A 100% renewable energy system in the year 2050: The case of Macedonia, *Energy*, Vol. **48**, no. 1, pp. 80–87. DOI: 10.1016/j.energy.2012.06.078.

Journal of Electrical Engineering and Information Technologies, Vol. **8,** No. 2, pp. 83–92 (2023)
Article 209
Received: October 15, 2023
Accepted: November 29, 2023
In print: ISSN 2545–4250
On line: ISSN 2545–4269
UDC: 004.7.056.57:004.85
https://doi.org/10.51466/JEEIT2382209083s

Original scientific paper

OVERVIEW OF DEEP LEARNING TECHNIQUES FOR NETWORK INTRUSION DETECTION SYSTEMS

Goce Stevanoski[1], Aleksandar Risteski[2], Marko Porjazoski[2]

[1]*Military Academy "General Mihailo Apostolski", Goce Delčev University in Štip, Vasko Karangelevski St., 1000 Skopje, Republic of North Macedonia*
[2]*Faculty of Electrical Engineering and Information Technologies, "Ss. Cyril and Methodius" University in Skopje, Rugjer Bošković bb, P.O.Box 574, 1001 Skopje, Republic of North Macedonia*
goce.stevanoski@ugd.edu.mk

A b s t r a c t: The rapid advances in the new digital world are producing vast amounts of data. This gives more opportunities in business management, but it can also help in implementing new security techniques. Intrusion detection systems (IDS) are enforcing processes for analyzing network data. This study is reviewing the main Deep Learning approaches for intrusion detection in IT network traffic. In the beginning, the study gives an overview of the various IDS types and their usability in the IT network. Then it presents some of the most used Deep Learning techniques proposed by the research community in recent years. By analyzing various papers on the subject, current achievements, and limitations in developing IDS are detected and presented. The study ends by providing the future reach of the newly proposed Deep Learning techniques in monitoring and detecting malicious activities in network traffic.

Key words; intrusion detection systems; machine learning algorithms; deep learning

ПРЕГЛЕД НА ТЕХНИКИ ЗА ДЛАБОКО УЧЕЊЕ НА СИСТЕМИ ЗА ДЕТЕКЦИЈА НА НАПАДИ ВО МРЕЖИ

А п с т р а к т: Брзиот напредок на дигиталното општество предизвикува генерирање голем број податоци. Овие податоци покрај тоа што ги зголемуваат можностите за напредок на бизнисот можат многу да помогнат во справување со безбедносните предизвици во ИТ-инфраструктурата. Улогата на системот за детекција на напади е да врши анализа на мрежниот сообраќај и да ги детектира можните закани. Во трудот се обработени позначајните техники на учењето во длабочина. Разгледани се преку презентирање на нивниот начин на функционирање и како се користат во поновата литература од таа област. Со анализа на релевантни објавени научни трудови на темата се претставени моменталните достигнувања и ограничувања на новите решенија на IDS предложени во последните години користејќи техники на учење во длабочина. На крајот трудот дава преглед на идниот опсег на достигнувањата кои можат да се постигнат со техниките на длабоко учење во делот на мониторинг и детекција на злонамерни активности во мрежен сообраќај.

Клучни зборови: системи за детекција на напади; машинко учење; учење во длабочина

1. INTRODUCTION

Intrusion detection systems (IDs) are a critical segment of every well-established information security posture in an organization. In the security of IT networks, an intrusion is defined as an act of compromising the network resources and servers' infrastructure. An implementation of IDS is providing monitoring, detecting, and intentionally preventing malicious activity on the network to secure the confidentiality, integrity, and availability of the data [1].

The fast-growing evolution of network infrastructure with the introduction of many new services for supporting business continuity is generating enormous quantities of data and information.

This becomes a heavy burden for the IT security personnel and well-positioned IDS can significantly help in mitigating the security risk to organizational data. The implementation of IDS in the network infrastructure can help in detecting and preventing unusual activity in the network traffic.

Traditional IDS are based on technology that is enforcing too many rules on network traffic and this becomes a headache for the IT staff. On the other hand, Machine Learning (ML) technologies are giving an innovative approach to developing and utilizing IDSs in the network infrastructure. Since the beginning of the adoption of ML algorithms in the science community, ML was seen as a new and a potential way ahead for improving the shortcomings of the traditional IDS. The first ML-based IDSs were applying traditional ML algorithms which were able to notable classify the bad traffic from the good network traffic. This led to the introduction of many new ML technologies for IDS implementation.

Nowadays, Deep Learning (DL) techniques are the front runners in the application of ML in IDSs. The innovative approaches are giving remarkable results for pattern recognition and anomaly detection in network traffic. These results provide a very good foundation for enforcing DL techniques in IDS.

?. *Related work*

In the literature, the relevant studies for reviewing the DL approach in building IDS are done for synthesizing the current trends and achievements of the scientific community. In [2] the authors have analyzed the research in IDS using the ML approach until 2019 with a specific interest in the dataset, DL techniques, and metrics. Concluding that soft computing techniques are on the rise and that researchers are using old datasets that can limit the development of ML-based IDSs.

In another paper, [3], is providing a review of the ML technologies until 2020 by studying the proposed methodology, evaluation metrics, and dataset selection and discussing the strengths and limitations of the proposed solutions. Here, the author highlights various research challenges for the future.

In one of the most recent papers on the topic, the authors of [4] have done an incredibly detailed comparative study on various ML techniques such as artificial neural networks, support vector machines, decision trees, and hybrid classifiers. This study presents some of the datasets used in ML and the performance metrics for evaluating the ML models. Future work is also discussed.

2. INTRUSION DETECTION SYSTEMS

An Intrusion Detection Systems (IDS) makes regular checks on the network traffic for malicious activity on all inbound and outbound packets. If malicious activity is detected IDS can also enforce a security mechanism for preventing damage to the network environment and notify the system administrator about the attack. In comparison to the Firewall, the IDS has better detection of interior attacks, and it provides more reliable strategies for securing the perimeter.

The IDS can be classified into distinct categories depending on the implementation in the operational environment or the detection mechanism. IDS can be implemented as a Host Intrusion Detection System (HIDS) and as a Network Intrusion Detection System (NIDS).

Host intrusion detection system (HIDS) inspects traffic that originates from/to one device in the network. This type is limited in performance and cannot detect what is going on in the other parts of the network environment. Usually detects unusual connections, file changes, and file removal on one system and notifies the user of that system.

For inspecting network traffic, a NIDS is used. NIDS is part of the overall network security infrastructure on the organizational level. Usually is implemented on the main entering network points (gateways, routers) and it inspects the incoming and outgoing network traffic. NIDS checks the traffic for the known attacks' signatures in the data packets. If a match is found, NIDS can prevent damage to the network infrastructure and sends and notifications to the system administrator.

Signature-based detection mechanisms usually mean that the IDS must be regularly updated with the signature of newly discovered attacks. Otherwise, the IDS will be unable to detect and prevent new attacks. So, the inability to detect unknown attacks is one of the main shortcomings of IDS [5] and is a challenge for IDS based on Machine Learning techniques.

Machine learning intrusion detection systems

Machine learning-based implementation of IDS is a process of learning different patterns in data by machines (computer systems) from previously collected data and applying those patterns to newly acquired data. By this, the machines can make predictions about what kind of data is and act on the data or other systems. ML can be categorized based on the learning approach and the functionality of how they work on new data. The three main types of ML techniques categorized by the learning approach are supervised learning, unsupervised learning, and semi-supervised learning.

In supervised learning, the machine learns from labeled data to construct a pattern for future predictions. This learning is used for both classification and regression problems. The following are some of the most common ML algorithms for supervised learning: k-Nearest Neighbor, Decision Tree, Naïve Bayes, Support Vector Machine, Random Forest Algorithm, and Linear Regression Algorithm.

On the other hand, in unsupervised learning, machine learning with unlabeled data detects unknown cases. Some common ML algorithms for unsupervised learning are Hidden Markov Model, K-means Self-Organizing Map.

In semi-supervised learning, the machine learns with both labeled and unlabeled data. Some examples of semi-supervised algorithms are SVM, Gaussian Fields Approach, and Spectral Graph Transducer.

Furthermore, ML algorithms can be classified as Shallow Learning and Deep Learning. ML techniques with few layers are known as Shallow Learning (SL) and they are better for less complex tasks. The newly raised technique which uses more layers of a neural network is named Deep Learning (DL). DL is used for complex tasks and on a larger dataset.

ML techniques are noted as one of the best approaches for the effective development of IDS by providing, a high positive alarm rate, low false alarm rate, and improved detection rate [6]. These types of IDSs are using learning-based systems that can detect classes of attacks by comparing normal (benign) and bad (attack) traffic behavior. In our work we discuss the latest DL techniques for intrusion detection in IT networks.

3. DEEP LEARNING TECHNIQUES FOR IDS

Neural Networks have brought a new approach to building ML models. The DL techniques have shown that traditional ML techniques can be replaced by more efficient and more accurate ML models. In the following part, we are presenting some of the most used DL techniques for building ML models for IDS.

Restricted Boltzmann machine

Restricted Boltzmann machine (RBM) can find patterns in the data by reconstructing the input. Hinton in [7] introduced an approach that created the restricted Boltzmann machine. RBM, depicted in Figure 1, is a shallow two-layer network with visible and hidden layers. Each node in the visible layer relates to each node in the hidden layer. RBM is considered restricted because no two nodes in the same layer share a connection. The nodes are conditionally independent of each other in the same layer. In the forward pass, RBM takes the input and translates that into the set of numbers that encodes the input. In the backward pass, RBM takes the output set of numbers and sends them back to the visible layer to reconstruct the input. A well-trained network will be able to make translations with a remarkably high level of accuracy. In RBM weights and biases have a particularly important role. They help the RBM to determine the relationships among the import features and help RBM to decide which features are most important when they detect patterns. The training process consists of many forward and backward passes that are helping the RBM to reconstruct the input data. In the beginning, every input is combined with every individual weight and one overall bias. The result may or may not activate the hidden neurons. The same process is done in the next step with the backward process. In the backward pass, the input is combined with every individual weight and the overall bias. In the visible layer, the returned result is compared to the initial input to determine the quality of the results.

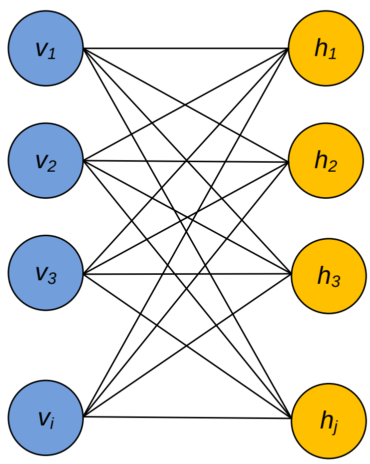

Fig. 1. Architecture of restricted Boltzmann machine (RBM)

This process is repeated until the input and the reconstructed result are as close as possible. Here learning means assigning a probability to every possible pair of visible/hidden vectors. The estimation of updating values is presented with Eqs. 1, 2, and 3 [8].

$$\Delta w_{ij} = \epsilon \left(v_i^{(0)} h_j^{(0)} - v_i^{(T)} h_j^{(t)} \right) \tag{1}$$

$$\Delta a_i = \epsilon \left(v_i^{(0)} - v_i^{(T)} \right) \tag{2}$$

$$\Delta b_j = \epsilon \left(h_j^{(0)} - h_j^{(t)} \right) \tag{3}$$

where:

v_i – is state of the visible unit *i*,

h_j – is state of the hidden unit *j*,

a_i – is bias of visible unit *i*,

b_j – is bias of hidden unit *j*,

w_{ij}– weight between visible unit and the hidden unit,

Δw_{ij}– is updating value for w_{ij},

Δa_i – is updating value for a_i,

Δb_j – is updating value for b_j,

ϵ – is the learning rate,

T – times of probabilistic distribution,

t – ????.

The application of RBM for network intrusion detection does not have many applications proposed by the scientific community. The authors in [9] are proposing an intrusion detection method with RBM as one phase in the methodology. In this paper, the authors are proposing the application of RBM for feature extraction since RBM has proven performance for unsupervised feature extraction which could be efficient to learn user behaviors from raw traffic data. Furthermore, the proposed method is utilizing the Feed-Forward Neural Network, automated FFNN, Random Forest (RF), and Support Vector Machine (SVM) ML techniques for classifying the network traffic in the observed domain. Their work shows that the proposed methodology can detect DDoS attacks efficiently and accurately.

Convolutional neural networks

Convolutional neural networks (CNNs) were introduced to overcome the problem of too many weights in neural networks. Used mostly in image recognition, CNN doesn't need data preprocessing, it can process raw data and extract the needed features. CNN is using spares connections and weight sharing which lowers the need for computational power and helps in the time complexity of the training. The data is transitioning over two layers, the convolutional layer, and the pooling layer of CNN. The process of training, depicted in Figure 2, is repeated for several convolutional – pooling iterations. In the convolutional layer the data is convoluted with fix sized kernels which sample the data to clusters – convoluted representation of the data and the kernel. Further, the pooling layer reduces the dimensionality of the convoluted data clusters. This reduction can be enforced with distinct functions but the most established are max-pooling and average pooling. With max-pooling the maximum value of the cluster is taken for the next iteration, whereas average pooling the average value of the processed cluster is taken for the next iteration.

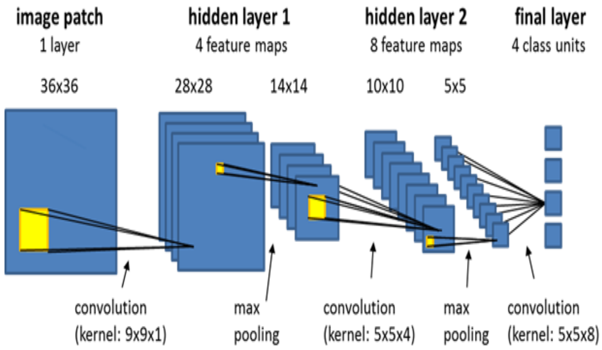

Fig. 2. Overview of the training process for CNN

As CNN is used for image recognition its use in IDS is challenging. There is much research done with CNN for IDS but developing a CNN model for IDS that will be reliable and effective is still a problem. The authors in [10] have notated this and proposed a method that will use evolutionary convolutional neural network (ECNN) for IDS. They are suggesting the use of multi-objective immune algorithm to optimize the accuracy and weights of CNNs. Their model has shown higher detection accuracy when compared to some state-of-the-art algorithms. Furthermore, the authors of [11] have suggested the use of IDS which can identify attacks by using model based on CNN. Here they are removing the redundant and irrelevant features in the network traffic data using various dimensionality reduction methods. Later the features from the dimensionality reduction data are extracted using CNN and the traffic vector had been converted to image so to reduce the computational cost. The authors proved that they method have not only theoretical value but also and the practical value by experimenting with the method on standard KDD-CUP99 dataset.

The authors at [12] have depict the usage of Binary Grey Wolf Optimization for detection of optimal features from the data. They have proposed a CNN approach named TreeNets. This method is identifying the attacks and segregates them into binary outcomes. With their work they exhibit three variants of TreeNets and made a comparison with a known state-of-the-art ML and DL models. The experiments have shown respectable results in detecting suspicious activity.

Overall, the scientific community is working on CNN application for IDS, but the work is not providing reliable and effective results. CNN can significantly improve the accuracy of classification but the convergence speed and ability for generalization of CNN is a problem that should be addressed in the future.

Recurrent neural networks

Recurrent Neural Network (RNN) is a type of Deep Learning network which is used for processing sequential data in layers of neurons. RNN is mostly used for supervised classification learning and incorporates input, hidden and output layers. Much of the work for data processing is done in the hidden layer. The architecture of RNN is shown in Figure 3. This network forms connections between the nodes in a directed structure and encompasses a feedback loop for applying the output values in the input layer. In building bigger models RNN is suffering from a vanishing/exploding gradient problem and the solution can be found in implementing Long-Short Term Memory (LSTM) and Gated Recurrent Units (GRU) models. These models possess an internal cell for storing input values which helps in processing directly corelated data from the dataset. The best results are achieved in applications where the output is predicted by analyzing the previous values of the data.

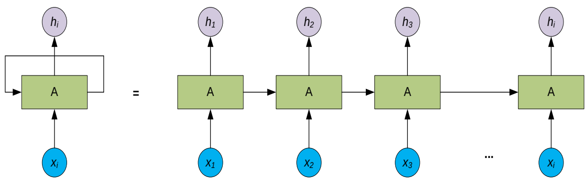

Fig. 3. Architecture of RNN

In [12] the authors are suggesting a hybrid DL model for IDS by using RNNs. The method is based on LSTM type of RNN and is proposed improved long-time memory tree model. This approach should have a secondary detection for solving problems with high false negative rate in RNN based IDS. For proving their work, they have made experiments with NSL-KDD data set. In another method, the authors of [13] have address the intrusion detection with combining two DL techniques CNN and RNN. Their work is done in two parts. The first is analyzing the payloads with CNN classification and the second part is detecting an attack with RNN classification. They are suggesting that the proposed model is learning the features without feature engineering, supports end-to-end detection and shows better results compared to some state-of-the-art methods. Similar approach is proposed by authors of [14] suggesting a hybrid model with CNN and LSTM-RNN networks. They are presenting that the model has obtained a high accuracy as 94.4% with previous hyper parameter tuning done by using deep learning architecture.

The ability of RNNs to store input values and use them later for making data correlation is a significant advantage in comparison to other NNs when are sequential data is processed. Combination of RNNs with various ML techniques in hybrid models has been seen as a right approach in application of RNNs for IDS.

AutoEncoder neural network

AutoEncoder (AE) is an unsupervised DL technique. It is used for building artificial neural networks that can learn data representations on the input of the network, to reconstruct as an output. AE is learning the features of a set of data, the purpose of it is for dimensionality reduction. The network, depicted in Figure 4, is symmetrically constructed and the numbers of neurons and layers on the input are the same as on the output. In the middle between the input and output layer, there is the smallest layer of all which is called the bottleneck layer.

The main reason for constructing this type of layer is to encode the input data from the input layer into the bottleneck layer and later decode the data on the output layer. Because of this functionality, the input layer is known as the encoder and the output layer is known as the decoder.

This process of reconstructing the input data on the output of the AE comes with some loss of level of data accuracy.

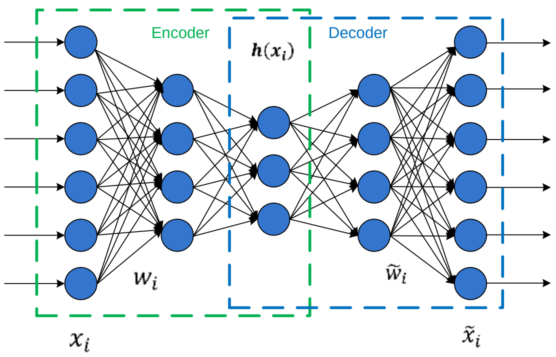

Fig. 4. Architecture of AutoEncoder neural network

If the AE is well-trained the loss is minimal. Eq. 4 represents the cost function of the AE.

$$J_{A,E} = \frac{1}{n}\sum_{i=1}^{n}\left(\frac{1}{2}\|\hat{x}_i - x_i\|^2\right), \quad (4)$$

where,

$J_{A,E}$ – is the value of the cost for input data,
n – is number of input samples,
x_i – is the value of the input data,
$\hat{x}_i$ – is the value of the output data.

The AE training is done in two stages in the first stage a Contrastive Divergence (CD) is used between neighboring pairs of input layers. In the second part with back backpropagation, the whole network is for finetuning. The process of reconstructing the data on the output is useful in many cases. A well-trained model can enforce noise reduction on the data and emphasize the meaningful feature of the input data, variational autoencoder can be trained to generate new data and by application on pattern recognition problems, the AE can detect the anomalies in sequential data.

In IDS AE is used for detecting anomalies in network traffic by segregating the usual traffic from the unusual traffic. This application of AE is constantly evolving, and the results are improving. In [15] the authors proposed a deep learning classification method in the process of data preprocessing for feature extraction. This approach has led them to the improved classification of performance and detection speed. The authors in [16] have proposed a similar method by combining DL and SL techniques. They presented an effective stacked contractive autoencoder (SCAE) for feature extraction from the raw network traffic. Further, they have used the SVM classification algorithm for improving the detection performance on two different evaluation datasets KDD Cup 99 and NSL-KDD. In the next paper [17] the authors are bringing together the AE and the Improved Genetic Algorithm BP (IGA-BP) in one proposed method. AE is used for the elimination of redundant information and for reducing data dimensionality. The IGA-BP network model solved the problems with slow detection rate and getting easy into local optimality in the BP network. Their findings from the experiments have shown that the proposed method has a significant effect on classification accuracy, false positives, and detection rate.

Overall, the work with autoencoders in the recent period is focused on improving the feature extraction in the preprocessing phase of the model building and combining the results with different ML techniques.

Generative adversarial networks

Generative Adversarial Networks (GANs) are a class of artificial intelligence algorithms used in unsupervised machine learning. GANs are implemented by a system of two neural networks contesting with each other in a zero-sum game framework. From a wide perspective GANs consist of two parts: the generator (G) and the discriminator (D), depicted in Figure 5.

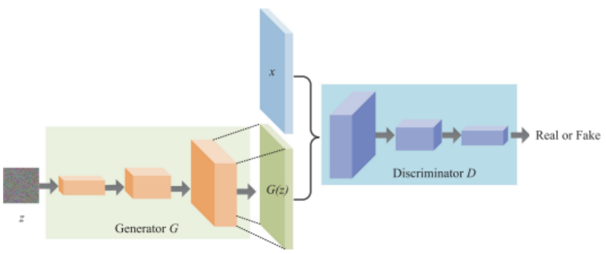

Fig. 5. The illustration of generative adversarial network

The generator creates data that is as realistic as possible, while the discriminator evaluates the data, trying to distinguish between real and generated data.

The primary goal of GANs is to generate high quality, realistic data, which makes them powerful tools for image generation, video generation, time-series data generation and more. In the system architecture generator and discriminator are typically deep neural networks. The architecture is designed such that both networks improve their performance in response to the other, creating a dynamic learning environment. During training, the generator's goal is to produce data that is indistinguishable from real data, thereby 'fooling' the discriminator. The discriminator learns to become better at distinguishing real data from the fake data created by the generator. This adversarial process continues until the generator produces data so close to real that the discriminator cannot reliably distinguish fake from real. Eq. 5 represents objective function of GANs that can be transformed into a minimax game,

$$\min \max V(D,G) = E_{x \sim p_{data(x)}}[\log D(x)] - \\ - E_{z \sim p_{z(z)}}[log(1 - D(G(z)))], \quad (5)$$

where x indicates the real data distribution from $p_{data(x)}$, E indicates the expectation, z indicates the vector from the random noise distribution $p_z(z)$, $G(z)$ and $D(x)$ indicates the samples generated by the generator, and the probability that D discriminates x as real data, respectively.

$D(G(z))$ indicates the probability that D determines the data generated by G. For the generator G, to fraud D, the discriminator probability $D(G(z))$ needs to be maximized, so $\log(1 - D(G(z)))$ will be minimized. For the discriminator D, a cross entropy function is used to distinguish between $G(z)$ and x, and D wants $V(D,G)$ to be maximized. In practice, G will be fixed firstly, and the parameters of discriminator D are updated to maximize the accuracy of D. And then, D is fixed to optimize G. When G and D have a sufficient capacity, the model will converge, and these two parts will reach the Nash equilibrium. At this time, $p_{data(x)} = pg(x)$, and the discriminator cannot determine the differences between these two distributions.

While primarily known for data generation in various fields including art generation, photo-realistic image synthesis, style transfer, and more, GANs can also be applied in anomaly detection for intrusion detection, where they learn to generate 'normal' data, and deviations from this can be flagged as anomalies. GANs are actively researched, and many researchers have shown the potential of GANs for intrusion detection.

AnoGAN was one of the first GAN that was proposed for anomaly detection in image data [18], and latter was applied to GAN-based intrusion detection in [19]. In AnoGAN, the generator receives information about a real instance and, if this was anomalous, it would learn to produce a fake benign instance using a technique called feature matching. A major disadvantage is that AnoGAN required a time-consuming backpropagation process to define the mapping for anomaly scoring and reconstruction of the data [20].

The project Efficient GAN-Based Anomaly Detection (EGBAD) improved the performance of AnoGAN by using a BiGAN design [19]. The EGBAD and AnoGAN were evaluated on the KDD-99 network intrusion dataset [21]. The influence of BiGAN encoder helped in eliminating much of the computation necessary for the scoring and reconstruction that originally influenced AnoGAN's training performance. This helped in increasing binary classification performance. For evaluation the authors used F1-scoring, which gives a clearer estimation of the performance then using raw accuracy. Results show that AnoGAN achieved an F1-score of 78.52%, EGBAD achieved 93.72% [18].

In IDSGAN, the generator was used for creating malicious traffic and the discriminator received responses from a simulated intrusion-detection system as input. In the research the model is tested on NSL-KDD dataset [21]. The IDSGAN was implemented based on a GAN using the performance metric of Wasserstein loss [22], this produced an "authenticity" score instead of a probability that an instance is part of the real dataset. With this the generator receives more specific information about how to adjust its weights and with that can create more stable model [23]. Here the intrusion-detection system was simulated with one of the following machine-learning algorithms: a Support-Vector Machine, Logistic Regression, Naive Bayes, k-Nearest Neighbors, Linear Programming, and Random Forest.

One proposal that has notably results was the Generative Adversarial Network Intrusion-Detection System (GIDS). The authors in this proposal are implementing a raw Controller Area Network (CAN) traffic data [24]. The CAN protocol it resembles industrial control system protocols and is used in automotive vehicles. The researchers tested two discriminators. The first one was trained on real traffic data, both malicious and benign. The second discriminator was trained on both fake and real data generated from the generator. Here the generator took a combination of normal and noise traffic data as input. For evaluation of the proposal the authors used accuracy, which is the proportion of correct predictions over total tested instances. In this research the first discriminator has detected over 99% of the malicious data that it was tested on, on the other hand, the second discriminator reached 98% accuracy on the attacks that were not known for the first discriminator. The proposed model shows that with combination of the two discriminators a 100% accuracy can be achieved.

Continuous advancements in GAN technology have led to more efficient and effective models. For instance, some research has focused on stabilizing the training process, which is traditionally challenging due to the adversarial nature of the networks.

In summary, GANs represent a significant breakthrough in the field of generative models, with their unique adversarial approach to learning, enabling a wide range of applications from realistic image generation to complex anomaly detection systems.

4. CHALLENGES AND OPPORTUNITIES IN FUTURE DL BASED IDS

Deep learning for intrusion detection systems (IDS) is a rapidly evolving field, with significant potential for advancements and innovations. We can highlight several areas that are interesting for future research and development. These areas not only focus on enhancing the accuracy and efficiency of intrusion detection but also address broader challenges such as adaptability, scalability, and integration with emerging technologies. Some of the future challenges include:

1. Federated learning for IDS [25]

This approach is working on developing federated learning approaches for IDS that enable collaborative learning across multiple devices or networks without sharing raw data, enhancing privacy and data security. This can lead to development of robust models that can learn from diverse network environments and adapt to local conditions without compromising sensitive data.

2. Explainable AI (XAI) in IDS [26]

Integrating XAI methods to make deep learning-based IDS more transparent and interpretable, helping security analysts understand and trust the decisions made by the system. They have the potential to develop IDS that provide actionable insights and explanations for detected threats, improving decision-making and response strategies.

3. Anomaly detection with advanced GANs [27]

In this approach advanced Generative Adversarial Networks (GANs) can be used for more sophisticated anomaly detection, especially for identifying novel or sophisticated attacks. In the future works GANs can simulate complex attack scenarios for better training of IDS and more effective detection of previously unseen attack types.

4. Integration with blockchain technology [28]

In this approach a combination of deep learning-based IDS with blockchain technology is used for ensuring secure and trustable network transactions. This can potentially lead to development of IDS solutions that ensure data integrity and traceability, enhancing accountability in security operations.

5. Handling encrypted traffic [29]

The main course of action for future work is in developing methods to detect malicious activities in encrypted traffic without decryption, respecting privacy while ensuring security. This can lead to potential novel approaches or models capable of analyzing encrypted data patterns to identify potential threats.

Future research in deep learning for intrusion detection systems is likely to focus on enhancing adaptability, explainability, real-time processing, and integration with other emerging technologies like IoT, Blockchain etc. These advancements aim not only to improve detection accuracy but also to address broader challenges in these technologies.

4. CONCLUSION

In this study, we made an overview of some of the most researched DL approaches applied in IDS. DL techniques are becoming more and more sophisticated and are taking over the field of ML for IDS from the traditional ML techniques. This is done by developing new DL applications or integrating the DL models with other techniques in various ensemble methods.

DL techniques, particularly those involving neural networks, are highly effective in detecting complex patterns and anomalies in data. They can identify subtle, non-linear relationships that traditional methods might not detect. Additionally, they can learn from new data continuously, allowing them to adapt to evolving cyber threats more effectively than traditional systems, which often rely on predefined rules and signatures. Applying these models it can help in automatically identify and extract relevant features from data, reducing the time and expertise required for system setup and maintenance.

Besides the positive aspects of DL for IDS there are shortcomings of these techniques that need to be addressed. The significant computational resources and power that these techniques require may not be feasible for smaller organizations or in environments with limited infrastructure. Additionally, due to their complexity, DL models are prone to overfitting, especially if not trained with sufficiently large and diverse datasets. Transparency and interpretability can be an issue too, since the DL models, particularly deep neural networks, are often seen as 'black boxes' due to their complex internal workings, making it difficult to understand the rationale behind specific detections or predictions.

The work has shown that the future of DL for IDS also brings many challenges and opportunities for development of new applications in various emerging technologies. This shows that DL for IDS is a very broad point for discussion in the field of cybersecurity and can contribute to the efforts for enhancing that field.

REFERENCES

[1] McHugh, J. (Aug. 2001): Intrusion and intrusion detection, *Int J Inf Secur*, Vol. **1**, no. 1, pp. 14–35. DOI: 10.1007/s102070100001

[2] Kok, S., Abdullah, A., Zaman, N., Supramaniam, M. (Nov. 2019): A review of intrusion detection system using machine learning approach, *International Journal of Engineering Research and Technology*, Vol. **12**, pp. 8–15.

[3] Ahmad, Z., Shahid Khan, Wai Shiang, A., C., Abdullah, J., Ahmad, F. (Jan. 2021): Network intrusion detection system: A systematic study of machine learning and deep learning approaches, *Transactions on Emerging Telecommunications Technologies*, Vol. **32**, no. 1. DOI: 10.1002/ett.4150

[4] Prethija, G., Katiravan, J. (2022): *Machine Learning and Deep Learning Approaches for Intrusion Detection: A Comparative Study*, Springer, pp. 75–95. DOI: 10.1007/978-981-16-5529-6_7

[5] Patcha, A., Park, J.-M. (Aug. 2007): An overview of anomaly detection techniques: Existing solutions and latest technological trends, *Computer Networks*, Vol. **51**, no. 12, pp. 3448–3470. DOI: 10.1016/j.comnet.2007.02.001

[6] Dayal, N., Maity, P., Srivastava, S., Khondoker, R. (Dec. 2016): Research trends in security and DDoS in SDN, *Security and Communication Networks*, Vol. **9**, no. 18, pp. 6386–6411. DOI: 10.1002/sec.1759

[7] Hinton, G. E. (Aug. 2002): Training products of experts by minimizing contrastive divergence, *Neural Comput*, Vol. **14**, no. 8, pp. 1771–1800. DOI:10.1162/089976602760128018

[8] Ogawa, S., Mori, H. (2019): A Gaussian-Gaussian-Restricted-Boltzmann-Machine-based Deep Neural Network Technique for Photovoltaic System Generation Forecasting, *IFAC-PapersOnLine*, Vol. **52**, no. 4, pp. 87–92. DOI: 10.1016/j.ifacol.2019.08.160

[9] Elsaeidy, A., Munasinghe, K. S., Sharma, D., Jamalipour, A. (Jun. 2019): Intrusion detection in smart cities using Restricted Boltzmann Machines, *Journal of Network and Computer Applications*, Vol. **135**, pp. 76–83. DOI: 10.1016/j.jnca.2019.02.026

[10] Chen, Y., Chen, S., Xuan, M., Lin, Q., Wei, W. (May 2021): Evolutionary convolutional neural network: An application to intrusion detection, In: *2021 13th International Conference on Advanced Computational Intelligence (ICACI)*, IEEE, pp. 245–252. DOI: 10.1109/ICACI52617.2021.9435859

[11] Xiao, Y., Xing, C., Zhang, T., Zhao, Z. (2019): *An intrusion detection model based on feature reduction and convolutional neural networks*, IEEE Access, Vol. **7**, pp. 42210–42219. DOI: 10.1109/ACCESS.2019.2904620

[12] Mishra, S., Dwivedula, R., Kshirsagar, V., Hota, C. (Jan. 2021): Robust detection of network intrusion using tree-based convolutional neural networks, In: *8th ACM IKDD CODS and 26th COMAD*, New York, NY, USA: ACM, pp. 233–237. DOI: 10.1145/3430984.3431036

[13] Wang, S., Xia, C., Wang, T. (May 2019): A novel intrusion detector based on deep learning hybrid methods, In: *2019 IEEE 5th Intl Conference on Big Data Security on Cloud (BigDataSecurity), IEEE Intl Conference on High Performance and Smart Computing, (HPSC) and IEEE Intl Conference on Intelligent Data and Security (IDS)*, IEEE, pp. 300–305. DOI: 10.1109/BigDataSecurity-HPSC-IDS.2019.00062

[14] Liu, H., Lang, B., Liu, M., H. Yan, M. (Jan. 2019): CNN and RNN based payload classification methods for attack detection, *Knowl Based Syst*, Vol. **163**, pp. 332–341. DOI: 10.1016/j.knosys.2018.08.036

[15] Akarsh, S., Simran, K., Poornachandran, P., Menon, V. K., Soman, K. P. (Mar. 2019): Deep learning framework and visualization for malware classification, In: *5th International Conference on Advanced Computing & Communication Systems (ICACCS)*, IEEE, pp. 1059–1063. DOI: 10.1109/ICACCS.2019.8728471

[16] Lee, J., Pak, J., Lee, M. (Oct. 2020): Network Intrusion detection system using feature extraction based on deep sparse autoencoder, In: *International Conference on Information and Communication Technology Convergence (ICTC)*, IEEE, pp. 1282–1287. DOI: 10.1109/ICTC49870.2020.9289253

[17] Deng, H., Yang, T. (Jul. 2021): Network intrusion detection based on sparse autoencoder and IGA-BP network, *Wirel Commun Mob Comput*, Vol. **2021**, pp. 1–11. DOI: 10.1155/2021/9510858.

[18] Di Mattia, F., Galeone, P., De Simoni, M., Ghelfi, E. (Jun. 2019): A Survey on GANs for Anomaly Detection.

[19] Zenati, H., Foo, C. S., Lecouat, B., Manek, G., Chandrasekhar, V. R. (Feb. 2018): *Efficient GAN-Based Anomaly Detection*.

[20] Schlegl, T., Seeböck, P., Waldstein, S. M., Schmidt-Erfurth, U., Langs, G. (March 2017): *Unsupervised Anomaly Detection with Generative Adversarial Networks to Guide Marker Discovery*.

[21] Tavallaee, M., Bagheri, E., Lu, W., Ghorbani, A. A. (July 2009): A detailed analysis of the KDD CUP 99 data set, In: *2009 IEEE Symposium on Computational Intelligence for Security and Defense Applications*, IEEE, pp. 1–6. DOI: 10.1109/CISDA.2009.5356528

[22] Martin Arjovsky, S. C. L. B. (2017): Wasserstein generative adversarial networks, In: *ICML'17: Proceedings of the 34th International Conference on Machine Learning*, pp. 214–223.

[23] Lucic, M., Kurach, K., Michalski, M., Gelly, S., Bousquet, O. (Nov. 2017): *Are GANs Created Equal?* A Large-Scale Study.

[24] Seo, E., Song, H. M., Kim, H. K. (Aug. 2018): GIDS: GAN based intrusion detection system for In-Vehicle Network, In: *16th Annual Conference on Privacy, Security and Trust (PST)*, IEEE, pp. 1–6. DOI: 10.1109/PST.2018.8514157

[25] Agrawal, S. et al. (Nov. 2022): Federated Learning for intrusion detection system: Concepts, challenges and future directions, *Comput Commun*, Vol. **195**, pp. 346–361. DOI: 10.1016/j.comcom.2022.09.012

[26] Patil, S. et al. (Sep. 2022): Explainable artificial intelligene for intrusion detection system, *Electronics (Basel)*, Vol. **11**, no. 19, p. 3079. DOI: 10.3390/electronics11193079

[27] Jain, S., Seth, G., Paruthi, A., Soni, U., Kumar, G. (Apr. 2022): Synthetic data augmentation for surface defect detection and classification using deep learning, *J Intell Manuf*, Vol. **33**, no. 4, pp. 1007–1020. DOI: 10.1007/s10845-020-01710-x

[28] Mathew, S. S., Hayawi, K., Dawit, N. A., Taleb, I., Trabelsi, Z. (Dec. 2022): Integration of blockchain and collaborative intrusion detection for secure data transactions in industrial IoT: a survey, *Cluster Comput*, Vol. **25**, no. 6, pp. 4129–4149. DOI: 10.1007/s10586-022-03645-9

[29] Bakhshi, T., Ghita, B. (Sep. 2021): Anomaly detection in encrypted internet traffic using hybrid deep learning, *Security and Communication Networks*, Vol. **2021**, pp. 1–16. DOI: 10.1155/2021/5363750

Journal of Electrical Engineering and Information Technologies, Vol. **8,** No. 2, pp. 93–100 (2023)
Article 210
In print: ISSN 2545–4250
Received: November 4, 2023
On line: ISSN 2545–4269
Accepted: December 6, 2023
UDC: 004.652.3-027.544/.545:[002:378.2
https://doi.org/10.51466/JEEIT2382210093r

Original scientific paper

DATABASE DESIGN IN A BLOCKCHAIN-BASED SYSTEM FOR GENERATING AND VERIFYING ACADEMIC CREDENTIALS

Avni Rustemi[1,2], Vladimir Atanasovski[1], Aleksandar Risteski[1]

[1]*Faculty of Electrical Engineering and Information Technologies, "Ss. Cyril and Methodius" University in Skopje, Rugjer Bošković bb, P.O.Box 574, 1001 Skopje, Republic of North Macedonia*
[2]*Department of Informatics, Faculty of Mathematics and Natural Sciences, Tetovo University, 1200 Tetovo, Republic of North Macedonia*
avni.rustemi@unite.edu.mk

A b s t r a c t: The management of data and their storage in the database for an indefinite time, whether in a centralized or decentralized form, is of great importance for the operation of the system and its efficiency. One of the challenges that decentralized systems are facing is the lack of decentralized management of databases, because they have limitations in terms of inserting, updating, and deleting data. The generation of diplomas is a more sensitive issue and one of the reasons why it has not been digitalized to date is the fact that centralized systems do not offer sufficient security for the generation of such documents, since the same systems must be controlled by third people or administrators of the system, where there is also the suspicion of data misuse. Through the paper, we will compare centralized and decentralized databases, the operation of decentralized databases, and finally present a scheme of our vision about the operation of the database in the blockchain-based system for the generation and verification of diplomas.

Key words: entralized database: decentralized database: blockchain system: diploma

ДИЗАЈН НА БАЗА НА ПОДАТОЦИ ВО СИСТЕМ ЗАСНОВАН НА БЛОКЧЕЈН ЗА ИЗДАВАЊЕ И ПРОВЕРКА НА АКАДЕМСКИ ДОКУМЕНТИ

А п с т р а к т: Управувањето со податоците и нивното складирање во базата на податоци на неопределено време, било во централизирана или децентрализирана форма, е од големо значење за функционирањето на системот и неговата ефикасност. Еден од предизвиците со кои се соочуваат децентрализираните системи е немањето децентрализирано управување со базите на податоци, бидејќи имаат ограничувања во однос на вметнување, ажурирање и бришење податоци. Издавањето дипломи е чувствително прашање и една од причините зошто до денес не е дигитализирано е фактот што централизираните системи не нудат доволна сигурност за издавање такви документи, бидејќи истите тие системи мора да бидат контролирани од трети лица или администратори на системот, бидејќи и кај нив постои сомнеж за злоупотреба на податоците. Во трудот ги споредуваме централизираните и децентрализираните бази на податоци, работата на децентрализираните бази на податоци и на крајот претставуваме шема за тоа како ја замислуваме работата на систем за издавање и верификација на дипломи базиран на блокчејн.

Клучни зборови: централизирана база на податоци; децентрализирана база на податоци; систем блокчејн; диплома

1. INTRODUCTION

Very important for a higher education institution is efficient management, real-time generation, safe and secure storage of data in certain databases for a longer period of time. During the creation of a certain system, it is very important to choose the platform where the same will be implemented, the auxiliary equipment and to provide opportunities for updating the system without affecting the data in the database. Also, the reuse of architectures, models and certain parts of the code, speed up the creation time, reduce costs, and make the system easily adaptable to different platforms. Blockchain technology is seen as a solution for digitizing services as a whole, including the process of generating and verifying diplomas. This technology offers distributed data processing networks, generating data automatically without the intervention of the third parties. However, despite the fact that blockchain technology is finding a wide application in many fields, in education, and especially in higher education institutions, it is encountering many difficulties. From the systematic literature review [1], it turns out that despite many challenges and obstacles, one of the main ones is that there is a lack of developers' interest in blockchain programming, and the creation of data management systems. There is a lack of interoperability between decentralized databases and programming languages with which the system is developed as a whole, and the smart contract in particular. The generation must be connected with the preliminary processes in the blockchain system, from enrollment process, evaluation to obtaining grades and credits in certain subjects. Smart contract and blockchain programming have certain limitations, because they are compatible only on the Ethereum platform, while the same platform cannot achieve the maximum performance, due to many characteristics. The automation of services has its challenges and limitations, where for every mistake the data cannot be updated, and requires deletion and regeneration of the same. Blockchain systems require much more auxiliary tools to carry out transactions than centralized systems. And finally, there is a lack of architectures and concrete standard models that describe the processes of generation and verification of diplomas, respectively there is a lack of literature. Table 1 gives a description of the characteristics that blockchain-based systems possess, where, among other things, the same should offer high security, identity protection, transparency of services, their classification and even the generation and verification of academic documents quickly and safely [2].

Despite the fact that so far several educational platforms have been implemented for the educational process in higher education institutions [3], even for the verification of diplomas [4], however, most of them have been tested with several data and there is no research that shows that the same are being used or have shown good or bad results during application.

Table 1

Characteristics of blockchain-based system

Characteristics	Description
Privacy	Divide the services into private and public
Traceability	The data is immutable, alerts any change
Transparency	Services are transparent, easy and fast verification of diplomas
Safety	Intelligent and cryptographic mechanisms
Trust	Gain people's trust from the characteristics it possesses

2. SMART CONTRACT USABILITY

Presented in the simplest form, the process of communication between the user and the blockchain network is given the Figure 1. Between the user interface and the execution of the smart contract is the web3 provider, as well as between blockchain network and smart contract it is blockchain api. Smart contracts are compatible with Solidity as a programming language while their execution is done on the Ethereum platform, as one of the platforms most compatible with smart contracts [5]. Each smart contract represents a digital object in a blockchain system. Every transaction on the Ethereum platform represents a smart contract [6].

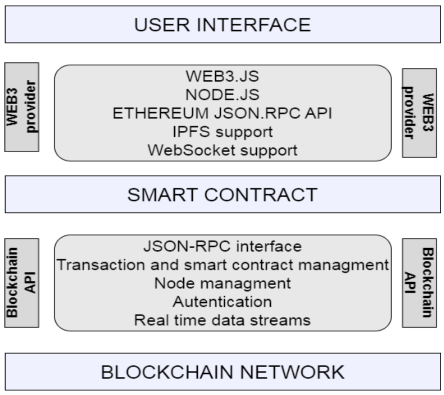

Fig. 1. Interaction between blockchain network and user

To support the work of smart contract developers, online environments called Remix IDE have been created. Smart contract can be used in banking systems for loans, automatic management of bank transactions related to large companies, in medicine for health insurance, automatic allocation of financial resources to clinics based on fulfilled conditions, in health insurance for damage assessment based on the conditions as well as many other areas, where a fair judgment with preliminary conditions is needed [7].

In medicine for the automatic processing of doctors' requests, for the allocation of financial resources to clinics. In electronic commerce for the management of payments, online orders. In aviation for automatic flight management, ticket booking, payment system.

Regarding the application of smart contract in higher education institutions, they are used in digital certificates, for the process of storing, verification and validation of certificates, as a supporting tool for many processes such as online learning, various online trainings for students and academic staff, the management of the bookstore in the institution of higher education, student payments, students' knowledge evaluate, student evidence, registration process [8]. Among the many challenges that we have mentioned in [9], there is also the challenge of standardizing smart contracts and their automatic generation on the Ethereum platform, since for higher education institutions, such a phenomenon is limited. Any error in the data must result in its re-generation, then the cost doubles, since the cost of maintaining the blockchain system itself is much higher than the cost of centralized systems. The immutability of smart contracts makes it even more difficult to adapt and reuse them.

Figure 2 presents the smart contract execution process, starting from the invoking smart contract until the successful implementation or not, depending on the money we have in the wallet, as long as Figure 3 summarizes some of the challenges facing blockchain technology in higher education institutions (HEI).

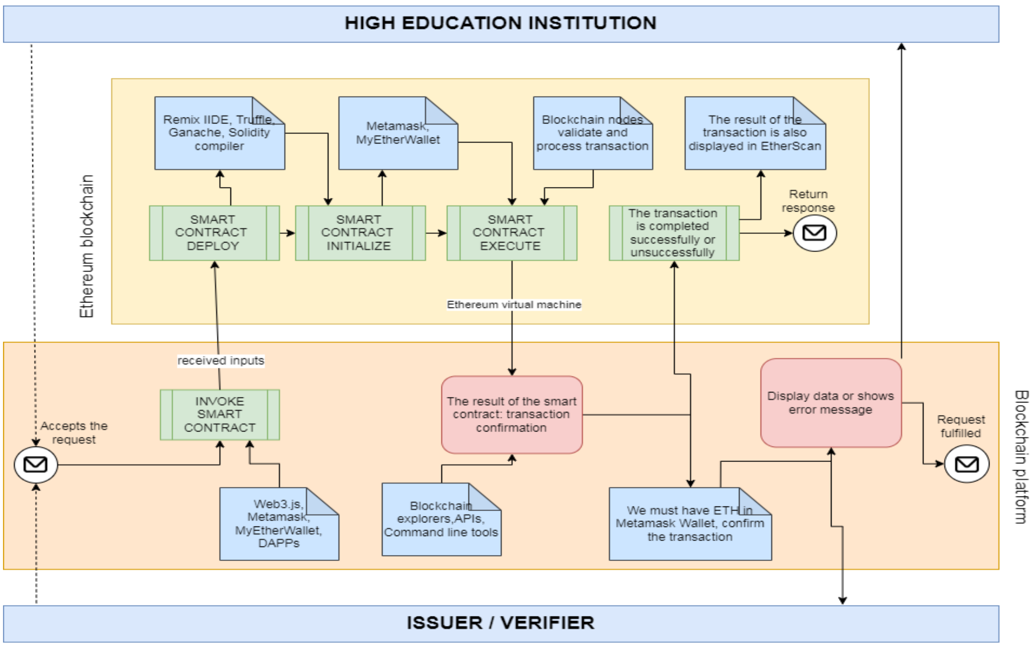

Fig. 2. Smart contract executing process

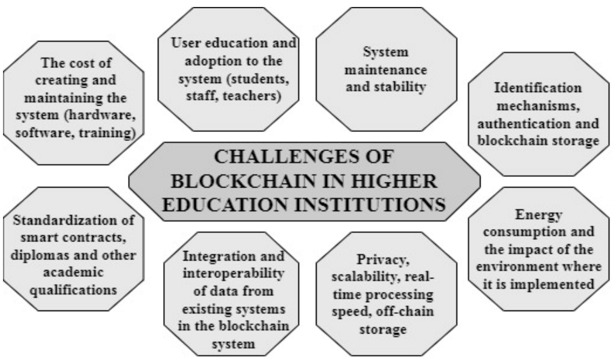

Fig. 3. Challenges of blockchain in HEI

3. DECENTRALIZED SYSTEM AND DATABASES CHARACTERISTICS

The development of information computer technologies (ICT) and the digitization of services has caused that in almost all spheres of life, most services are digitized and generated electronically through various devices. Compared to the past, with traditional learning methods, where students have had the opportunity to acquire knowledge only through books, nowadays they can access any information they need in digital form in a very short time through digital devices [17]. Learning Management Systems (LMS) also facilitate the educational process in higher education institutions. Today, the distribution of literature, electronic learning, real-time tasks, electronic evidence, distance learning, and the classroom, are just some of the many opportunities that students have thanks to LMS. It is worth emphasizing a great help of Youtube in this direction, where through videos the teachers very easily share to the students the lessons with relevant explanations, which luckily the same can be shared into the LMS and in the classroom [20]. Centralized systems always have a third intermediary in the generation of each service, respectively every service must be generated by the administrative staff, or other responsible persons, up to the administrator. The application of artificial intelligence in centralized systems has helped to develop processes in an independent form, respectively intelligent devices have the ability to learn from human actions, however, centralized systems must have an administrator who controls every process in the system and is responsible for whatever happens in the system. [18]. Despite the fact that there are many developments in centralized systems, offering fast, secure data processing, by the word itself we mean that someone has access to the data, and he is definitely the system administrator. Precisely for this reason, privacy, authentication and even the possible misuse of data and the use of the same for malicious purposes are put into question. What is more worrying, in such systems, in institutions of higher education, in addition to the administrator, IT managers and the higher management of the institution have access, which means that the possibility of misuse is even higher. And the system lacks a traceability that cannot be hidden, but that shows precisely every possible change of the data and by whom it was made [19].

Decentralized systems in comparison to centralized ones have some advantages, however, the respective limitations. In the following, we will mention some differences of the same to continue with the types and clarification of decentralized databases.

- Privacy, transparency, traceability, identity [10]. Lack of self-identification mechanisms, the target of numerous attacks, the cause of transparency
- Reuse and adaptability, decentralization and distributed ledger [11].Reuse depends on standardization, adaptation is difficult especially from centralized to decentralized systems, decentralization has more deficiencies in storage for a longer period of time and response in real time.
- Immutability of smart contract and blockchain platform [12, 14]. Every error requires the regeneration of the smart contract, smart contracts are only compatible with the Ethereum platform, which limits it in many features
- Safety and cost, electricity consumption, maintenance [13, 14]. The generation and verification of diplomas have a low cost, but their maintenance for a longer time is expensive, because blockchain itself is an expensive technology.
- Decentralized data storage, off-chain storage [15]. All current systems work with centralized databases, and adaptation to decentralized databases is very difficult.
- User interface, compatibility, guide and documentation [15]. The design of the system must be compatible for all intelligent devices, lack of documentation and experts in this field.
- Fast generation, verification, online support all the time [13–15]. It requires high costs, because it is in direct proportion to the energy consumed and the blockchain auxiliary equipment used for the system. There is a lack of programmers and experts in this direction

As for decentralized databases, there are several of them, whether as file storage, cloud platforms or even blockchain databases, among which we will mention:

- Interplanetary file storage (IPFS), which has shown good results in data management in certain capacities with blockchain systems, which is based on the peer-to-peer protocol, and uses the addressing method to store and receive data.
- BigChainDB, combines blockchain technology with decentralized databases. In fact, it is used for storing and processing the largest amounts of data in the blockchain network.
- Swarm, is a peer to peer protocol, which stores data in an unchangeable form. It runs on the Ethereum platform [16].
- Cassandra, is a NoSQL database, which is based on the addition of more nodes for data storage, which is actually known as the continuation of SQL databases, and those who are familiar with it, find it very easy to use Cassandra.
- ChainifyDB, is a blockchain layer that has recently been used as an auxiliary tool for existing blockchain databases, and is also used as a connecting tool for data in the blockchain network.
- CovenantSQL, is a blockchain database that attempts to combine the characteristics of central-

ized databases with the characteristics of blockchain, giving primary importance to the issue of privacy and data security.

- Modex Blockchain Database (BCDB), developed by the company Modex, known for its research in the field of blockchain. It aims to combine the advantages of traditional centralized databases with the immutability and transparency of the blockchain.
- Postchain, developed by ChromaWay company, specialized in smart contract and decentralized applications. It also aims to combine relational databases with blockchain technology.

4. DATABASE DESIGN FOR BLOCKCHAIN SYSTEM

Very important for the selection of the blockchain database are several factors such as the data structure, consensus mechanisms, node types, block structure, determining the amount of data to be stored and processed, up to security strategies, scalability, transparency. In order to have a clearer overview of the functioning of the blockchain system, for the generation and verification of diplomas, including the database, we will present a class diagram through Figure 4, as part of the UML diagrams. In this diagram, we have simultaneously presented the most important elements that are necessary for the implementation of the blockchain system for the generation and verification of diplomas, including the blockchain database. Both processes, the generation of diplomas and the verification, are connected to the blockchain database. And the blockchain database works through the Ethereum blockchain platform, with which the data is mined, validated, encrypted and sent in a distributed form to the respective database. Very important for the efficient generation of diplomas, is the insertion of data in a detailed form in the system, taking special care for all information not to be mistaken, because every mistake has its own cost in the blockchain system. It is of little importance whether Homomorphic Encryption, Zero-Knowledge Proofs or Elliptic Curve Cryptography will be used, as they aim to preserve data security, privacy, collaboration and database management in a protected way [16].

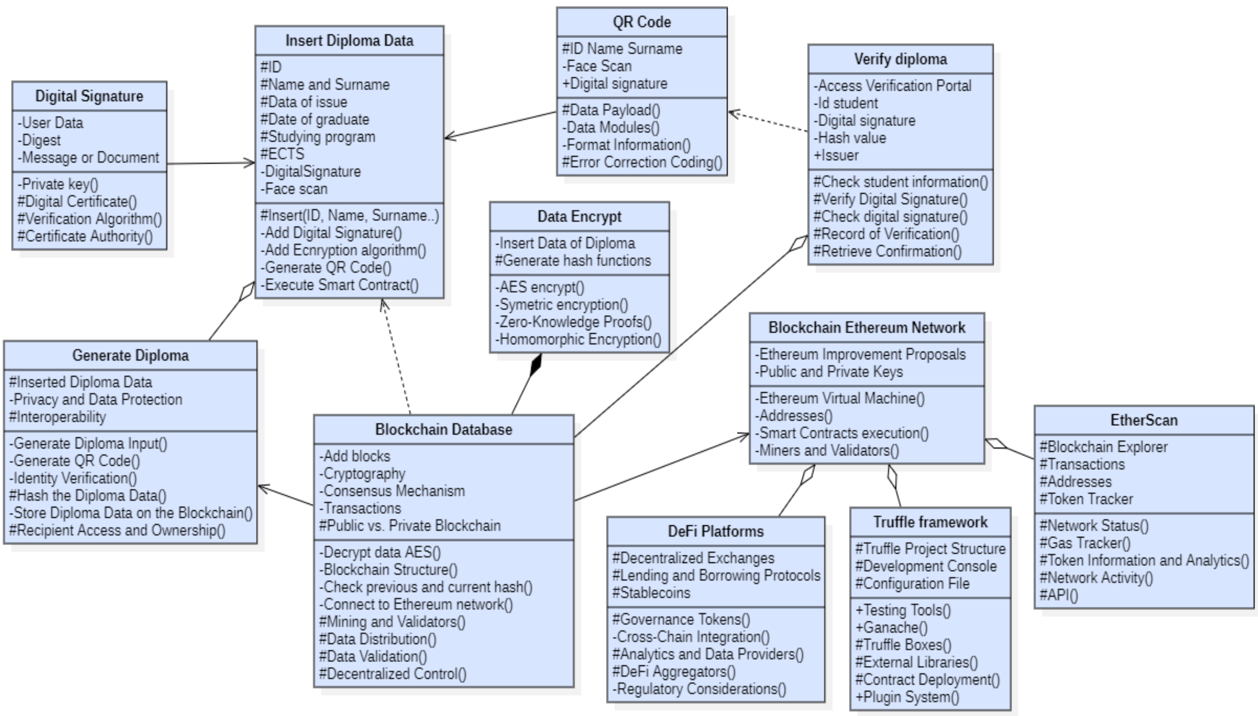

Fig. 4. Class diagram for blockchain system and database design

The digital signature is very important during the insertion of the data in the database, as the same must be signed at the end by the student but also by the institution's management. As part of the digital signature, we have operations such as: private key generation, digital certificates, certificate authorization, algorithms for verification. It is very important for quick verification to attach the QR code to the generation of the diploma. QR code, on the one hand, verifies the immutability of the data, since all the data is generated in the QR code, but on the other hand, it is very easy to verify the data, since the data that is part of the QR code can be verified through very easy applications. Within the blockchain database, we have presented the following operations: data decryption and encryption, blockchain structure for data storage and distribution, checking previous and current hash values, connection to Ethereum blockchain network, mining and validation, decentralized data control. Additionally to description of the class diagram for blockchain system and database design presented on Figure 4, Figure 5 illustrates the sequential diagram of the process of generating the diploma in electronic form, digitally signed by both the student and the institution of higher education.

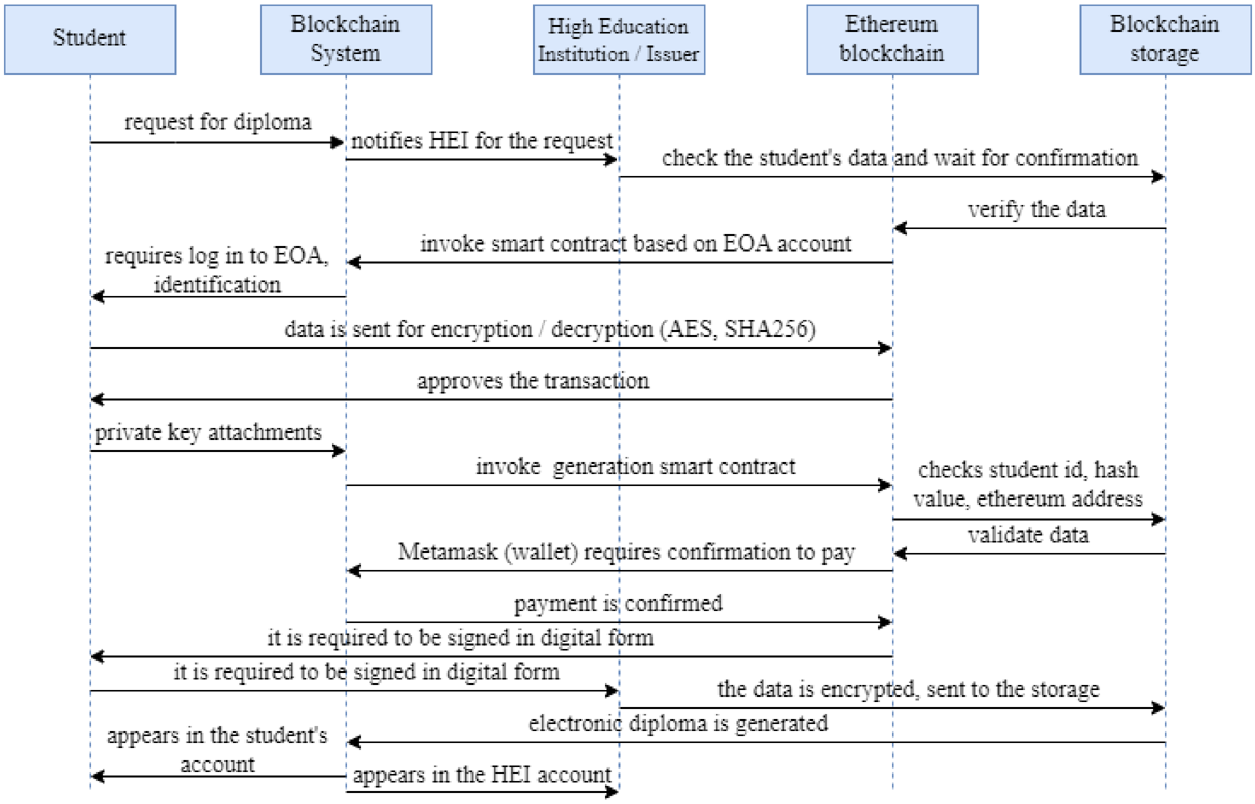

Fig 5. Sequence diagram of diploma generation form blockchain system

Based on the systematic literature review [1], which we have done regarding the implementation of blockchain in higher education institutions, it turns out that there are only few architectures, models and adequate literature that show the details of the implementation of systems or blockchain solutions in this direction. Although there is a considerable number of blockchain solutions, again there is no research that shows the success or failure of the ones or their practical implementation in any institution of higher education. It is characteristic that most blockchain solutions have used the Ethereum platform, Solidity for smart contract programming, and Truffle suite as a package with the tools for the development of the blockchain network infrastructure. Because we are in the phase of designing a system based on blockchain technology for the generation and verification of diplomas, after numerous analyses of the numerous challenges and limitations in terms of the practical implementation of the smart contract, it is very important to include all the details of implementation, to be as accurate as possible in programming the smart contract and overcoming the limitations so far. Only after we have implemented the initial prototype based on the architecture and the conceptual model we are developing, we will be able to have analyses and comparisons, respectively quantitative analyses of the performance of the system in real time, to test the validity of the same based on the defined architecture. The optimization and testing of the smart contract is of great importance for the creation of the blockchain system for the generation and verification of diplomas. There are different smart contract testing techniques, such as Mutation testing, OYENTE, Zeus, Vandal, ContractFuzzer, GasSaver, SmartBug, while optimization has to do with the detailed analysis of the code during programming and the overcoming of useless and unnecessary elements with the aim of reducing the cost and execution time of the smart contract [21].

5. CONCLUSION

Regarding the application of blockchain in higher education institutions, we have done a lot of research, review, definition of architecture, use case diagrams and scenarios for the main actors in this system. We also designed the conceptual model, describing in detail the process of inserting and verifying diplomas, in the form of systematic architectures. This means that detailed analyses have been made in terms of the practical application of the system. Through this paper, after describing the importance of blockchain for higher education institutions, we described the importance of smart contracts and the challenges in terms of their application in higher education institutions. Through the paper we tried to make a comparison between centralized and decentralized systems, and then also the description of some decentralized databases that are towards development recently. And in the end, we paid special attention to the design through the class diagram of the blockchain system and in particular to describe the importance of the blockchain-based database for the blockchain system. The primary importance of this work is the creation of the architecture of how the smart contract execution process flows, the design and importance of the blockchain database in the creation of the blockchain system. The next challenge is the practical implementation of the system, quantitative analysis of the code's performance, including real-time analysis and results of the generation and verification of diplomas, which we will present in the next research.

REFERENCES

[1] Rustemi A., Dalipi F., Atanasovski V., Risteski A. (2023): A systematic literature review on blockchain-based systems for academic certificate verification, *IEEE Access*, Vol. **11**, pp. 64679–64696. DOI: 10.1109/ACCESS.2023.3289598

[2] Peng Y., Yang X., Zhou H. (2021): Blockchain technology and higher education: characteristics, dilemma and development path. In: *Proceedings of the 2020 4th International Conference on Education and E-Learning (ICEEL '20)*. Association for Computing Machinery, New York, NY, USA, 173–176. https://doi.org/10.1145/3439147.3439185

[3] Saleh O., Ghazali O., Rana, M. E. (2020): Blockchain based framework for educational certificates verification. *Journal of Critical Reviews*. **7**. 79–84. 10.31838/jcr.07.03.13.

[4] Hsu, C. S., Tu, S. F., Chiu, P. C. (2022): Design of an e-diploma system based on consortium blockchain and facial recognition. *Educ Inf Technol* **27**, 5495–5519. https://doi.org/10.1007/s10639-021-10840-5

[5] Gugnani P., Godfrey W. W., Sadhya D. (2022): Ethereum based smart contract for event management system, In: *2022 IEEE 6th Conference on Information and Communication Technology (CICT)*, Gwalior, India, pp. 1–5. DOi: 10.1109/CICT56698.2022.9997939

[6] Nguyen D.-H., Nguyen-Duc D.-N., Huynh-Tuong N., H.-A. (2018): CVSS: A blockchainized certificate verifying support system. In: *Proceedings of the 9th International Symposium on Information and Communication Technology (SoICT '18)*. Association for Computing Machinery, New York, NY.

[7] Geroni, D. (September 16, 2021): Top 12 Smart coctract use cases, [Online]. Available: https://101blockchains.com/smart-contract-use-cases/

[8] Awaji, B., Solaiman, E., Albshri, A. (2020): Blockchain-based applications in higher education: a systematic mapping study. In: *Proceedings of the 5th International Conference on Information and Education Innovations (ICIEI '20)*. ACM, New York, NY, USA, 96–104. https://doi.org/10.1145/3411681.3411688

[9] Rustemi, A., Atanasovski, V., Risteski, A. (2023): Identification during verification of diplomas. In: *The Blockchain System. 2023 30th International Conference on Systems, Signals and Image Processing (IWSSIP)*, Ohrid, North Macedonia, pp. 1–5. DOI: 10.1109/IWSSIP58668.2023.10180241

[10] Cernian, A., Vlasceanu, E., Tiganoaia, B., Iftemi, A. (2021): Deploying blockchain technology for storing digital diplomas. In: *23rd International Conference on Control Systems and Computer Science (CSCS)*, Bucharest, Romania, pp. 322–327. DOI: 10.1109/CSCS52396.2021.00059

[11] Pandey, S., et al. (2022): Do-it-yourself recommender system: Rreusing and Recycling with Blockchain and Deep Learning., In: *IEEE Access*, Vol. **10**, pp. 90056–90067. DOI: 10.1109/ACCESS.2022.3199661

[12] Zhu P., Hu J., Zhang Y., Li X. (2020): A blockchain based solution for medication anti-counterfeiting and traceability, *IEEE Access*, Vol. **8**, pp. 184256–184272. DOI: 10.1109/ACCESS.2020.3029196

[13] Ge, X. et al. (2023): Blockchain and green certificates based market structure and transaction mechanism of direct power-purchase for industrial users. In: *IEEE Transactions on Industry Applications*, Vol. **59**, no. 3, pp. 2892–2903. DOI: 10.1109/TIA.2023.3246966

[14] Kaur, J., Rani, R., Kalra, N. (2022): an automated liver disease detection system using machine learning and smart contract, *2022 IEEE International Conference on Current Development in Engineering and Technology (CCET)*, Bhopal, India, pp. 1–5. DOI: 10.1109/CCET56606.2022

[15] Wang, Y., Su, Z., Xu, Q., Li, R., Luan, T. H., Wang, P. (2022): A secure and intelligent data sharing scheme for uav-assisted disaster rescue, *IEEE/ACM Transactions on Networking*. DOI: 10.1109/TNET.2022.3226458

[16] Rustemi, A., Atanasovski, V., Risteski, A. (2022): Overview of blockchain data storage and privacy protection, *2022 International Balkan Conference on Communications and Networking (Balkan Com)*, Sarajevo, Bosnia and Herzegovina, pp. 90–94. DOI: 10.1109/BalkanCom55633.2022.9900867

[17] Dneprovskaya, N. V., Bayaskalanova, T. A., Ruposov, V. L., ShevtsovaI, V. (2018): Study of digitization of Russian higher education as basis for smart education, *2018 IEEE International Conference*

"Quality Management, Transport and Information Security, Information Technologies" (IT&QM&IS), St. Petersburg, Russia, pp. 607–611,
DOI: 10.1109/ITMQIS.2018.8524945

[18] Dwivedi, A. (2018): Digitizing academic delivery in higher education issues and challenges, *2018 5th International Symposium on Emerging Trends and Technologies in Libraries and Information Services (ETTLIS)*, Noida, India, pp. 179–182.
DOI: 10.1109/ETTLIS.2018.8485251

[19] Ehsan, I., Khalid, M. I., Ricci, L., Iqbal, J., Alabrah, A., Ullah, S. S., Alfakih, T. M. (2022): A conceptual model for blockchain-based agriculture food supply chain system, *Scientific Programming*, Vol. **2022**, 15 pages, Article ID 7358354.
https://doi.org/10.1155/2022/7358354

[20] Shoufan, A., Mohamed, F. (2022): YouTube and education: A scoping review, *IEEE Access*, Vol. **10**, pp. 125576–125599.
DOI: 10.1109/ACCESS.2022.3225419

[21] Rustemi, A., Atanasovski, V., Risteski, A. (2023): Design of the blockchain system for the generation and verification of diplomas, *2023 XXXII International Scientific Conference Electronics (ET)*, Sozopol, Bulgaria, 2023, pp. 1–6.
DOI: 10.1109/ET59121.2023.10279743

Journal of Electrical Engineering and Information Technologies, Vol. **8,** No. 2, pp. 101–107 (2023)
Article 211
Received: November 9, 2023
Accepted: December 6, 2023
In print: ISSN 2545–4250
On line: ISSN 2545–4269
UDC: 621.317.76.029.426:006.91.067
https://doi.org/10.51466/JEEIT2382211111d

Original scientific paper

CONTRIBUTION TO IMPROVED MEASUREMENT AND CALIBRATION CAPABILITIES IN THE FIELD OF MEASURING INSTRUMENTS FOR HIGH FREQUENCIES

Ǵorǵi Dimitrovski, Marija Čundeva-Blajer, Kiril Demerdžiev

Faculty of Electrical Engineering and Information Technologies,
"Ss. Cyril and Methodius" University in Skopje,
Rugjer Bošković bb, P.O.Box 574, 1001 Skopje, Republic of North Macedonia
gorgi.dimitrovski@hotmail.com

A b s t r a c t: In the paper, analysis of the measurement infrastructure for examination and calibration of measuring instruments (oscilloscopes and counters) at extremely high-frequencies at the international, regional and national levels is made. The analysis is carried out within the framework of the scientific research project "Development and Upgrade of Laboratory Resources for Research and Introduction of New Analytical Methods in Electrical Metrology", which is implemented under the program for financing scientific and research projects of public interest for 2021 by the Ministry of Education and Science of the Republic of North Macedonia. The main emphasis of the paper is on the development of a procedure and calculation of measurement uncertainty for the calibration of high-frequency meters, according to Euramet Guideline No.7, Calibration of Oscilloscopes. The paper describes the newly installed reference standard measurement system in the Laboratory for Electrical Measurements at UKIM-FEEIT for calibration of instruments for high frequencies, as well as specific measurement results, evaluation of the budget of measurement uncertainties, and established traceability chain in the field of high frequencies.

Key words: measurement uncertainty; calibration; instruments for high-frequencies; measurement traceability

ПРИДОНЕС КОН ПОДОБРЕНИ МЕРНИ И КАЛИБРАЦИОНИ МОЖНОСТИ ВО ОБЛАСТА НА МЕРНИ ИНСТРУМЕНТИ ЗА ВИСОКИ ФРЕКВЕНЦИИ

А п с т р а к т: Во овој труд е направена анализа на мерна инфраструктура за испитување и калибрација на мерни инструменти (осцилоскопи и мерила) при екстремно високи фреквенции, на интернационално, регионално и национално ниво. Анализата е спроведена во рамките на научно-истражувачкиот проект „Развој и надградба на лабораториски ресурси за истражување и воведување нови аналитички методи во електрична метрологија", кој е имплементиран во програмата за финансирање на научноистражувачки проекти од јавен интерес за 2021 година од страна на Министерството за образование и наука на Република Северна Македонија. Главен акцент на трудот е ставен на развојот на постапка и пресметка на мерна неодреденост за калибрација на мерила за високи фреквенции, согласно упатството Еурамет бр. 7, Калибрација на осцилоскопи. Во трудот е даден и опис на новоинсталираниот мерен систем со референтен еталон за калибрација на мерила за високи фреквенции во Лабораторијата за електрични мерења при УКИМ-ФЕИТ, како и мерни резултати, оцена на буџетот на мерна неодреденост и воспоставен е редослед на мерната следливост на високи фревенции.

Клучни зборови: мерна неодреденост; калибрација; мерила за високи фреквенции; мерна следливост

1. INTRODUCTION

The Laboratory of Electrical Measurements (LEM) at the Faculty of Electrical Engineering and Information Technologies (FEEIT) of the "Ss. Cyril and Methodius" University in Skopje (UKIM) [1] is an accredited calibration laboratory according to the standard MKS EN ISO/IEC 17025:2018 [2] with traceability to the international primary reference standards of the International Bureau of Weights and Measures (Bureau International des Poids et

Mesures – BIPM) [3] in certain ranges of several electrical quantities.

The laboratory's mission is to disseminate its international traceability for the needs of electrical measurements in the Republic of North Macedonia, the region of Southeast Europe and beyond. The laboratory's services for the calibration of various types of instruments are continuously used by many national companies and companies from the region of Southeast Europe that perform electrical measurements with various levels of accuracy [1]. LEM has the ability to calibrate a wide range of electrical measuring instruments such as: multimeters, sources of direct and alternating voltages and currents, instruments for specific purposes and reference standards. Furthermore, work is being done on the analysis and development of new analytical methods in the field of measuring electrical quantities, within the framework of the scientific research project "Development and Upgrade of Laboratory Resources for Research and Introduction of New Analytical Methods in Electrical Metrology", implemented under the program for financing scientific research projects of special and public interest for 2021 by the Ministry of Education and Science of Republic of North Macedonia [4].

The aim of the paper is to present the achieved contribution to improvement of the measurement and calibration capabilities (CMC) in the field of high frequency measuring instruments, primarily calibration of oscilloscopes, including new laboratory equipment, for strategic expansion of the scope of accreditation of LEM. The developed measurements procedures, and the analysis of the obtained results from the calculation of the measurement uncertainties are in accordance with the Calibration Guide Euramet cg-7, Calibration of oscilloscopes, TC-EM, version 1.0, 06/2011 [5].

The result of each measurement contains a certain uncertainty, which means that it is not possible to obtain an ideally accurate value of the measured quantity [6]. In order to achieve uniformity in the expression of measurement results, in 2008 BIPM published the new version of the Guide to the expression of uncertainty in measurement [7]. To quantify the uncertainty, two parameters are required, the first is the width of the margin or interval of measurement uncertainty, and the second is the reliability or probability, which defines that the "correct value" is within the limits of the given interval [8].

In practice, five elements complete the measurement process: the measurand, the measuring instrument, the reference standard, the measurement method and the operator [9]. The standard is expected to have been checked in the appropriate competent calibration laboratory, either accreditied by European Accreditation Multilateral Agreement (EA/MLA) [9] signatory national accreditation body or a national metrology institute with officially published CMC in the Key Comparison Data Base (KCDB) of BIPM [3], and thus establishing the unbroken chain of traceability in the international metrology system. Traceability in measurements is realized within the framework of the national measurement system, which should be in a traceable relationship with the international SI system of measurement units.

Laboratories accredited by the accreditation bodies that are members of the European cooperation for Accreditation of Laboratories (EAL) [10] must enter the expanded uncertainty U in their calibration certificates. It is calculated according to the expression:

$$U = k \cdot u_c(y), \tag{1}$$

where k is the coverage factor and u_c is the combined measurement uncertainty. The results of the measurements are conventionally expressed as:

$$Y = y \pm U, \tag{2}$$

which is interpreted as an interval from $y–U$ to $y+U$ in which the measurement results are found with a given probability.

2. ANALYSIS OF THE CURRENT-STATE-OF-THE-ART OF THE BEST MEASUREMENT AND CALIBRATION CAPABILITIES FOR HIGH-FREQUENCIES AT INTERNATIONAL AND REGIONAL LEVEL

The state-of-the-art analysis of the best measurement and calibration capabilities for high frequencies at the international and regional level started from a survey of published measurement and calibration capabilities of the top national metrology institutes (NMIs) at international level (CMCs in KCDB base of BIPM), but also at the regional level through published CMCs by the national accreditation bodies. The main emphasis is on the comparison of the values for the expanded measurement uncertainties at each NMI. Bellow are the results of the extensive survey which is done for high-frequencies (at 500 kHz and at 1 MHz) for two voltage levels (1 V and 10 V). The expanded uncertainty is presented with a coverage factor of $k = 2$, with a statistical probability of 95%.

In Figures 1 and 2, the comparison of the values of the expanded measurement uncertainties of the national metrology institutes (NMIs) at the international level when measuring alternating voltages of 1 V and 10 V at very high frequencies of 500 kHz and 1 MHz, is given.

Figures 1 and 2 show that the national metrology institute of FR Germany – PTB, has the smallest values of the expanded measurement uncertainty for the considered frequencies at both voltage levels.

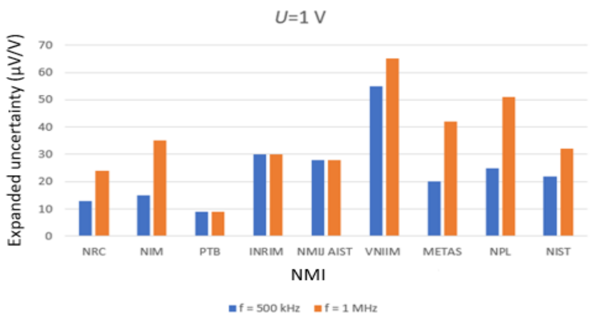

Fig. 1. Expanded measurement uncertainty of 1 V AC voltage at frequency of 500 kHz and 1 MHz at the international NMIs level

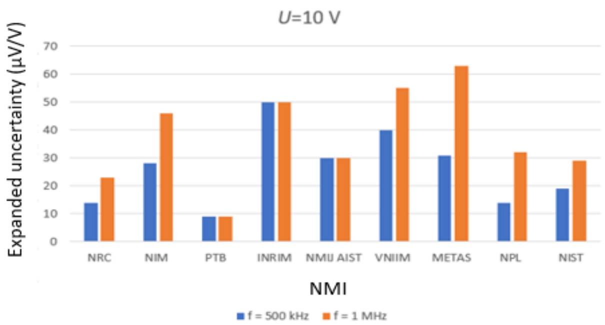

Fig. 2. Expanded measurement uncertainty at 10 V AC voltage at frequency of 500 kHz and 1 MHz at the international NMIs level

Table 1 presents the standards and measurement methods used by the NMIs at the international level that obtained the values of the expanded measurement uncertainties shown above.

In Figures 3 and 4, the comparison of the values of the expanded measurement uncertainties of the national metrology institutes (NMIs) at the regional level in Southeast Europe when measuring alternating voltages of 1 V and 10 V at very high frequencies of 500 kHz and 1 MHz, is given.

According to Figures 3 and 4, it can be concluded that the national metrology institute of R. Slovenia – MIRS/SIQ/Metrology, has the best values of expanded maesurement uncertainty for the considered frequencies at both voltage levels. On the other hand, the national metrology institute of R. Croatia – FER-PEL, has reported the highest values of expanded uncetainty in all analyzed cases.

Table 1

Standards and measurement methods used by NMIs at the international level

Metrology institute	Standard	Measurement method
NRC (Canada)	AC-DC transfer standard / Thermal voltage converter	Direct comparison
NIM (China)	Multifunction calibrator	Comparison
PTB (Germany)	AC voltmeter, multimeter	AC/DC transfer
INRIM (Italy)	AC-DC transfer standard	Resistive dividers
NMIJ AIST (Japan)	AC voltmeter	Comparison
VNIIM (Russian Federation)	AC-DC transfer standard / Thermal voltage converter	Thermal transfer standard
NPL (UK)	AC voltmeter, multimeter	Digital sampling
NIST (USA)	Multimeter	Comparison with reference

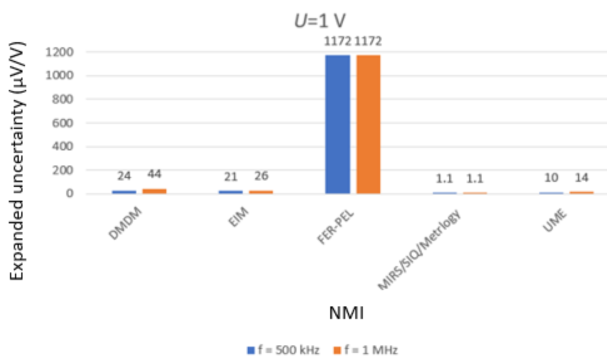

Fig. 3. Expanded measurement uncertainty at 1 V AC voltage at frequency of 500 kHz and 1 MHz at the regional NMIs level (Southeast Europe)

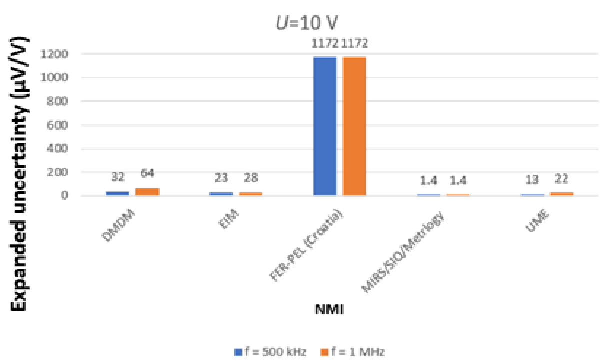

Fig. 4. Expanded measurement uncertainty at 10 V AC voltage at frequency of 500 kHz and 1 MHz at the international NMIs level (Southeast Europe)

The metrology institutes UME from R. Turkiye and MIRS/SIQ/Metrology from R. Slovenia use an AC-DC transfer standard and a thermal voltage converter for direct comparison. The national metrology institutes of R. Serbia (DMDM) and R. Greece (EIM) use standards whose working principle is similar to the standards used by the metrology institutes UME and MIRS/SIQ/ Metrology, with which satisfactory results are obtained in terms of uncertainty. Their standards can be used for calibration of standards of a lower accuracy class as well as for support in the process of calibration of standards from surrounding countires.

3. ANALYSIS OF THE CURRENT-STATE-OF-THE-ART OF THE BEST MEASUREMENT AND CALIBRATION CAPABILITIES FOR HIGH-FREQUENCIES OF THE LABORATORY FOR ELECTRICAL MEASUREMENTS AT UKIM-FEEIT

The Laboratory of Electrical Measurements at UKIM-FEEIT operates with several reference standards in the field of electrical measurements [1]. For the development of new calibration procedures in the field of high-frequencies, in order to expand the scope of accreditation of the laboratory, a new laboratory equipment was acquired – the standard Transmille 4015 Advanced Multiproduct Calibrator [11], shown in Figure 5.

The Transmille calibrator [11] of the 4000 series enables calibration of a wide variety of electrical measuring instruments and is a functional and precise programmable calibration standard. Regarding the need to perform measurements and develop measurement procedures for the calibration of meters in domain of high-frequencies, there are measurement possibilities for the calibration of oscilloscopes with frequency ranges up to 630 MHz. The Transmille 4015 Advanced Multiproduct Calibrator has multiple calibration functions, using built-in software, and has a baseline calibration accuracy of 8 ppm DC voltage measurement ranges [11].

As artefacts of calibration, owned by LEM, two oscilloscopes are used:

• Rigol Digital Oscilloscope 100 MHz DS1102E [12], shown in Figure 6 – an eight-bit, two-channel oscilloscope with a maximum real-time sampling rate of 1 GSa/s and a maximum equivalent sample rate of 25 GSa/s s, with a frequency bandwidth of 100 MHz per channel.

• GW Instek GDS-1072B Digital Storage Oscilloscope 70 MHz 1GS/s [13] – two-channel oscilloscope with a maximum sampling rate of 1 GSa/s in real time with a frequency bandwidth of 70 MHz per channel.

Fig. 5. Transmille 4015 Advanced Multiproduct Calibrator

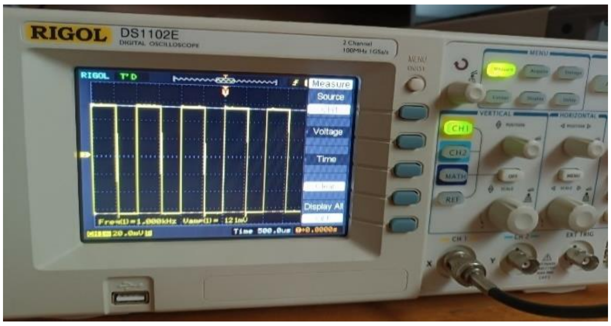

Fig. 6. Rigol Digital Oscilloscope 100 MHz DS1102E

According to the international guideline for calibration of oscilloscopes Euramet cg-7 Ver. 1.0 (06/2011) [5], an in-house original calibration procedure for oscilloscopes was developed with Transmille 4015 as a reference standard.

Calibration of oscilloscopes includes two main stages [5]:

• calibration of the vertical deflection (amplitude calibration),

• calibration of the bandwidth (frequency measurement along the horizontal axis).

The two main stages are independent of each other, but both are necessary to perform a complete procedure of oscilloscope calibration. With the reference standard measurement signals are generated as inputs to the oscilloscopes, through which the measurement procedure is experimentally realized. Each set reference value is measured with 12 repetitions according to [5]. The specified measurement values correspond to the analyzed measurement points provided in the Transmille Calibration Certificate [14], issued by the Transmille Calibration Laboratory, accredited by the UKAS (United Kingdom Accreditation Service) [15]. The reported expanded measurement uncertainties are based on the standard (combined) uncertainty multiplied by a coverage factor of $k = 2$ and a statistical probability of approximately 95%.

When estimating the measurement uncertainties and deviation intervals at each measurement point, the standard (combined) measurement uncertainty budget is composed of four influential factors:

• measurement uncertainty Type A – u_A (which corresponds to the standard deviation of all 12 repeated measurements divided by the square root of the number of measurements),

• measurement uncertainty from the resolution of the oscilloscope (the artefact of calibration),

• measurement uncertainty from the specification of the reference standard (for a period of 2 years) [11],

• measurement uncertainty from the calibration certificate of the reference standard (according to the last available Transmille Reference Standard Calibration Certificate) [14].

In this paper, the same measuring points, which were compared in Chapter 2, are analyzed, in order to make a valid and traceable comparison of the obtained results.

Table 2 and Table 3 present the calculated expanded measurement uncertainties U_{MU} and deviations of the voltage ΔU and of the frequency Δf from the given reference value, based on the measured values with the oscilloscopes, at the voltage measurement ranges of 1 V/Div and 10 V/Div as well as at frequencies of 500 kHz (1 µs/Div) and 1 MHz (2 µs/Div), respectively. Figures 7 and 8 show the respective measurement results with the accompanying uncertainties.

T a b l e 2

Expanded measurement uncertainties and deviations from the reference value, based on the measured values by the oscilloscopes at the voltage levels of 1 V/Div and 10 V/Div

Oscilloscope	Standard	Measurement method	U_{MU} at U = 1 V/Div	ΔU at U = 1 V/Div
Rigol Digital Oscilloscope 100 MHz	Transmille 4015	Direct comparison	0.017646 V	0.018 V
Gwinstek GDS-1072B Digital Storage Oscilloscope 70 MHz	Transmille 4015	Direct comparison	0.059349 V	0 V
Oscilloscope	Standard	Measurement method	U_{MU} at U = 10 V/Div	ΔU at U = 10 V/Div
Rigol Digital Oscilloscope 100 MHz	Transmille 4015	Direct comparison	0.08933 V	0.74 V
Gwinstek GDS-1072B Digital Storage Oscilloscope 70 MHz	Transmille 4015	Direct Comparison	0.101961 V	0 V

T a b l e 3

Expanded measurement uncertainties and deviations from the reference value, based on the measured values by the oscilloscopes at the high-frequencies of 500 kHz and 1 MHz

Oscilloscope	Standard	Measurement method	U_{MN} at f = 500 kHz	Δf at f = 500 kHz
Rigol Digital Oscilloscope 100 MHz	Transmille 4015	Direct comparison	2.007403 kHz	1.42 kHz
Gwinstek GDS-1072B Digital Storage Oscilloscope 70 MHz	Transmille 4015	Direct comparison	0.12159 kHz	0.12 kHz
Oscilloscope	Standard	Measurement method	U_{MN} at f = 1MHz	Δf at f = 1 MHz
Rigol Digital Oscilloscope 100 MHz	Transmille 4015	Direct comparison	0.012087 MHz	0.001 MHz
Gwinstek GDS-1072B Digital Storage Oscilloscope 70 MHz	Transmille 4015	Direct comparison	0.00051 MHz	8.3×10^{-6} MHz

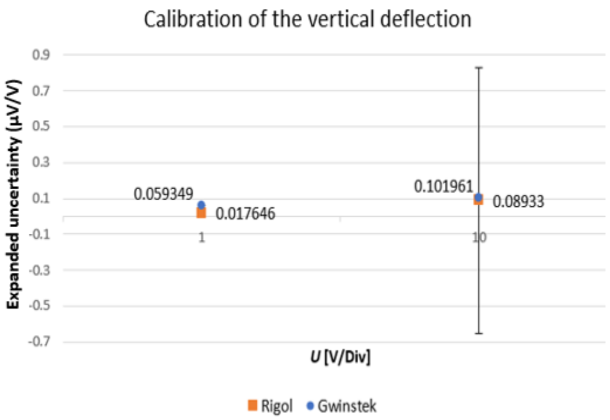

Fig. 7. Expanded measurement uncertainties based on the measured values by the oscilloscopes at the voltage levels of 1 V/Div and 10 V/Div

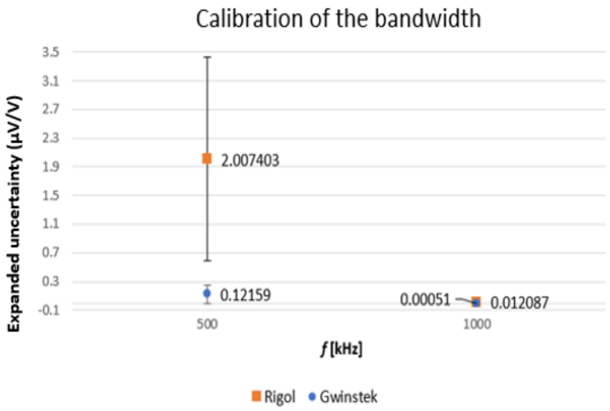

Fig. 8. Expanded measurement uncertainties based on the measured values by the oscilloscopes at the high-frequencies of 500 kHz and 1 MHz

CONCLUSIONS

In this paper, a brief overview of the work, objectives and equipment available in the Laboratory of Electrical Measurements at UKIM-FEEIT for the calibration in the field of high-frequency is provided. The identification of the available test equipment (oscilloscopes) which are artifacts for calibration during the development of measurement procedures in the field of high-frequency has been made. The calibration set-up of newly acquired reference standard Transmille 4015 Advanced Multiproduct Calibrator is briefly described, enabling expansion of the scope of accreditation of the LEM and providing the calibration and measurement capability of oscilloscopes and other high frequency instruments with a frequency bandwidth of up to 630 MHz.

The comparison of the best measurement and calibration capabilities in the field of high-frequencies, reported by the NMIs at the international and regional level, expressed through the values of the expanded measurement uncertainty for several measurement points is conducted. The analyzed measurement points were chosen in such a way to enable comparable traceability at the largest number of national metrology institutes.

To achieve long-term sustainability of the recently acquired laboratory equipment and the extended calibration infrastructure, new and modified laboratory procedures are developed and adopted, their accreditation is planned, with the objective of expanding the measurement and calibration capabilities of LEM.

Finally, from the calibration measurements performed in LEM, using both oscilloscopes and Transmille as a reference standard, it can be concluded that the obtained values for the expanded measurement uncertainty are comparable to the reported BIPM values by the national metrology institutes analyzed in this paper. The level of repeatability is acceptable and the all the necessary quality assurance measures for confidence, traceability to SI and unity of the calibration results are performed with appropriate validation methods. The obtained results of the performed calibration enabled the development of a new calibration procedure for high frequency meters, in compliance to the international guideline Euramet cg-7 Ver. 1.0 (06/2011). This makes a significant contribution to the metrological infrastructure for the calibration of high-frequency meters in Republic of North Macedonia and in the region of Southeast Europe.

Acknowledgement. The research is conducted within the scientific project “Development and Upgrade of Laboratory Resources for Research and Introduction of New Analytical Methods in Electrical Metrology”, Contract No.15-15590/22, 22.11.2021, financed by the Ministry of Education and Science of the Republic of North Macedonia and co-financed by the Faculty of Electrical Engineering and Information Technologies at the Ss. Cyril and Methodius University in Skopje.

REFERENCES

[1] Demeržiev, K., Čundeva-Blajer, M., Dimčev, V., Srbinovska, M., Kokolanski, Z. (2018): Improvement of the FEIT Laboratory of Electrical Measurements Best CMC Through Internationally Traceable Calibrations and Inter-Laboratory Comparisons, *Conf. Proc. of Int. Conf. ETAI 2018*, Struga, R. Macedonia, 20–22 September 2018 (ETAI 6–4).

[2] EN ISO/IEC 17025 (2005): *General Requirements for the Competence of Testing and Calibration Laboratories*, Cenelec, Brussels.

[3] https://www.bipm.org/en/ (retrieved on: 16.06.2023)

[4] https://mon.gov.mk/ (retrieved on: 16.06.2023)

[5] EURAMET cg-7: *Calibration of Measuring Devices for Electrical Quantities Calibration of Oscilloscopes*, Calibration Guide, Version 1.0 (06/2011).

[6] Гавровски, Ц. (2011): *Основи на мерна шехника*, второ преработено и дополнето издание, УКИМ, ФЕИТ, Скопје.

[7] https://www.bipm.org/documents/20126/2071204/JCGM_100_2008_E.pdf/cb0ef43f-baa5-11cf-3f85-4dcd86f77bd6 (retrieved on: 26.03.2023).

[8] Чундева-Блајер, М. (2020): *Иншерна скрийша йо йредмешош Мерења во елекшрошехника*, УКИМ-ФЕИТ, Скопје.

[9] The Measurement Quality Division (2012): Jay L. Bucher (Editor), *The Metrology Handbook*, Second Edition, AASQ Quality Press, Milwaukee, Wisconsin.

10] https://eal.org.uk/ (retrieved on: 16.06.2023)

[11] Transmille 4015 Advanced Multiproduct Calibrator, Extended specifications, Transmille Ltd., Unit 4, Select Business Centre, Lodge Road, Staplehurst, Kent, 2022.

[12] Rigol, *User's Guide*, DS1000E, DS1000D Series, Digital Oscilloscopes, Sept. 2010.

[13] Gwinstek, User Manual, Digital Storage Oscillscope, GDS-1000B Series.

[14] Certificate of Calibration, Certificate Number 46981, Transmille Ltd., Unit 4, Select Business Centre, Lodge Road, Staplehurst, Kent, 06 September 2022.

[15] https://www.ukas.com/ (retrieved on: 16.06.2023)

[16] Čundeva-Blajer, M., Dimitrovski, Gj., Sapundžiovski V., Dimčev, V., Demerdžiev K. (2022): Infrastructure development for extreme electrical metrology, *Journal of Electrical Engineering and Information Technologies*, Vol. **7,** no. 2, pp. 101–109.
DOI: https://doi.org/10.51466/JEEIT2272201101chb

[17] Cundeva-Blajer, M., Dimitrovski, Gj., Demerdziev, K. (2023): Implementation and validation of calibration methods in the area of high frequencies, *Proceedings of the IMEKO TC8&TC11&TC24 Joint International Conference*, 11–13. 10. 2023, Funchal – Madeira Islands, Portugal.

[18] Dimitrovski, Gj., Čundeva-Blajer, M., Demerdžiev K. (2023): Contribution to improved measurement and calibration capabilities in the field of mesuring instruments for high-frequencies, *International Conference MakoCigre 2023*, 17–19.09.2023, Ohrid, North Macedonia.

[19] https://european-accreditation.org/mutual-recognition/the-ea-mla/ (retrieved on: 11.11.2023).

Journal of Electrical Engineering and Information Technologies, Vol. **8,** No. 2, pp. 109–116 (2023)
Article 212
Received: November 3, 2023
Accepted: December 7, 2023
In print: ISSN 2545–4250
On line: ISSN 2545–4269
UDC: 004.925.84:004.356]:[004.89:616.717-77
https://doi.org/10.51466/JEEIT2382209073h

Original scientific paper

MECHANICAL DESIGN OF A LOW-COST 3D PRINTED FOREARM PROSTHESIS WITH THE ABILITY FOR INDIVIDUAL FINGER CONTROL

Blagoj Hristov, Arjun Nair, Goran Rafajlovski, Vesna Ojleska Latkoska, Gorjan Nadžinski

Faculty of Electrical Engineering and Information Technologies,
"Ss. Cyril and Methodius" University in Skopje,
Rugjer Bošković bb, P.O.Box 574, 1001 Skopje, Republic of North Macedonia
hristovb@feit.ukim.edu.mk

A b s t r a c t: The prosthesis technology has had a renaissance in recent years, although the improved and natural control coupled with fast and fluid movements have led to devices which are very expensive and not attainable by the majority of people who need them. In this paper we present a mechanical design of a low-cost of 3D printed forearm prosthesis which has the ability for individual finger control using a sophisticated software solution by incorporating artificial intelligence. By using two actuators for each finger instead of one we allow for more precise and robust movements of the prosthetic, and by using affordable yet high-torque servomotors we can keep the price low while offering performance similar to much more expensive devices available on the market. The use of 3D printing is also used in order to drive down the cost of the prosthesis, by implementing materials which are inexpensive yet light, strong and durable.

Key words; electric prosthesis; 3D printing; mechanical design; electromyography; artificial intelligence

МЕХАНИЧКИ ДИЗАЈН НА НИСКОБУЏЕТНА 3D ПЕЧАТЕНА ПРОТЕЗА НА ПОДЛАКТНИЦА СО СПОСОБНОСТ ЗА ИНДИВИДУАЛНО УПРАВУВАЊЕ НА ПРСТИТЕ

А п с т р а к т: Науката за вештачки делови на телото (протези) има доживеано преродба во последните неколку години, но подобреното и природно управување заедно со брзите и глатки движења доведе до уреди коишто се многу скапи и не се достапни за мнозинството на лица на кои протезите им се потребни. Во овој труд е предложен механички дизајн на нискобуџетна 3D печатена протеза на подлактница која има способност за индивидуално управување на прстите со примена на софистицирано софтверско решение базирано на вештачка интелигенција. Со користење на два актуатора за секој прст наместо еден се овозможуваат попрецизни и поробусни движења на протезата, а со примената на евтини сервомотори, кои се карактеризираат со релативно висок вртежен момент, се задржува ниската цена на уредот, а се обезбедуваат перформанси слични на многу поскапи уреди достапни на пазарот. Употребата на 3D печатење исто така се користи со цел да се намали крајната цена на протезата, бидејќи се користат материјали кои се евтини, а сепак лесни, јаки и издржливи.

Клучни зборови: електрични протези; 3D печатење; механички дизајн; електромиографија; вештачка интелигенција

1. INTRODUCTION

The difficult task of replacing a missing limb can make one properly understand the complexities of the human body. Throughout the ages, innovators have been attempting to use artificial limbs to replace lost natural ones. There are numerous prosthetic devices that are shown to be from ancient civilizations all around the world, exhibiting the development of artificial limb technology. The technological development of prosthetic limb design has been relatively gradual up until recently.

Prostheses have largely remained passive tools that provide limited control and mobility, although as time went on and technology improved, designs began to incorporate hinges and pulley systems as well as better materials. This resulted in the development of basic mechanical body-powered gadgets, for example, metal hooks that can open and close when a person bends their elbow. Recently however, there has been a significant improvement in prosthetic devices and the demand for completely functional prostheses is at an all-time high as the number of amputees worldwide continuously rises each year [1]. Although today there are more options readily available for amputees in the market, acquiring a fully functional prosthetic is still an expensive process. A recent technological advance in this field has been the introduction of 3D printers. 3D printers allow for a multitude of new possibilities as this device is capable of creating different objects using recycled plastics and biodegradable materials, which is not only cost-effective but also better for the environment [2].

While in the past the most advanced prosthetics which used hinges and pulley systems were able to achieve some level of control, they were still basic mechanical devices. The prosthetics that are available today have become electrical devices which focus not only on the physical aspects of the device, but also on the level and ease of control through complex biofeedback systems. Perhaps sometime in the future prosthetic devices will be even faster, stronger, and overall better than biological limbs. To be able to achieve this, the prosthesis should not only be able to perform the desired movement of the user, but also be durable, lightweight and easy to put on.

The goal of this paper is to present an easy to build artificial forearm prosthetic through the use of 3D printing, made from an adequate material which is strong and robust yet not too expensive. By using readily available low-cost materials we can design a prosthetic device which is not only easily controllable by the user but also costs less than the prosthetics that are already available on the market.

The paper is structured as follows: in Section 2 we discuss different types of prosthetic device which already exist but have flaws which we aim to improve upon thorough the research in this paper. Then, in Section 3 we present the mechanical design of the proposed prosthetic device and explain the design process of the model as well as the drive system which is used to actuate the fingers. In Section 4 we make a comparison between different types of materials for the 3D printing of the prosthesis in order to find the one which offers the best strength and durability. Finally, in Section 5, we close the paper by discussing the pros and cons of the presented solution and propose further possible ideas and improvements which can be implemented in the future.

2. RELATED WORK

A prosthetic device should ideally be as simple and effortless to use as possible. The prosthesis would not be helpful in any practical sense if the user has to struggle to perform even the most basic elementary movements, such as gripping and object or pointing. While there are multiple options for electrical prosthesis on the market, a fully functional prosthetic is either hard to find or unaffordable.

A functional prosthetic arm must be able to overcome various design and manufacturing obstacles. The degree to which the mechanical device replicates the human arm and the degree of mobility that it can provide are determined by the complexity of the mechanical and electrical systems which are implemented, which is also the reason they are usually highly priced. Many prosthesis on the market use electromyography (EMG) for the detection and measuring of electrical impulses in the residual limb of the user while particular flexions are performed [3]. By analyzing these measurements through signal processing or machine learning methods, one can extract the type of movement the user was trying to perform. An example of a myoelectric forearm prosthesis is shown on Figure 1.

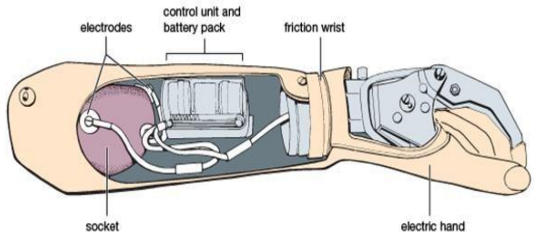

Fig. 1. Visual representation of a myoelectric forearm prosthesis [10]

There have been many successful attempts at classifying the movements carried out by users through the use of electromyography, although most fall short due to the use of multiple expensive EMG sensors [4], complex solutions that cannot be easily implemented in an embedded system [5, 6] , or a limited array of possible movements [7]. We have already addressed some of these issues in previous publications where we successfully achieved the classification of individual finger flexions using only two-channel electromyography with an F1 score of 91.3% [8], as well as individual and combined finger flexions with an F1 score of 96.6% [9].

In the early days of prosthetic arm development, the heavy weight of the device used to be a major problem which made most of the functions difficult to perform and even caused the user to feel uncomfortable due to having to carry the prosthetic for long periods of time [11]. The materials that were used were also inadequate as they absorbed sweat, which made the maintenance of such devices difficult. With the introduction of 3D printing, the whole outlook of the market eventually changed. Lighter materials were being used to create prosthetics and the cost was also able to be significantly reduced.

There is a large variety of prosthetic devices which can be categorized according to their method of operation. Simple, immobile devices known as passive prostheses are mainly used for aesthetic appeal and while they help amputees regain their confidence and normality in everyday life, these types of devices offer basic functionality and control, if any. A separate kind of passive prosthesis is a customized silicone restoration device that serves primarily as a cosmetic item. The transparent silicone glove can be painted to precisely match the user's skin tone, body hair, and other natural traits. This particular and thorough style of painting and design allow the prosthetic to have the look of a real arm, without any of the functionality. The simplicity of these devices usually means they are very affordable and inexpensive, which is the reason they are the most common option for amputees when choosing a prosthetic device [12].

Another type of prosthesis that is available is a body powered prosthetic device where the control is carried out through a harness fastened to the user. These prosthesis typically consist of a straightforward tool, like a mechanical hook, that is connected to the shoulder and elbow and moves along with them. Although these gadgets are very simple and offer very limited control, they continue to be a common type of prosthesis due to their lower cost [13].

In this paper we present an electric forearm prosthesis which is affordable yet offers high functionality through fast, easy and natural control by the user. The control of the devices is accomplished using electromyography with just two EMG sensors placed on the residual limb. The electrodes of the sensors are used to measure to electrical impulses when flexing the muscles which flex and extend the fingers of the hand. After being amplified, these signals are then transmitted to a microcontroller, which uses the data to analyze them in order to detect the desired movement, i.e. which finger (or fingers) the user wanted to flex or extend. When the movement is detected, the microcontroller sends a signal to the necessary internal actuators and carries out the movement on the prosthesis. Due to this complex system of measurement-classification-actuation, mechanical prostheses cannot be controlled to the same extent as myoelectric ones.

The main focus of the paper is the mechanical design of this proposed prosthesis and the different aspects considered while designing the device to be cost effective yet efficient and robust in terms of weight, usability and durability. The signal processing and control aspects have already been covered in [8] and [9], and the discussion on the mechanical considerations presented here represents the next step in the overall design of a low-cost fully functioning forearm prosthesis.

3. MECHANICAL DESIGN

Some of the current limitations of prosthetic arms available on the market today include:

- **Price** – not everyone who has the need for a prosthetic arm can afford it due to their high cost.
- **Robustness** – prosthesis are susceptible to damage and require frequent repairs and/or replacements.
- **Functionality** – currently existing prosthetic arms may not be as functional as minimally necessary for users to decide to use them in everyday life; in order to replicate a real human arm the functionality of the prosthesis must be fast and fluid and the implementation of sensory feedback, such as a feeling of touch, is also a needed but difficult task.
- **Comfort** – prosthetic arms are usually not comfortable to wear for extended periods of time and this can make the user reluctant to use them.
- **Weight** – depending on the material the prosthesis is made out of, the weight of the device also plays a major factor in the decision of the user to continue using the prosthetic.

The first and main focus of the mechanical design of the proposed prosthesis was to make it inexpensive to produce thus making it affordable for the majority of people who need it. Seeing as the majority of the cost of the prosthesis is driven by the material which is used to produce it, the first approach to making it affordable is the use of basic yet durable plastics and 3D printing. Although this can be achieved, there are a lot of aspects to consider while designing and building the device, such as the shape and geometry of the palm and fingers, the material of the mechanical joints, the actuators which will be used to carry out the flexions etc. Keeping these aspects in mind, as well as the previously mentioned flaws of current prosthesis, multiple iterations and designs for the prosthetic arm were created.

a) *Early ideas*

Before the process of designing the prosthetic arm, certain key decisions had to be made for the basis of the design, such as the actuation mechanism, the number of servo motors to be used and the placement of the motors in the prosthesis. It was decided initially that for the actuation, ten servo motors (two per finger) would be housed in the body of the prosthesis in order to increase the strength and efficiency of the flexions. Figuring out a way to house the actuators while also finding a way to implement the correct actuation technique proved to be a challenge during the initial steps of the design process. The locking of the coil was another important aspect to consider in prior to creating the model as, if not locked properly, the flexions would not be carried out smoothly and this would affect the functionality of the prosthesis.

It was decided that the best option for the actuation method of the fingers would be a basic pulley and string design which mimics the biological actuation of fingers through tendons present in a real human arm. The CAD model of the prosthesis was then designed using SolidWorks.

b) *Finger design*

Each of the four fingers is made up of three different printed parts that are connected using 3D printed pins. To produce a tendon locking point, the artificial tendon coils around the inside of the fingertip. This tendon forms a closed loop by navigating guide pathways inside the finger. All of the joints experience a rotational stress as the tendon is tugged by the servo motor, which causes the finger to curl up. As mentioned previously, in this design each finger has two tendon coils, one for the distal interphalangeal joint (DIP) at the fingertip, and another for the proximal interphalangeal joint (PIP) in the middle of the finger. It is crucial for each tendon to have a locking point in order to increase the efficiency of the spin or grip hold during flexion. If a locking mechanism is missing there is a possibility that the tendon would simply slip under tension, preventing the finger from moving. The extension of the fingers is done by applying tension to the other end of the tendon. It is necessary to use a high-quality braided string to ensure that it will stretch very little under tension. The final design of one of the fingers is shown on Figure 2.

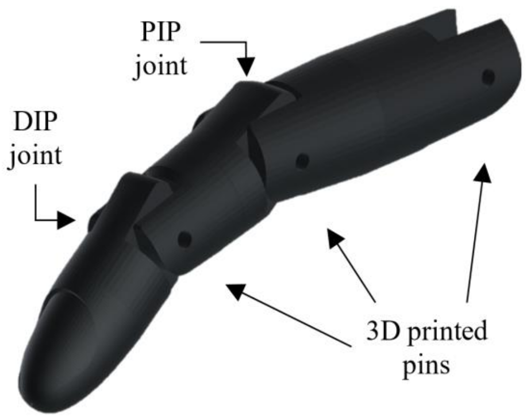

Fig. 2. Finger design concept for the artificial prosthesis

c) *Thumb design*

Due to the complexity of the movement of the thumb, its design was different in comparison to the rest of the fingers. The majority of commercial and research prostheses strive to offer at least two degrees of freedom for the movement of the thumb, and the same approach has been taken in this paper as well. Without considering the extension, the thumb is consists mainly of two parts representing the interphalangeal (IP) and metacarpophalangeal (MP) joint. In both parts a tendon lock is used for carrying out the flexions. As in a real biological hand, the thumb is the most integral part of almost every movement carried out by the hand as it is the locking finger in most gripping techniques. In order to optimize tendon orientation and avoid tendon lines becoming snagged on a sharp edge, guide holes have been integrated into the design of both the fingers and the thumb. The design of the thumb is shown on Figure 3.

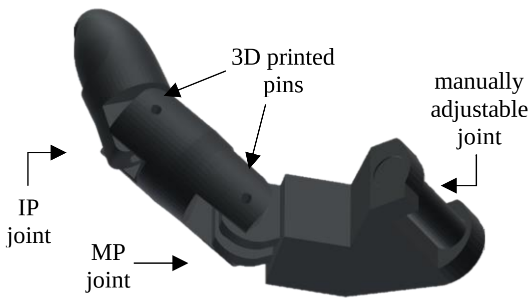

Fig. 3. Thumb design concept for the prosthesis

d) *Palm design*

Each of the fingers connects to the palm by using 3D printed pins. In this paper, the palm was the most redesigned part as initially the plan was to have two parts combining to form the body of the palm, where the main part was used to connect the thumb, index and middle finger and the other part was consisted of separate moving extensions for the ring and little finger. The two extensions would be fixed to the main part using screws. This design was initially considered for better grips, but due to the complexity in the design as well as the aesthetic appeal, the design was later changed in order to keep the palm as a single rigid part on to which the fingers would be fixed, as shown on Figure 4.

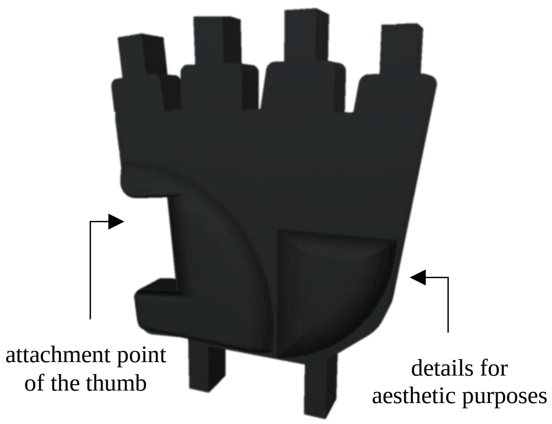

Fig. 4. Palm design concept for the prosthesis

e) *Forearm design*

Even though the forearm section contains no moving parts it is still a challenge to design as it needs to house most of the electrical components and actuators, as well as the power source for the whole device. After the complete forearm section was designed it was split into separate components which could then be assembled using screws. If the forearm was 3D printed as a single large component it would not be possible to place the servo motors and tendons inside the palm. A robust and durable material is necessary for the production of the forearm as the screws can easily break and crack weaker plastics, even though the guide holes for the which have been incorporated into the design have enough material to firmly support the screw. The two large sections of the forearm can be 3D printed as a single piece without affecting the assembly of the device, however most basic 3D printers are simply not large enough to print an object of this size. The final model of the forearm is shown on Figure 5.

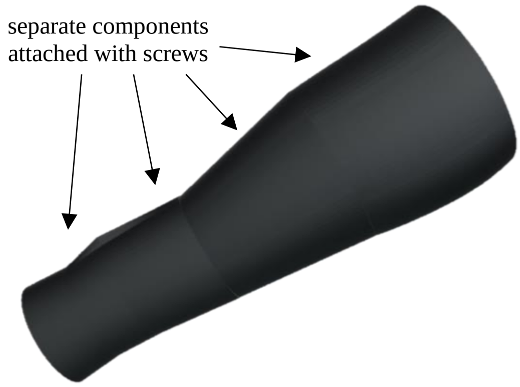

Fig. 5. Forearm design concept for the prosthesis

f) *Drive system*

As stated previously, the drive system of the proposed prosthesis is based on a biological actuation mechanism where the string is meant to mimic the tendons in the palm, while the servo motors, which are the driving force of the prosthesis, mimic the muscles. The string is pulled when the servo motor turns in one direction, flexing the finger. If the servo motor turns in the opposite direction, the finger will extend. An individual pulley is used to attach the thumb, index and middle finger. Each of the fingers has a separate servo motor system attached to it. The ring and little finger are joined to one pulley system due to the constrained space inside the palm. In a way this actually mimics the dependence of neighboring fingers in a real biological hand, so no meaningful functionality will be lost due to this simplification.

The actuators which are used for the movement of the fingers of the prosthesis are standard servo motors. These motors can be controlled to rotate to angular positions of up to ±90° from their initial position which is adequate for the small and limited range of motion of the joints of the fingers. Relatively inexpensive servo motors with sufficient torque and speed have been used in this system to maintain the low cost of the prosthesis. The use of higher quality servo motors would lead to an increase in finger strength and precision, but the exponential increase in cost is not worth the minimal improvement they would bring.

g) *Power supply*

It is of outmost importance that the prosthesis is fully portable and capable of multiple hours of constant use without the need for power by external sources. As such, an internal power supply capable of providing enough power for the whole device while lasting an adequate amount of time is required [14]. The servo motors are the main users of power in the system due to the significant amount of current which is necessary during operation. Disposable batteries would not be a good solution since the servo motors would drain power too quickly, meaning they would need to be replaced frequently. Lithium Polymer (LiPo) batteries offer a high energy density and are rechargeable, meaning they are a decent option for the task at hand, but they would need to be taken out of the prosthesis, recharged, and put back in on an almost daily basis, which can be a hassle for some users. In order to reprimand this, an alternative source of power was used, i.e. a power bank device, which can be easily recharged by connecting it to a wall plug by a regular USB-C cable. The power bank is housed on an exterior pouch on the forearm of the prosthesis, meaning it is easily accessible to recharge as well as replace when needed.

4. MATERIAL COMPARISON

When creating a 3D printed product one must consider the material that will be used, which depends on the type of product that is being created, the environment in which it will be used, as well as the price-to-quality ratio of the material. Three of the most popular 3D printing materials are polylactic acid (PLA), acrylonitrile butadiene styrene (ABS), and nylon. They can all be extruded using a basic 3D printer and at their low price of around \$20–\$30 per spool, they are among the most affordable filaments available on the market today. When making a simple prototype which will not be used as a final product, the choice of material is usually between PLA and ABS, and nylon and its copolymers are often used when there is a need for a higher quality item. The comparison between these materials will be made using a simplified qualitative approach in terms of what is necessary for the task of this paper. A more detailed review of the materials can be found in [15].

4.1. *Polylactic acid*

Polylactic acid (PLA) is a user-friendly thermoplastic with a higher strength and stiffness than both ABS and nylon. The low melting temperature and minimal warping make PLA one of the easiest materials to 3D print successfully, which is the reason it is the most often used when prototyping new designs [16]. One of the drawbacks to using PLA is its low melting point, which causes it to lose almost all of its stiffness and strength at temperatures above 50° Celsius. In addition to that, PLA is also very brittle which causes parts to have poor durability and impact resistance, often virtually falling apart after a short amount of time. A comparison of the characteristics of this material is given in Table 1. Even though PLA is the strongest of the three proposed plastics, the poor chemical and heat resistance make it unsuitable for anything other than the initial printing of the prototype in order to tune the tolerances between the individual parts, as it is the cheapest and most widely available material to use.

T a b l e 1

Characteristics of PLA

PLA	Bad	Good	Great
Strength	■	■	
Stiffness	■	■	
Durability	■		
Printability	■	■	■
Heat resistance	■		
Chemical resistance	■		

4.2. *Acrylonitrile butadiene styrene (ABS)*

Weaker and less rigid than PLA, ABS is a tougher and lighter filament which is suitable for applications that require somewhat higher quality products. This plastic is characterized with a higher durability, is about 25% lighter and has around four times the impact resistance compared to PLA. Seeing as ABS is more heat resistant and prone to warping, it is more difficult to 3D print [17]. It is necessary to have a heated bed for the 3D printer as well as an extruder which is able to get 40°–50° Celsius hotter. Even though ABS is not prized for its heat resistance, it still has superior heat deflection temperature in comparison to PLA and nylon. These characteristics, as shown in Table 2, make ABS the perfect option for printing the initial full prototypes of the proposed prosthesis which can be used to test the device, while still remaining a relatively low-cost option.

Table 2

Characteristics of ABS

ABS	Bad	Good	Great
Strength	■	■	
Stiffness	■	■	
Durability	■	■	
Printability	■	■	
Heat resistance	■	■	
Chemical resistance	■		

4.3. *Nylon*

In contrast to PLA and ABS, nylon is a flexible and durable material with less strength and stiffness. The signature malleability leads to an increase in toughness and an impact resistance that is ten times that of ABS. Nylon is also characterized with a surprisingly high chemical resistance which leads to it being used in more industrial applications. Similarly to ABS, nylon is more difficult to 3D print than PLA as it needs to be extruded at very high temperatures. It must also be kept dry before printing due to its tendency to soak up moisture from the air. The main downside to nylon in comparison to PLA and ABS is its lower strength and rigidity which makes in unsuitable for most serious applications. As a result, nylon is usually altered such that it is combined with other plastics in the form of a copolymer, but the best quality nylon filaments are usually a form of nylon-fiber mixtures.

Filled nylon is a type of mixture of nylon with tiny particles of a stronger material such as fiberglass or carbon fiber. The goal of these mixtures is to preserve the favorable flexibility and chemical resistance of nylon while adding a considerable amount of strength, stiffness, head resistance as well as making it easier to print [18]. A comparison between the characteristics of regular nylon and nylon filled with carbon fibers is given in Table 3 and Table 4. This type of filament is one of the best ones available on the market today, and while it is slightly more expensive than its counterparts, it is a great option for fully functional prototypes as well as end use products. The final version of the prosthesis is to be constructed using a mixture of Nylon PA12 and 20% carbon fibers which will result in an optimally resistant, strong and durable device.

Table 3

Characteristics of nylon

Nylon	Bad	Good	Great
Strength	■		
Stiffness	■		
Durability	■	■	■
Printability	■		
Heat resistance	■		
Chemical resistance	■	■	■

Table 4

Characteristics of filled nylon

Nylon + CF	Bad	Good	Great
Strength	■	■	■
Stiffness	■	■	■
Durability	■	■	■
Printability	■	■	
Heat resistance	■	■	
Chemical resistance	■	■	■

5. CONCLUSION

The initial idea of this research was to design and build a high quality forearm prosthesis from a strong, resistant and durable material which is inexpensive to produce and yet offers high functionality with natural control by the user. After multiple iterations of the design of the fingers and palm, a design that was satisfactory in both aesthetics and usability was created. Finding a design that can host ten servo motors was a challenging task, but with the extent of research and the approach of experimenting with different variables in the design allowed us to create a prosthesis that has double the power and precision in comparison to most prosthetic devices which use only one actuator per finger. Extensive research was also done on the material to be used for the 3D printing of the device, and finally it was decided that Nylon PA12 mixed with carbon fiber would be the optimal solution for the final product.

To ensure that the proposed prosthesis is able to be used in real-world situations for extended periods of time, certain aspects of the system still need to be tested and analyzed, such as:

Detailed and thorough testing of the strength, rigidity, heat and chemical resistance and overall durability of the finished prosthesis.

Design of a comfortable yet stable socket connection in order to better attach the device to the residual limb of the user.

Further improvements of the control system of the device and the classification algorithm, as well as expanding the range of possible movements.

Real-world trial studies using amputees to better ascertain the pros and cons of the proposed device in order to improve upon possible flaws that may have been overlooked.

In conclusion, the design for a low-cost myoelectric forearm prosthesis with the ability for individual finger control that was presented in this paper is a solid base for the production of an affordable yet functional device which can improve upon the lives of many people. After the completion and implementation of the aforementioned improvements, we can ensure that the device will be a strong contender in the market due to the innovative hardware and software approaches that were used in its creation, while also allowing it to be available to a larger number of people who have a need for it.

Acknowledgment: This work is part of the project "Realization of a myoelectric robotic arm prosthesis with the ability for individual finger flexions", which is supported by the University of "Ss. Cyril and Methodius" in Skopje, Faculty of Electrical Engineering and Information Technologies.

REFERENCES

[1] Yuan, B., Hu, D., Gu. S., Xiao, S., Song, F. (2023): The global burden of traumatic amputation in 204 countries and territories, *Frontiers in Public Health,* Vol. **11**.

[2] Tabassum, T., Mir, A. A. (2023): A review of 3D printing technology – the future of sustainable construction, *Materials Today: Proceedings*.

[3] Marinelli, A. et al. (2023): Active upper limb prostheses: a review on current, *Progress in Biomedical Engineering*, Vol. **5**. 012001. DOI: 10.1088/2516-1091/acac57

[4] Tsenov, G. et al. (2006): Neural networks for online classification of hand and finger movements using surface EMG signals, *2006 8th Seminar on Neural Network Applications in Electrical Engineering*, pp. 167–171.

[5] Lee, K. H., Min, J. Y., Byun, S. (2022): Electromyogram-based classification of hand and finger gestures using artificial neural networks, *Sensors,*Vol. **22**, p. 225.

[6] Nahid, N., Rahman, A., Ahad, M. A. R. (2020): Deep learning based surface EMG hand gesture classification for low-cost myoelectric prosthetic hand, In: *2020 Joint 9th International Conference on Informatics, Electronics & Vision (ICIEV) and 2020 4th International Conference on Imaging, Vision & Pattern Recognition (icIVPR)*, Kitakyushu, Japan.

[7] Jung, S.-Y., Kim, S.-G., Kim, J.-H., Park, S.-H. (2021): Development of multifunctional myoelectric hand prosthesis system with easy and effective mode change control method based on the thumb position and state, *Applied Sciences*, Vol. **11**, no. 16.

[8] Hristov, B., Nadzinski, G. (2021): Detection of individual finger flexions using two-channel electromyography, In: *ETAI 2021*.

[9] Hristov B., Nadzinski, G., Latkoska, V. O., Zlatinov, S. (2022): Classification of individual and combined finger flexions using machine learning approaches, In: *2022 IEEE 17th International Conference on Control & Automation (ICCA)*, Naples, Italy.

[10] *Encyclopaedia Britannica* (2012). [Online].

[11] Cordella, F. et al. (2016): Literature review on needs of upper limb prosthesis users, *Frontiers in Neuroscience,* Vol. **10**.

[12] Zuo, K. J., Olson, J. L. (2014): The evolution of functional hand replacement: From iron prostheses to hand transplantation, *Plast Surg (Oakv),* Vol. **22**, no. 1.

[13] Satriawan, A., et al. (2023): Karla: A Simple and affordable 3-D printed body-powered prosthetic hand with versatile gripping technology, *Designs,* Vol. **8**, no. 2.

[14] Malewski, M., Cowell, D. M. J., Freear, S. (2018): Review of battery powered embedded systems design for mission-critical low-power applications, *International Journal of Electronics*, Vol. **105**, no. 6.

[15] Iftekar, S. F., Aabid, A., Amir, A., Baig M. (2023): Advancements and limitations in 3D printing materials and technologies: A critical review, *Polymers,* Vol. **15**, no. 11.

[16] Liu, Z. et al. (2019): A critical review of fused deposition modeling 3D printing technology in manufacturing polylactic acid parts, *The International Journal of Advanced Manufacturing Technology,* Vol. **102**.

[17] Moradi, M. et. al. (2022): 3D Printing of acrylonitrile butadiene styrene by fused deposition modeling: artificial neural network and response surface method analyses, *Journal of Materials Engineering and Performance,* Vol. **32**.

[18] Mohammadizadeh, M., Fidan, I. (2021): Tensile performance of 3D-printed continuous fiber-reinforced nylon composites, *Journal of Manufacturing and Materials Processing,* Vol. **5**, no. 3.

Journal of Electrical Engineering and Information Technologies, Vol. **8,** No. 2, pp. 117–128 (2023)
Article 213
Received: November 12, 2023
Accepted: December 6, 2023
In print: ISSN 2545–4250
On line: ISSN 2545–4269
UDC: 621.372.63.064:621.315.592
https://doi.org/10.51466/JEEIT2382213117r

Original scientific paper

A COMPARATIVE STUDY OF SWITCHING PERFORMANCES AND EFFICIENCY OF GaN, SiC AND Si BASED DC-DC CONVERTERS

Marko Kamilovski, Katerina Raleva, Mario Makraduli

Faculty of Electrical Engineering and Information Technologies,
"Ss. Cyril and Methodius" University in Skopje,
Rugjer Bošković bb, P.O.Box 574, 1001 Skopje, Republic of North Macedonia
catherin@feit.ukim.edu.mk

A b s t r a c t: Wide bandgap (WBG) semiconductors offer many advantages over conventional silicon (Si) based devices such as faster switching speeds, lower internal capacitances, smaller size, lower power losses and higher efficiency. Due to their exceptional properties, these materials have gained significant attention in the field of power electronics. The wide bandgap of GaN (gallium-nitride) and the high-temperature tolerance of SiC (silicon carbide) make them ideal candidates for various power applications, from electric vehicles to renewable energy systems. This paper analyzes the overall efficiency and switching performances of three topologies of DC-DC converters in GaN technology and compare them with Si and SiC counterparts. The simulation results for the switching frequencies in the range of 100 kHz to 500 kHz show that the GaN based DC-DC converters provide smaller switching times and superior efficiency when compared to the same Si or SiC based DC-DC converters.

Key words; wide bandgap semiconductors; GaN devices; on-resistance; DC-DC converters; power efficiency; switching times

КОМПАРАТИВНА СТУДИЈА ЗА ПРЕКИНУВАЧКИТЕ КАРАКТЕРИСТИКИ И КОЕФИЦИЕНТОТ НА ПОЛЕЗНО ДЕЈСТВО НА DC-DC КОНВЕРТОРИ ВО GaN, SiC И Si ТЕХНОЛОГИЈА

А п с т р а к т: Полуспроводниците со голема широчина на забранетата зона (WBG) во однос на силициумските полуспроводнички елементи нудат многу предности: поголема брзина на вклучување и исклучување, помала интерна капацитивност, помали димензии, помали загуби на моќност и голем коефициент на полезно дејство. Поради нивните исклучителни својства, овие материјали привлекоа значајно внимание во енергетската електроника. Големата широчина на забранетата зона на GaN (галиумнитрид) и високата температурна толерација на SiC (силициумкарбид) ги прават идеални кандидати за различни енергетски апликации, од електрични возила до системи за обновлива енергија. Во овој труд се прави анализа на прекинувачките карактеристики и на коефициентот на полезно дејство на три топологии на DC-DC конвертори реализирани во GaN-технологија и се споредуваат со истите топологии на конвертори во Si и SiC технологија. Резултатите од симулацијата добиени за прекинувачки фреквенции од 100 kHz до 500 kHz покажуваат дека DC-DC-конверторите со GaN транзистори имаат многу мали времиња на вклучување и исклучување и извонреден коефициент на полезно дејство споредено со DC-DC конвертори базирани на Si и SiC.

Клучни зборови: полуспроводници со голема широчина на забранета зона; GaN електронски елементи; отпорност при вклучена состојба; DC-DC конвертори; коефициент на полезно дејство; прекинувачки времиња

1. INTRODUCTION

Silicon (Si) has been the dominant semiconductor for power electronic devices for over five decades. However, in the continuously evolving world of electronics, the power electronics field imposes unique demands on the next generation of high-voltage, high-current transistors-particularly for switching power supplies or motor drives. Two wide bandgap (WBG) materials that have been at the forefront of this technological revolution are silicon carbide (SiC) and gallium nitride (GaN) [1], [2]. While 4H-SiC technology [3] is mature in terms of crystalline quality and available device performances, gallium nitride (GaN) is still affected by several materials and technology concerns, limiting its full exploitation in power electronics applications [4].

Gallium nitride (GaN) has better material properties compared to Si and SiC (see Table 1). Due to the wider bandgap, higher critical electric field and higher saturation velocity, GaN is a promising semiconductor for the next generation of high-power and high-frequency devices. Also, the intrinsic carrier concentration of GaN is several orders of magnitude lower than Si which gives a possibility of GaN devices to operate at higher temperatures. All of the above mentioned characteristics have made GaN devices a very attractive choice in many applications such as automotive electronics, power supplies, communication infrastructures and other power systems.

Table 1

Relevant physical and electronic properties of Si, 4H-SiC and GaN

Property	Si	4H-SiC	GaN
Bandgap (eV)	1.12	3.2	3.4
Critical field (MV/cm)	0.25	3.0	4.0
Dielectric constant ε	11.8	9.7	9.5
Saturation velocity vs (107 cm/s)	1	2	3
Electron mobility μ (cm^2/Vs)	1350	800	1300 (2DEG)
Intrinsic carrier concentration n_i (cm^{-3}) at 300 K	1010	10−7	10−10
Thermal conductivity k (W/cmK)	1.5	4.9	1.3

Key to numerous applications in power electronics are conversion processes, in which switching frequencies have a major influence on device dimensions. Operation at higher frequencies provides a reduction in dimensions and weight of passive elements, which is especially important for compact DC-DC converters. The reduced power losses offered by gallium nitride, as well as the high temperature coefficient, allow reducing the size of the heat sinks, and thus reducing the dimensions of the converters. Many studies have shown the significant improvement in switching performances and efficiency when GaN transistors are used in DC-DC converters. In [5], a 160 W GaN-HEMT based synchronous boost converter is compared with a Si based converter with the same specifications in terms of efficiency and power losses over a wide range of operating conditions. The results (simulation and experiments) show that GaN has an efficiency of over 98.5% over the frequency range of 100–400 kHz. Ref. [6] presents a GaN-based flyback converter that achieves a maximum power conversion efficiency of 99.6% at 1 MHz. The switching performances and efficiency for a bidirectional buck-boost converter operating in buck mode were analyzed in [7]. In it, the cascode GaN-FET based converter showed lower switching losses and higher overall efficiency than the Si-CoolMOS based converter, due to the low on-state resistance and ultra-low reverse recovery charge of the cascode GaN-FET. Similar analysis for both, buck and boost mode of the bidirectional buck-boost converter was performed in [8], where an e-mode GaN is used instead of cascode mode. Ref. [9] presents a comparison of Si and GaN based buck converter, where the results show that GaN based buck converters show higher efficiency at higher frequencies and for different load currents. A comparative study between Si, SiC and GaN based buck converters is presented in [10], where the wide bandgap semiconductors show better overall performances than the Si-MOSFET with the GaN-FET edging out the SiC-MOSFET in both efficiency and switching performance. In [11], the analysis shows that GaN-HEMT based boost converter show much lower losses and consequently higher efficiency compared to their Si-MOSFET counterpart. Moreover, the converters are compared in terms of power density and cost. GaN-HEMTs show overall higher power density and even though they are costlier than Si-MOSFETs, their cost gap may close in the future with the further development of GaN technology. Also, the study compares the performance of hard-switched and soft-switched converters. The simulation and experimental results show that hard-switched converters have a better overall performance.

The goal of this paper is to investigate the advantages of using GaN devices in different topologies of DC-DC converters operating in continuous conduction mode (CCM) compared to SiC and Si switches. A method for selecting the optimal power switch in GaN technology for a given DC-DC converter application is presented. The simulation results of the most popular DC-DC topologies (buck, boost and buck-boost) with GaN, SiC and Si switches were performed and some relevant conclusions were derived. The paper is organized as follows: the topology of the three chosen DC-DC converters is presented in Section 2. Section 3 explains the parameters that affect the performances of the analyzed DC-DC converters, while in Section 4 are given the simulation results for all three converter topologies. In the last section, final conclusions are summarized.

2. SELECTED TOPOLOGIES FOR THE SIMULATIONS

Figure 1 presents the buck converter circuit diagram. It is used to step down the input voltage to a certain value according to the equation $V_{out}/V_{in} = D$, where D is the duty cycle.

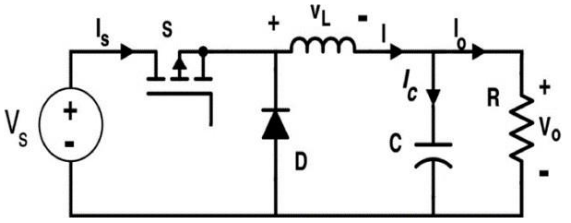

Fig. 1. Buck converter circuit diagram

The boost converter is used to step-up (increase) the input voltage to a certain output voltage value. Its circuit diagram is presented in Figure 2. The equation $V_{out}/V_{in} = 1/(1–D)$ gives the relation between input voltage, output voltage and duty cycle.

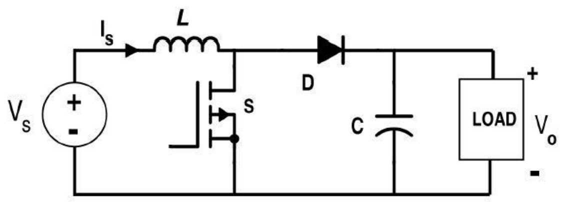

Fig. 2. Boost converter circuit diagram

The bidirectional buck-boost converter circuit diagram is shown in Figure 3. It consists of two switches, two capacitors, an inductor, and a load. The two diodes represent the anti-parallel body diodes of the power MOSFETs. This converter has two modes of operation: buck-mode and boost-mode.

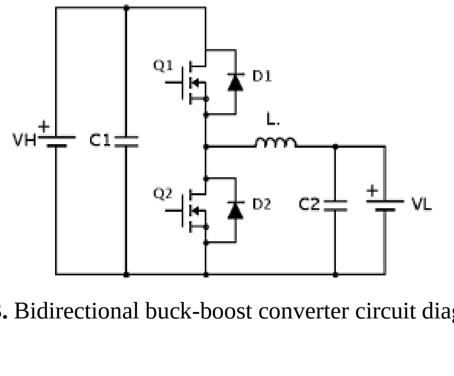

Fig. 3. Bidirectional buck-boost converter circuit diagram

3. PARAMETERS THAT AFFECT CONVERTER PERFORMANCES

The performance of a DC-DC converter is dependent on several factors: the switching frequency, the selected switch, the size of the passive elements, ripple of the output voltage and inductor current, etc. When selecting the switch three factors should be considered: voltage and current rating, on-resistance and the switching speed of the switch. The latter two are very important in the overall performance of the converter. Selecting a switch with optimal on-resistance can lead to lower power dissipation in the switch during the on-processes. On the other hand, faster switching speed leads to lower power dissipation during the switching process. By lowering these power losses an overall higher efficiency can be achieved in the DC-DC converter.

The key parameters that determine the performance of DC-DC converters according to the analyzed literature are the switching times and the efficiency of the converter.

The efficiency of DC-DC converters is calculated by:

$$\eta = P_o / (P_o + P_{loss}), \tag{1}$$

where P_o is the output power and P_{loss} is the total power losses in the converter. The power losses of the selected converter are defined as the sum of the power losses in the switch (P_{switch}), power losses in the passive elements (P_L, P_C), power losses in the diode (P_{diode}) and losses in the gate driver (P_{drive}) as shown in equation (2):

$$P_{loss} = P_{switch} + P_{diode} + P_C + P_L + P_{drive} \tag{2}$$

In terms of power losses during the switching, the power loss in the switch is of the outmost interest. It can be divided in switching losses and conduction losses of the switch. The switching losses occur when the switch changes from on to off state and vice versa. These power losses are dependent on the parasitic components of the switch and the switching frequency. On the other hand, the conduction losses of the switch are proportional to the on-resistance (R_{on}).

Balancing these two power losses is crucial in order to achieve higher overall efficiency of the specific power converter. In [12] a method for selecting the optimal power switch for a given dc-dc converter application is presented. The method uses datasheet information for the on-resistance (R_{on}) and the effective output capacitance ($C_{o(er)}$) and is demonstrated using a family of commercial Si and

SiC-MOSFETs. The specific technological parameters of the analyzed switch family can be grouped by the constant k.

$$R_{on} \cdot C_{OSS} = k\,. \quad (3)$$

Since the output capacitance (C_{OSS}) is quite nonlinear, the effective output capacitance ($C_{o(er)}$), defined as the capacitance that gives the same stored energy as the C_{OSS} while the drain-to-source voltage is rising from 0 to 80% of the drain-source breakdown voltage, can be used in the Eq. 3. Thus the equation can be rewritten as:

$$R_{on} \cdot C_{O(er)} = k\,. \quad (4)$$

The conduction losses of the switch can be expressed by the equation:

$$P_{conduction} = D \cdot R_{on} \cdot I^2, \quad (5)$$

where D is the duty cycle, R_{on} is the on-resistance of the switch, and I is the root-mean square drain current.

The switching losses due to the charging/discharging of $C_{o(er)}$ are expressed as:

$$P_{switching} = f \cdot C_{O(er)} \cdot V^2, \quad (6)$$

where f is the switching frequency and V is the drain-source voltage. Using the Eq. (4), one can express the switching losses in terms of the on-resistance as:

$$P_{switching} = f \cdot k \cdot V^2 / R_{on}\,. \quad (7)$$

Combining (5) and (7), the total power loss can be expressed as:

$$P_{total} = D \cdot R_{on} \cdot I^2 + f \cdot k \cdot V^2 / R_{on}\,. \quad (8)$$

In order to minimize the total power loss with respect to R_{on}, the derivative of (8) is set to zero and the optimal R_{on} is derived as:

$$R_{on} = \frac{V}{t} \cdot \frac{\sqrt{f \cdot k}}{D}\,. \quad (9)$$

The minimum of the total power loss can be achieved for a specific R_{on}, that depends on V, I, f, k and D, as shown in (9).

In order to verify this method for switches in GaN technology, a family of five 650V GaN-HEMTs by GaN-Systems is analyzed. The boost converter topology in which the switches were analyzed was arbitrarily chosen for the verification of the method. The GaN switches used in the simulations in Section 4 for the different converter topologies were chosen using the method presented in this section.

The parameters of each GaN-HEMT for drain-to-source voltage of 400 V is given in Table 2. The value of constant k is calculated using Eq. (4). The mean value of all k's is 4.953 ps and it is used in the further calculations. Using equations (5) and (7) the conduction, switching and total power losses are calculated for three different switching frequencies and are presented in Tables 3 – 5.

Table 2

Datasheet parameters of the analyzed GaN switches

Switch	R_{on} (mΩ)	C_{oss} (IpF)	$C_{o(er)}$ (pF)	k (ps)
GS66502B	200	17	25	5,00
GS66504B	100	31	47	4.70
GS66506T	67	49	73	4.89
GS66508T	50	65	100	5.00
GS66516T	25	126	207	5.18

Table 3

Power losses for a frequency of 100 kHz (W)

Switch	$P_{conduction}$	$P_{switching}$	P_{total}
GS66502B	8.44	0.40	8.83
GS66504B	4.24	0.79	5.01
GS66506T	2.83	1.18	4.00
GS66508T	2.11	1.58	3.69
GS66516T	1.06	3.17	4.22

Table 4

Power losses for a frequency of 200 kHz (W)

Switch	$P_{conduction}$	$P_{switching}$	P_{total}
GS66502B	8.44	0.79	9.22
GS66504B	4.22	1.58	5.80
GS66506T	2.83	2.36	5.19
GS66508T	2.11	3.16	5.27
GS66516T	1.055	6.32	7.38

Table 5

Power losses for a frequency of 500 kHz (W)

Switch	$P_{conduction}$	$P_{switching}$	P_{total}
GS66502B	8.44	1.98	10.42
GS66504B	4.22	3.96	8.18
GS66506T	2.83	5.91	8.74
GS66508T	2.11	7.92	10.00
GS66516T	1.06	15.84	16.90

The obtained results are graphically presented in Figures 4 – 6 with the green dotted line representing the switch with the lowest power losses and thus optimal on-resistance. From these figures, one can conclude that optimal value of the on-resistance R_{on} increases as the switching frequency is increased, which follows the trend seen in [12]. For switching frequency of 100 kHz, using switch GS66508T results in the lowest total power loss. The case for $f = 200$ kHz confirms the selection of switch GS66506T, used in the boost converter simulations in Section 4, as the switch which has the lowest power loss and thus the highest efficiency in the boost converter under the specified parameters.

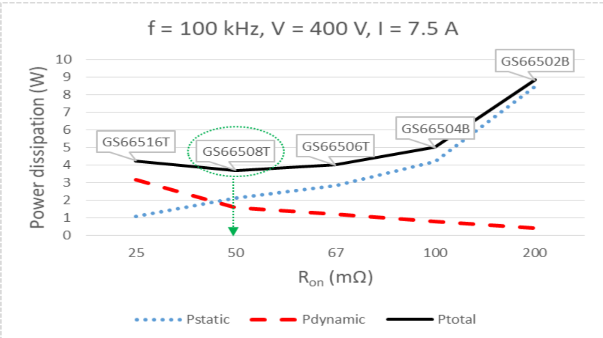

Fig. 4. Total power dissipation vs. on-resistance for a switching frequency of 100 kHz

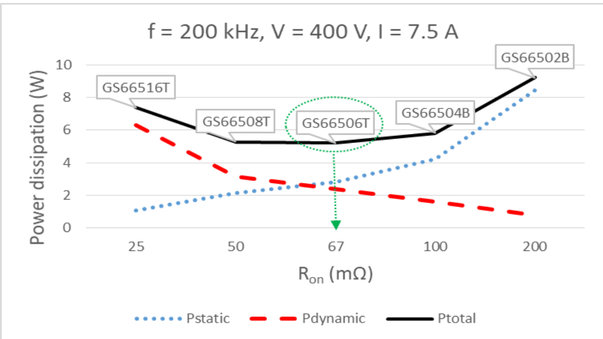

Fig. 5. Total power dissipation vs. on-resistance for a switching frequency of 200 kHz

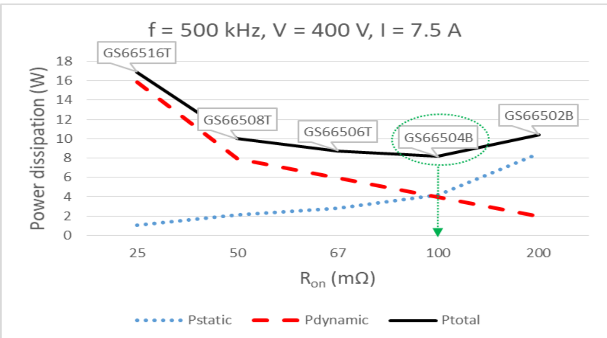

Fig. 6. Total power dissipation vs. on-resistance or a switching frequency of 500 kHz

The analyzed GaN switches were then simulated using the parameters of the boost converter in Section 4, given in Table 8. Figure 7 shows the simulation results in terms of overall efficiency of the boost converter for a switching frequency of 100, 200, and 500 kHz. The results show that for the switching frequency of 200 kHz, using switch GS66506T results in the highest efficiency of the boost converter, while for the frequencies of 100 and 500 kHz the optimal switches are GS66508T and GS66504B, respectively. Thus the calculated results match the obtained simulation results.

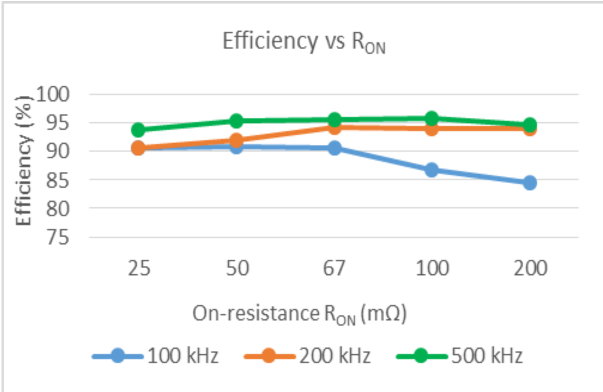

Fig. 7. Simulation of efficiency results for switching frequency of 100, 200, and 500 kHz

4. SIMULATION RESULTS

Three types of switches for each of the three topologies have been used in simulations: Si-MOSFET, SiC-MOSFET and GaN-HEMT/FET, with the models being provided by the manufacturer's producers. There are a large number of GaN models found in literature, which are developed by academia. The manufacturer models capture device-specific parameters and behavior that might not be fully reflected in the literature-based models, which could affect simulation accuracy for the particular device. When compared to the models of the manufacturers, these model have several disadvantages. Some of those disadvantages are: absence of thermal modeling, inability to reproduce both static and dynamic behavior, limited scope of focus (some models focus on certain aspects of device behavior), compatibility with other GaN-devices, high computational complexity, etc. In addition, literature/ academia based models might lack the extensive validation against measured data that manufacturer provided models undergo. With that being said, GaN models provided by their manufacturers are a better choice for fast and accurate simulations.

All simulations are performed in continuous conduction mode (CCM) where the current flowing through the inductor never reaches zero during its commutation period. In CCM the output voltage of the converter depends only on the duty cycle. On the other hand, in discontinuous conduction mode (DCM) the output voltage depends on multiple factors (switching frequency, duty cycle, inductor size). Additionally, DCM allows the use of smaller inductors (thus reducing the overall converter size) and decreases the power dissipation which occurs during the switching processes since the current at the start of each switching process is equal to zero. In CCM mode, there is greater power dissipation in the switches during the switching transitions, which significantly impacts the overall behavior of the converters. Nonetheless, this power dissipation in the switch is critical in the scope of this research; hence, the continuous current mode was chosen for analysis.

The inductor and capacitor used in the converters are dependent on the working conditions of the converter. The equations for the inductance (L) and capacitance (C) according to [13] are:

$$L = \left(V_0 \cdot \frac{1-D}{\Delta i_L \cdot fsw}\right) \quad (10)$$

$$C = \frac{1-D}{8 \cdot L \cdot \left(\frac{\Delta V_0}{V_0}\right) \cdot fsw} \quad (11)$$

$$L = \frac{Vin \cdot D}{\Delta i_L \cdot fsw} \quad (12)$$

$$C = \frac{D}{R \cdot \left(\frac{\Delta V_0}{V_0}\right) \cdot fsw} \quad (13)$$

where V_{in}, V_o, D, f_{sw}, Δi_L, ΔV_0 and R are the input voltage, output voltage, duty cycle, switching frequency, inductor current ripple, output voltage ripple, and resistance (load), respectively. Equations (10) and (11) are used for the buck converter and the buck-mode of the bidirectional buck-boost converter, while (12) and (13) are used for the boost converter as well as the boost-mode of the bidirectional buck-boost converter.

4.1. *Buck converter*

A DC-DC buck converter is used to step down the input voltage from 48 V to 12 V, using a GaN-FET (EPC2045), SCT20N120 (SiC-MOSFET) and a Si-MOSFET (FDA18N50) and the results are compared. The basic parameters of the converter are given in Table 6, while Table 7 shows the important parameters of the GaN-FET, SiC-MOSFET and Si-MOSFET, all of which were selected to have a similar current rating. The important waveforms of the simulated buck convertor are shown in Figure 7.

T a b l e 6

Parameters of the buck converter

Parameter	Value
Input voltage	48 V
Output voltage	12 V
Output current	6 A
Duty cycle	0.25
Switching frequency	100 – 500 kHz

T a b l e 7

Parameters of the used switches in buck converter

Parameter	FDA18N50 Si-MOSFET	SCT20N120 SiC-MOSFET	EPC2045 GaN-FET
Breakdown voltage	500 V	1200 V	100 V
Current	19 A	20 A	16 A
On-resistance	220 mΩ	189 mΩ	7 mΩ

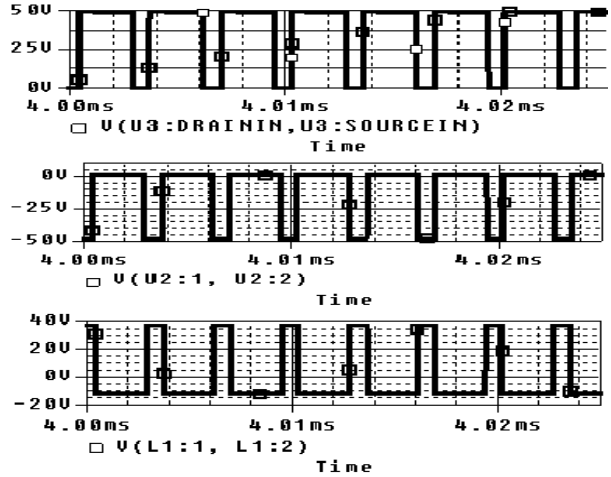

a)

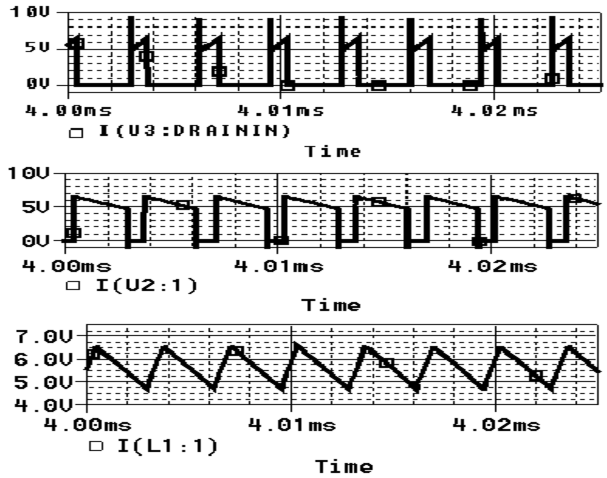

b)

Fig. 8. Key waveforms of the buck converter: a) switch voltage (top), diode voltage (middle) and inductor voltage (bottom); b) switch current (top), diode current (middle) and inductor current (bottom)

a) *Switching characteristics*

The switching performance of the buck convertor is analyzed in terms of on-delay, off-delay, rise and fall time, as well as the total on and off times. Both circuits are tested under the same switching frequency of 300 kHz. The Si-MOSFET requires a gate-source voltage of 15 V to securely turn on the switch and the SiC-MOSFET requires +18 V gate-source voltage for turn-on and –3 V for turn-off. The GaN-FET has a very low reverse recovery charge and it requires a gate-source voltage of +6 V for turning-on and –3 V for turning-off.

The turn-on time is calculated as the sum of the rise time and turn-on delay, where the rise time is the time from 90% to 10% of the fall of the drain-source voltage (V_{DS}) and the turn-on delay is the time between 10% of the rise of the gate-source voltage and 90% of V_{DS}. Similarly, the turn off -time is the sum of the fall time (time from 10% to 90% of the rise of V_{DS}) and the turn-off delay (time between 90% of the fall of V_{GS} and 10% of the rise of V_{DS}). Simulation results, presented in Figure 9, show that the GaN-FET has a turn-on time of around 8.9 ns which is almost five times smaller than the turn-on time of the Si-MOSFET (42.7 ns), while the SiC-MOSFET has halt the turn-on time of the Si-MOSFET (21.6 ns). In addition, the turn-off time of the GaN-FET is 11.57 ns and the turn-off time of the SiC-MOSFET is 13.9 ns, which are nearly ten times lower than the Si-MOSFET (108.3 ns).

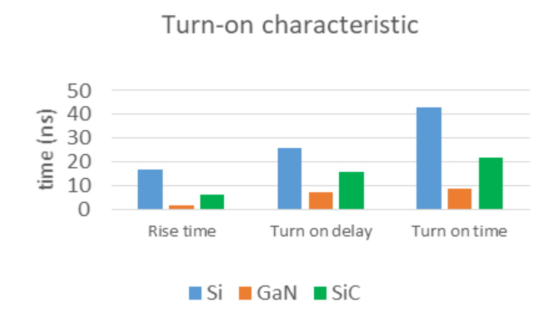

a)

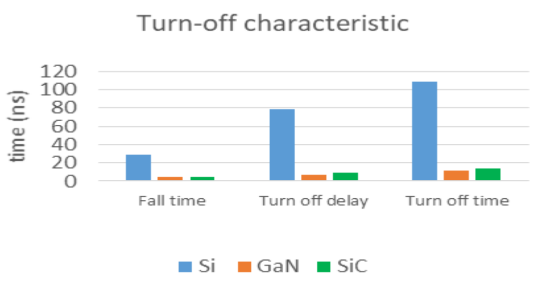

b)

Fig. 9. Switching characteristic of the buck converter a) turn-on and b) turn-off characteristics

b) *Efficiency*

The power losses in the gate driver are neglected in this analysis. By using the above mentioned formulas and operating under a switching frequency of 300 kHz, the efficiency of the buck converter with the Si-MOSFET is 88.8%, with the SiC-MOSFET is 90.6% while the efficiency of the same converter with a GaN-FET switch is 92.8%. The results are as expected due to GaN's lower on-state resistance, which results in lower conduction losses. As seen from the switching characteristics, GaN has a much shorter on and off times which result in an even lower switching losses.

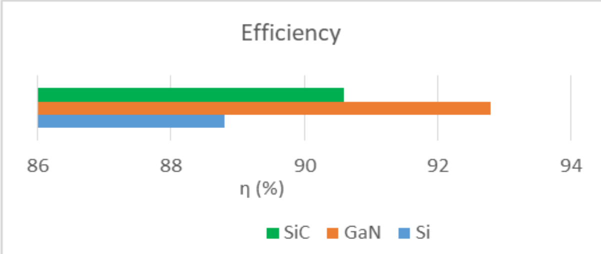

Fig. 10. Buck converter efficiency results for a switching frequency of 300 kHz

4.2. *Boost converter*

The boost converter is used to step-up the input voltage of 100 V to 400 V at the output, using GaN-HEMT, SiC-MOSFET and Si-MOSFET switches. The parameters of the boost converter are given in Table 8. The important parameters for each of the selected switches are given in Table 9.

Table 8

Parameters of the boost converter

Parameter	Value
Input voltage	100 V
Output voltage	400 V
Output current	1.25 A
Duty cycle	0.75
Switching frequency	100 – 500 kHz

Table 9.

Parameters of boost converter switch

Parameter	IPA60R120 P Si-MOSFET	SCT3120Al SiC-MOSFET	GS66506T GaN-HEMT
Breakdown voltage	650 V	650 V	650 V
Current	26 A	21 A	22.5 A
On-resistance	120 mΩ	120 mΩ	67 mΩ

The key waveforms of the boost converter are presented in Figure 11.

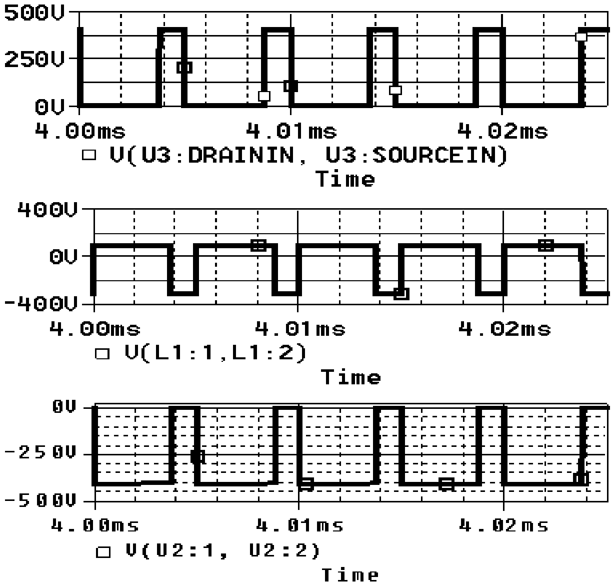

a)

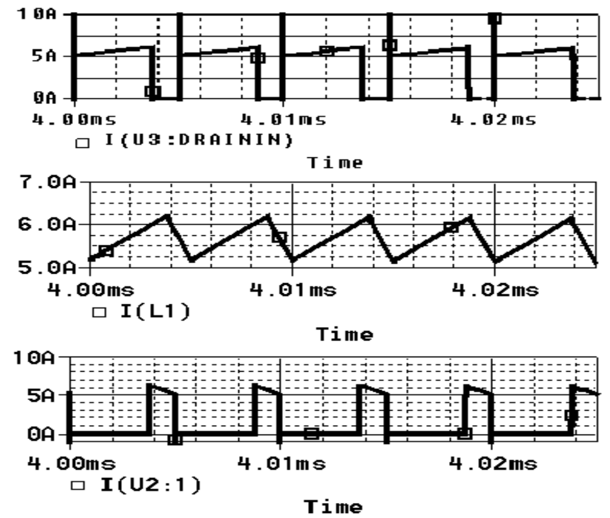

b)

Fig. 11. Key waveforms of the boost converter: a) switch voltage (top), inductor voltage (middle) and diode voltage (bottom); b) switch current (top), inductor current (middle), and diode current (bottom)

a) *Switching characteristics*

In this analysis both circuits are evaluated operating in boost converter mode at a switching frequency of 200 kHz. The E-series Si power MOSFET (SIHG24N65E) is driven on by a 12 V source. The GaN-HEMT (GS66506T) is turned on by a 6 V gate-source voltage and turned off by applying a –3 V, while the SiC-MOSFET (SCT3120A) is turned on with 18V and turned off with –3V. Figure 12 presents the simulation results for the switching characteristics for both circuits. Both turn-on and turn-off time of the GaN switch, which are 8.2 ns and 22 ns, respectively, are almost three times smaller than the Si turn-on (22.1 ns) and turn-off (57.6 ns) times. The SiC-MOSFET has a similar turn-on time to the Si-MOSFET (27.2 ns) and the smallest turn-off time of 19.14 ns.

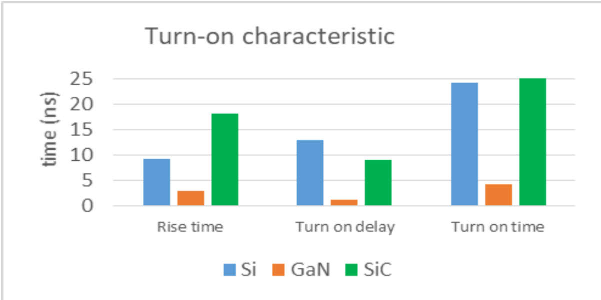

a)

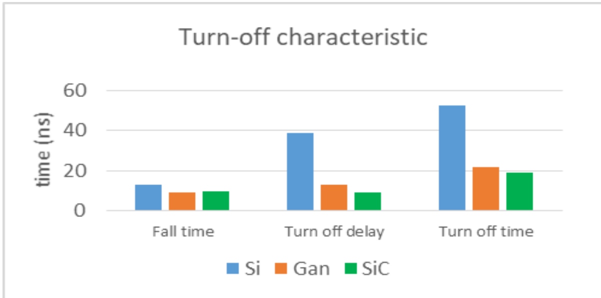

b)

Fig. 12. Switching characteristic of the boost converter a) turn-on b) turn-off

b) *Efficiency*

The efficiency of the boost converter is calculated using the same formulas as explained in Section 3. The E-series Si power MOSFET shows better performance than most of the conventionally used Si-MOSFETS and therefore it is expected to have a higher efficiency. Calculated at a frequency of 200 kHz. The efficiency of the boost converter is 91.8% with Si-MOSFET, 92.7% with SiC-MOSFET and 94.2% with GaN-HEMT for a switching frequency of 200 kHz. Simulation results in terms of efficiency are presented in Figure 13.

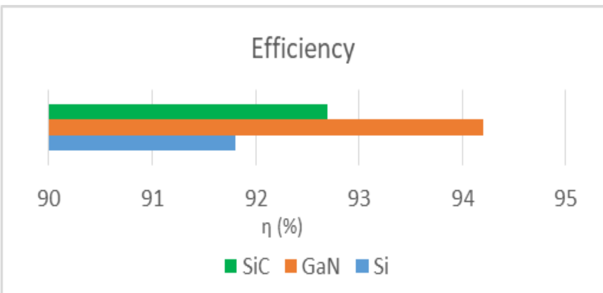

Fig. 13. Efficiency results for switching frequency of 200 kHz

4.3. *Bidirectional buck-boost converter*

In this analysis a bidirectional buck-boost converter is chosen. Both the buck and boost mode of operation are used under the same operating conditions and the parameters are calculated by using the same equations as for the buck and boost converter. The full list of parameters for the bidirectional buck-boost converter operating in both modes is given in Table 10. The three switches (Si-Cool-MOS, SiC-MOSFET and GaN-FET) were selected based on their similar electrical specifications and parameters as well as the suitability in the converter's operating mode and the method presented in Section 3. Their electrical specifications are given in Table 11.

Table 10

Parameters for buck mode of the bidirectional buck-boost converter

Parameters	Value
High side voltage	400 V
Low side voltage	96 V
Power rating	500 W
Duty cycle	0.24 and 0.76, respectively
Switching frequency	100 – 500 kHz

Table 11

Electrical specifications of chosen switches

Parameter	IPA65R045C Si-MOSFET	SCT20N120 SiC-MOSFET	GS66508B GaN-HEMT
Breakdown voltage	700 V	1200 V	650 V
Current	18 A	20 A	30 A
On-resistance	45 mΩ	190 mΩ	50 mΩ

a) *Switching characteristics*

The Si-CoolMOS has an overall better performance compared to other state of the art Si-MOSFETs. Its lower on state resistance and higher switching speeds lowers the conduction and switching losses. In comparison with the previous Si-MOSFETS, the Si-CoolMOS has the overall lowest turn-on and turn-off times. On the other hand, GaN-FET has an even smaller on-resistance and lower reverse recovery charge, resulting in a higher switching speed. Figure 14 shows the turn-on and turn-off characteristic. The GaN based converter for both modes of operation has exceptionally lower on and off times. For the buck mode the turn-on time for the GaN-FET is 10.92 ns, while the SiC-MOSFET and Si-Cool-MOS turn-on time are 25.2 ns and 26.4 ns, respectively. On the other hand, the boost mode has longer turn-on time for the Si-Cool-MOS with 121.77 ns, the SiC-MOSFET with 24.91 ns, and the GaN-FET has a turn-on time of 10.96 ns. The turn-off times for the GaN-FET are 10.97 ns for the buck mode and 10.96 ns for the boost mode. The SiC-MOSFET follows second with turn-off times of 18.82 ns and 18.23 ns for the buck and boost mode, respectively. The Si-CoolMOS has the longest turn-off times with a turn-off time of 34.58 ns for the buck mode, and 110.5 ns for the boost mode of operation.

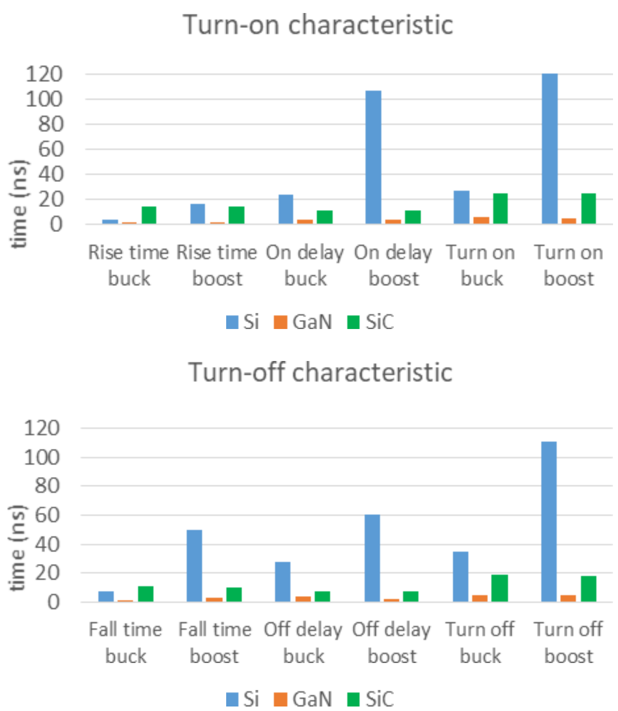

Fig. 14. Switching characteristic for both modes of operation: turn-on (top) and turn-off (bottom)

b) *Efficiency*

Similarly, to the buck and boost converter, the efficiency is calculated using equations (1) and (2). Using a switching frequency of 100 kHz, for the buck mode of operation the efficiency of the Si-CoolMOS is 91.8%, 92% for the SiC-MOSFET, while the GaN-FET based converter shows an efficiency of around 92.3%. On the other hand, when operating in boost mode, the efficiency of the Si based converter is 95.7%, 95.8 for the SiC based bidirectional converter and 96% for the GaN based converter. The results are shown in Figure 15.

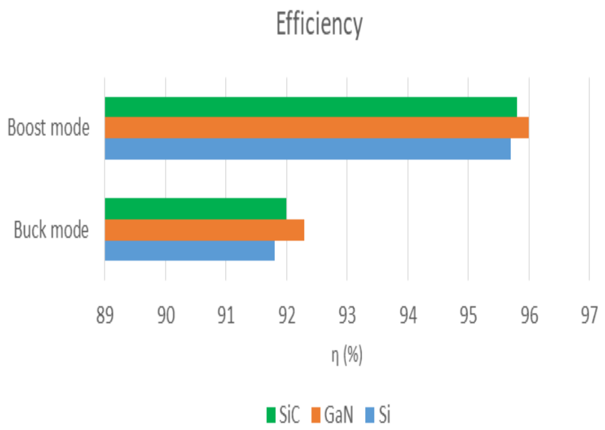

Fig. 15. Efficiency results for switching frequency of 100 kHz

Influence of the operating frequency on efficiency and switching times

Simulations were performed for all converters at different operating frequencies. As the switching frequency increases, the passive components are optimized accordingly using the equations (10)–(13) to calculate the appropriate capacitance and inductance for the different frequencies. Tables 12 to 15 show the change in efficiency and switching times as the frequency is increased from 100 kHz to 500 kHz with a step of 100 kHz for each of the analyzed converters. The switching times vary with the change of frequency. As it can be seen GaN devices show superior efficiency and switching times even at higher frequencies.

Table 12

Buck converter performance for the frequency range of 100 kHz – 500 kHz

Frequency (kHz)	t_{on} (ns)			t_{off} (ns)			η (%)		
	Si	SiC	GaN	Si	SiC	GaN	Si	SiC	GaN
100	40.91	21.51	**9.10**	110.40	13.10	**11.69**	90.0	91.40	**93.1**
200	40.38	21.45	**8.99**	107.84	13.33	**12.12**	89.7	91.10	**93.1**
300	42.70	21.6	**8.90**	108.30	13.90	**11.57**	88.8	90.10	**92.8**
400	45.00	21.13	**11.70**	109.46	13.77	**12**	88.2	89.92	**92.7**
500	41.87	20.98	**9.00**	108.80	13.86	**11.8**	87.6	89.60	**92.6**

Table 13

Boost converter performance for the frequency range of 100 kHz – 500 kHz

Frequency (kHz)	t_{on} (ns)			t_{off} (ns)			η (%)		
	Si	SiC	GaN	Si	SiC	GaN	Si	SiC	GaN
100	25.20	27.3	**4.63**	66.2	19.00	**17.50**	90.72	**92.90**	90.7
200	24.30	27.2	**4.3**	52.4	**19.44**	22.00	92.40	92.70	**94.2**
300	23.22	26.4	**4.50**	72.32	**20.00**	20.60	92.48	93.32	**95.1**
400	23.53	26.64	**5.40**	69.2	**20.41**	20.55	92.70	93.37	**95.4**
500	22.87	27.00	**5.43**	66	**20.17**	20.35	93.22	93.40	**95.6**

Table 14

Buck-boost (buck mode) converter performance for the frequency range of 100 kHz – 500 kHz

Frequency (kHz)	t_{on} (ns)			t_{off} (ns)			η (%)		
	Si	SiC	GaN	Si	SiC	GaN	Si	SiC	GaN
100	26.4	25.10	**5.27**	34.58	18.82	**5.23**	91.8	92.0	**92.3**
200	80.0	25.00	**5.35**	120	18.82	**5.20**	90.7	**91.8**	91.6
300	83.0	25.00	**5.27**	123	18.85	**5.18**	88.8	**90.5**	90.3
400	91.7	25.10	**5.24**	122	18.85	**5.20**	85.3	89.5	**89.7**
500	118.0	25.09	**5.23**	105	18.9	**5.20**	84.2	88.2	**88.6**

Table 15

Buck-boost (boost mode) converter performance for the frequency range of 100 kHz – 500 kHz

Frequency (kHz)	t_{on} (ns)			t_{off} (ns)			η (%)		
	Si	SiC	GaN	Si	SiC	GaN	Si	SiC	GaN
100	121.77	24.91	5.20	110.5	18.23	5.22	95.7	95.8	96.0
200	122.7	24.94	5.26	111.5	18.72	5.29	94.2	94.4	94.8
300	121.5	24.91	5.12	91.2	18.66	5.07	92.3	93.1	93.4
400	117.00	24.92	5.20	137.5	18.70	5.18	90.7	91.8	92.1
500	119.8	24.90	5.23	89.5	18.86	5.22	88.9	90.8	91.3

5. CONCLUSION

The paper presents a comparative study of switching performances and efficiency of the basic topologies of DC-DC converters in GaN, SiC and Si technologies. The simulation results show that the WBG devices, especially GaN devices, offer better performance (switching times and efficiency) than the state of the art Si devices. In all WBG based converter topologies, the switching times (on and off times) are notably smaller than the ones of the Si based converters. Furthermore, the results show that the WBG switches make the converters more efficient than their Si counterpart, with the efficiency of the GaN based converters never falling below 90%. Even though the technology of SiC and GaN devices is not as developed as the Si technology, these results show that the use of WBG semiconductors can improve the overall performance of DC-DC converters. The switching times of GaN switches are smaller than those of SiC switches for the entire frequency range of 100 kHz to 500 kHz and in some instances the difference is significant. On the other hand, the efficiency results show similar values for the switching frequency of 100 kHz, but as the frequency increases up to 500 kHz GaN switches stand out as the better choice for high frequency and low-medium voltage applications for DC-DC converters.

The popularity of GaN technologies in power electronics continues to rise with the ever growing demand for greater efficiency, higher frequencies and lower cost of production. When compared to Si and SiC, GaN technology is relatively young and has some material and technology concerns, mostly the production of GaN substrates, which limits its full potential. Another area of concern is the modelling of GaN-devices. Although, there are available manufacturer models, the proposed models for GaN transistors in the literature required several improvements such as, modelling of the parasitic components and their behavior and thermal modelling. These improvements will lead to faster and more accurate models, which is critical when predicting the behavior and reliability of the devices under different working conditions. Analyzing DC-DC converters in the discontinuous conduction mode (DCM) can be another area of future work. In it, special focus will be given to the effect of the passive elements (especially the inductor) on the converter performance.

REFERENCES

[1] Millán, J., Godignon. P., Perpiñà, X., Pérez-Tomás, A., Rebollo, J. (2014): A Survey of wide bandgap power semiconductor devices, *IEEE Transactions on Power Electronics*, Vol. **29**, no. 5, pp. 2155–2163. DOI: 10.1109/TPEL.2013.2268900.

[2] Ren F., Zolper, J. C. (2003): *Wide Energy Band Gap Electronic Devices,* World Scientific. https://doi.org/10.1142/5173

[3] Stefano Lovati (Oct. 2021): SiC technology: chalanges and future perspectives, *Power Electronics News*.

[4] Roccaforte, F., Greco, G., Fiorenza, P., Iucolano, F. (2019): An overview of normally-off gan-based high electron mobility transistors, *Materials*, **12** (10), 1599. https://doi.org/10.3390/ma12101599

[5] Han, D., Sarlioglu, B. (2015): Performance Evaluation of GaN-based synchronous boost converter under various output voltage, load current, and switching frequency operations, *Journal of Power Electronics*, **15** (6), pp. 1489–1498. DOI:10.6113/JPE.2015.15.6.1489

[6] Ahmet, O., Butt, M. A., Khonina, S. N., Kazanskiy, S. N. (2022): Performance comparison of silicon- and gallium-nitride-based MOSFETs for a power-efficient, DC-to-DC flyback converter, *Electronics,* **11** (8), 1222. https://doi.org/10.3390/electronics11081222

[7] Salah S. Alharbi, Saleh S. Alharbi, Ali M. S. Al-bayati, Yehuwalashet A. Tesema, Mohammad Matin (2018): Impact of cascode GaN power devices on a bidirectional DC-DC buck/boost converter in DC Microgrids, *Proc.*

SPIE 10754, Wide Bandgap Power and Energy Devices and Applications III, https://doi.org/10.1117/12.2322808

[8] Frivaldský, M., Morgoš, J., Zelnik, R. (2020): Evaluation of GaN power transistor switching performance on characteristics of bidirectional DC-DC converter. *Elektronika ir elektrotechnika,* **26**, pp 18–24.

[9] Lenzhofer, M., Frank, A. (2018): Efficiency and Near-Field Emission Comparisons of a Si- and GaN Based Buck Converter Topology, *2018 IEEE 18th International Power Electronics and Motion Control Conference (PEMC)*, Budapest, Hungary, pp. 818–823, DOI: 10.1109/EPEPEMC.2018.8521839.

[10] Khaled Alatawi, Fahad Almasoudi, Mohammad Matin (Sep. 2016): Switching performance and efficiency investigation of GaN based DC-DC buck converter for low voltage and high current applications, *Proc. SPIE 9957, Wide Bandgap Power Devices and Applications*, 99570C. https://doi.org/10.1117/12.2238142

[11] Ansari, S., Davidson, J., Foster, M. (2021): Evaluation of silicon MOSFETs and GaN HEMTs in soft-switched and hard-switched DC-DC boost converters for domestic PV applications, *IET Power Electronics*, **14** (5), pp 1032–1043. https.//doi.org/10.1049/pel2.12085

[12] Jadli U., Mohd-Yasin F., Moghadam H. A., Pande P., Chaturvedi M., Dimitrijev S. (2021): A method for selection of power MOSFETs to minimize power dissipation", *Electronics*, **10** (17), 2150. https://doi.org/10.3390/electronics 10172150

[13] Hart, D. W. (2011): *Power Electronics*, The McGraw-Hill Companies, Inc., pp. 203–225.

Journal of Electrical Engineering and Information Technologies, Vol. **8,** No. 2, pp. 129–132(2023
In print: ISSN 2545–4250
On line: ISSN 2545–4269

INSTRUCTIONS FOR AUTHORS

The *Journal of Electrical Engeneering and Information Technologies* is published twice yearly. The journal publishes **original scientific papers, short communications, reviews** and **professional papers** from all fields of electrical engineering.

The journal also publishes (continuously or occasionally) the bibliographies of the members of the Faculty, book reviews, reports on meetings, informations of future meetings, important events and data, and various rubrics which contribute to the development of the corresponding scientific field.

Original scientific papers should contain hitherto unpublished results of completed original scientific research. The number of pages (including tables and figures) should not exceed 15 (28 000 characters).

Short communications should also contain completed but briefly presented results of original scientific research. The number of pages should not exceed 5 (10 000 characters) including tables and figures.

Reviews are submitted at the invitation of the Editorial Board. They should be surveys of the investigations and knowledge of several authors in a given research area. The competency of the authors should be assured by their own published results.

Professional papers report on useful practical results that are not original but help the results of the original scientific research to be adopted into scientific and production use. The number of pages (including tables and figures) should not exceed 10 (18 000 characters).

Acceptance for publication in the Journal obliges the authors not to publish the same results elsewhere.

SUBMISSION

The article and annexes should be written on A4 paper with margins of 2.5 cm on each side with a standard font Times New Roman 11 points and should be named with the surname of the first author and then if more and numbered. It is strongly recommended that on MS Word 2003 or MS Word 2007 and on PDF files of the manuscript be sent by e-mail:

JEEIT@feit.ukim.edu.mk.

A letter must accompany all submissions, clearly indicating the following: title, author(s), corresponding author's name, address and e-mail addres(es), suggested category of the manuscript and a suggestion of five referees (their names, e-mail and affiliation).

Articles received by the Editorial Board are sent to two referees (one in the case of professional papers). The suggestions of the referees and Editorial Board are sent to the author(s) for further action. The corrected text should be returned to the Editorial Board as soon as possible but in not more than 30 days.

PREPARATION OF MANUSCRIPT

The papers should be written in the shortest possible way and without unnecessary repetition.

The original scientific papers, short communications and reviews should be written in English, while the professional papers may also be submitted in Macedonian.

Only SI (Système Internationale d'Unites) quantities and units are to be used.

Double subscripts and superscripts should be avoided whenever possible. Thus it is better to write $\nu_3(PO_4)$ than $\nu_{3_{PO_4}}$ or exp(–E/RT) than $e^{-E/RT}$. Strokes (/) should not be used instead of parentheses.

When a large number of compound have been analyzed, the results should be given in tabular form.

Manuscript should containt: title, author(s) full-name(s), surname(s), address(es) and e-mail of the corresponding author, short abstract, key words, introduction, experimental or theoretical back-ground, results and discussion, acknowledgment (if desired) and references.

The **title** should correspond to the contents of the manuscript. It should be brief and informative and include the majority of the key words.

Each paper should contain an **abstract** that should not exceed 150 words and **3–5 key words**. The abstract should include the purpose of the research, the most important results and conclusions.

The **title**, **abstract** and **key words** should be translated in Macedonian language. The ones written by foreign authors will be translate by the Editorial Board.

In the **introduction** only the most important previous results related to the problem in hand should be briefly reviewed and the aim and importance of the research should be stated.

The **experimental** section should be written as a separate section and should contain a description of the materials used and methods employed – in form which makes the results reproducible, but without detailed description of already known methods.

Manuscripts that are related to **theoretical studies**, instead of experimental material, should contain a sub-heading and the **theoretical background** where the necessary details for verifying the results obtained should be stated.

The **results** and **discussion** should be given in the same section. The discussion should contain an analysis of the results and the **conclusions** that can be drawn.

Figures (photographs, diagrams and sketches) and **mathematical formulae** should be inserted in the correct place in the manuscript, being horizontally reduced to 8 or 16 cm. The size of the symbols for the physical quantities and units as well as the size of the numbers and letters used in the reduced figures should be comparable with the size of the letters in the main text of the paper. Diagrams and structural formulae should be drawn in such a way (e.g. black Indian ink on white or tracing paper) as to permit high quality reproduction. The use of photographs should be avoided. The tables and the figures should be numbered in Arabic numerals (e.g. Table 1, Figure 1). Tables and figures should be self-contained, i.e. should have captions making them legible without resort to the main text. The presentation of the same results in the form of tables and figures (diagrams) is not permitted.

Figures and tables must be centred in the column. Large figures and tables may span across both columns (Figure 1).

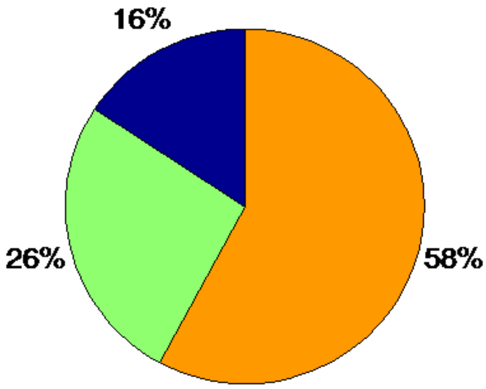

Fig. 1. Example of a graph and a single-line caption (collour)

Graphics may be full colour. Please use only colours which contrast well both on screen and on a black-and-white hardcopy because the Journal is published in black-and-white, as shown in Figure 2. The colour version is only for the electronic version of the Journal.

Please check all figures in your paper both on screen and on a black-and-white hardcopy. When you check your paper on a black-and-white hardcopy, please ensure that:

– the colours used in each figure contrast well,

– the image used in each figure is clear,

– all text labels in each figure are legible.

Please check all figures in your paper both on screen and on a black-and-white hardcopy. When you check your paper on a black-and-white hardcopy, please ensure that the image used in each figure is clear and all text labels in each figure are legible.

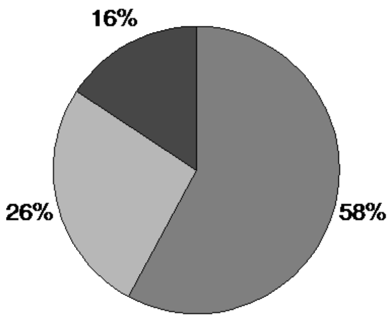

Fig. 2. Example of a graph and a single-line caption (black-and-white)

Fig. 3. Example of an image as it will appear at the electronic version of the Journal and a multi-line caption

Footnotes are also not permitted.

The **reference** should be given in a separate section in the order in which they appear in the text. The surname of one or two authors may be given in the text, whereas in the case of more than two authors they should be quoted as, for example:

Examples of reference items of different categories shown in the References section include:

- example of a book in [1]
- example of a book in a series in [2]
- example of a journal article in [3]
- example of a conference paper in [4]
- example of a patent in [5]
- example of a website in [6]
- example of a web page in [7]
- example of a databook as a manual in [8]
- example of a datasheet in [9]
- example of a master/Ph.D. thesis in [10]
- example of a technical report in [11]
- example of a standard in [12]

All reference items must be in 9 pt font. Please use Regular and Italic styles to distinguish different fields as shown in the References section. Number the reference items consecutively in square brackets (e.g. [1]).

When referring to a reference item, please simply use the reference number, as in [2]. Do not use “Ref. [3]” or “Reference [3]” except at the beginning of a sentence, e.g. “Reference [3] shows …”. Multiple references are each numbered with separate brackets (e.g. [2, 3], [4–8]).

The **category** of the paper is proposed by the author(s), but the Editorial Board reserves for itself the right, on the basis of the referees' opinion, to make the final choice.

Proofs are sent to the author(s) to correct printers' errors. Except for this, alterations to the text are not permitted. The proofs should be returned to the Editorial Board in 2 days.

The author(s) will receive, free of charge, 1 reprint of every paper published in the Journal.

REFERENCES

[1] Surname, N(ame).; Surname, N(ame). (Year): *Name of the Book*, Publisher.

[2] Surname, N(ame).: Surname, N(ame). (Year): *Name of the Book*, Name of the Series. Publisher, **vol.** XXX.

[3] Surname, N(ame).; Surname N(ame). (Year): Title of the article, *Name of the Journal*, **Vol. XX,** No. XX, pp. XXX–XXX.

[4] Surname, N(ame).; Surname N(ame). (Year): Title of the article, *Proceedings of the Conference (Name),* **Vol. XX,** pp. XXX–XXX.

[5] Surname, N(ame).; Surname N(ame). (Date dd. mm. yyyy): *Name of the Patent*, Institution that issued the patent & Number of the patent.

[6] N.N. (Year): *The XXX web site*, web address.

[7] Surname, N. (Year): *XXX homepage on XXX*, web address.

[8] N.N. (Year): *Title of the Manual*, Name of the Organization.

[9] N.N.: *XXX data sheet*, Name of the Organization.

[10] Surname, N. (Year): *Title of the Thesis*, Master/Ph.D. thesis (in Language), Institution.

[11] Surname, N(ame)., Surname, N(ame). (Year): *Title of the Report*, organization that issued the report, Number of the report.

[12] Institution that issued the standard, *Name of the Standard*, & Number of the standard (Year).